AD-A081 180 IOWA INST OF HYDRAULIC RESEARCH IOWA CITY F/G 20/4
EXPERIMENTS ON TRANSITIONAL OSCILLATORY PIPE FLOW,(U)
AUG 79 B R RAMAPRIAN, S W TU DAAG-29-79-G-0017
UNCLASSIFIED IIHR-221 NL

1 OF
AD
A081180

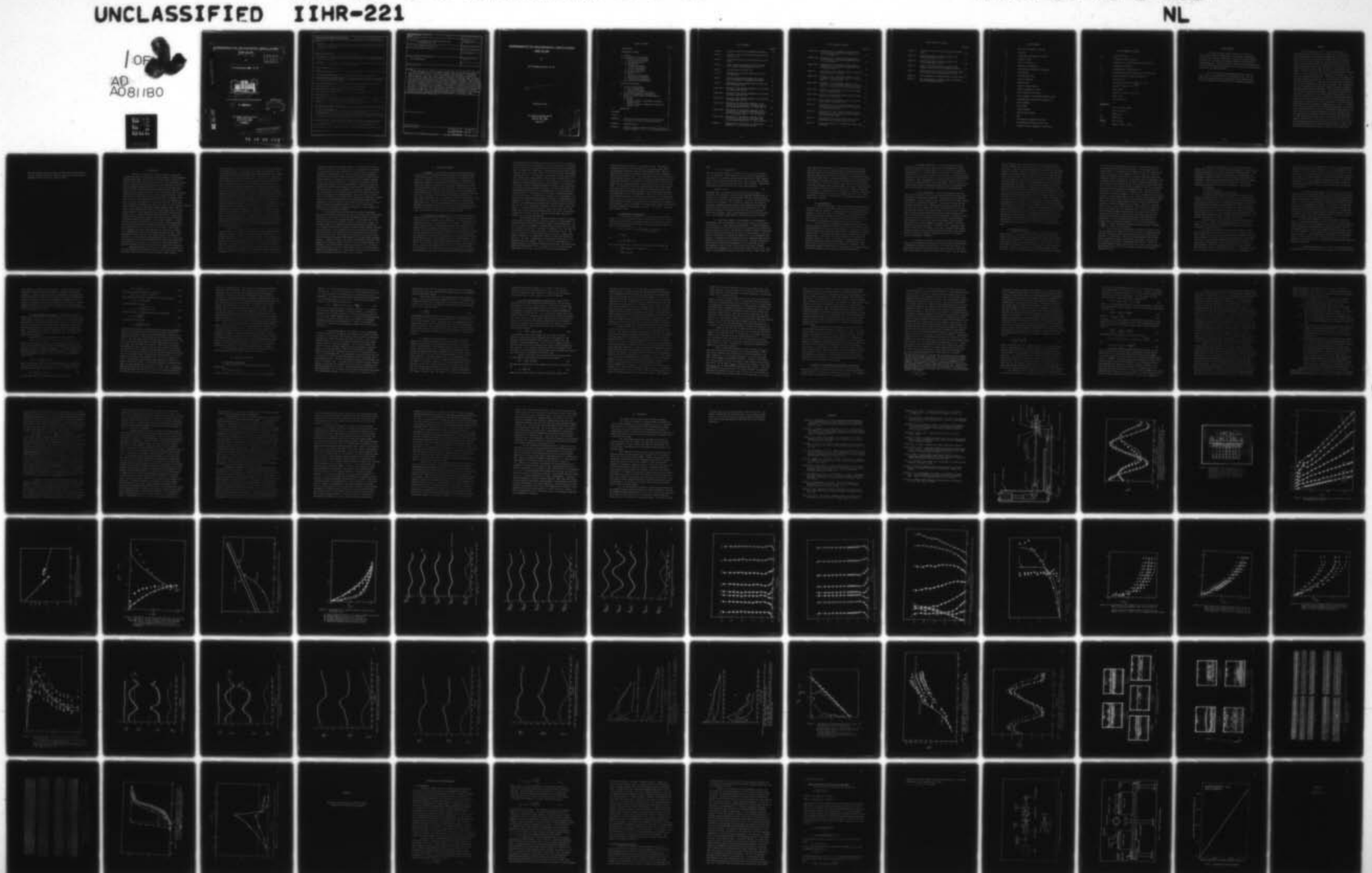

1 OF 1

AD A081180

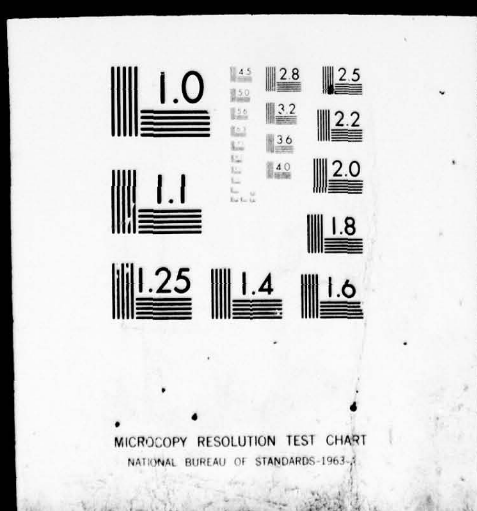

6

EXPERIMENTS ON TRANSITIONAL OSCILLATORY PIPE FLOW

1

by

10

B. R. Ramaprian [redacted] S. W. Tu

Contract DAAG-29-79-G-0017

15

14 IIHR [redacted] 221

Iowa Insti[redacted] of Hydraulic Research
~~The University of Iowa~~
Iowa City, ~~Iowa 52242~~

12 125

11 Aug[redacted]979

188 300

INSTRUCTIONS FOR COMPLETING FORM NTIS-35 (Bibliographic Data Sheet based on COSATI Guidelines to Format Standards for Scientific and Technical Reports Prepared by or for the Federal Government, PB-180 600).

1. **Report Number.** Each individually bound report shall carry a unique alphanumeric designation selected by the performing organization or provided by the sponsoring organization. Use uppercase letters and Arabic numerals only. Examples FASEB-NS-73-87 and FAA-RD-73-09.

2. Leave blank.

3. **Recipient's Accession Number.** Reserved for use by each report recipient.

4. **Title and Subtitle.** Title should indicate clearly and briefly the subject coverage of the report, subordinate subtitle to the main title. When a report is prepared in more than one volume, repeat the primary title, add volume number and include subtitle for the specific volume.

5. **Report Date.** Each report shall carry a date indicating at least month and year. Indicate the basis on which it was selected (e.g., date of issue, date of approval, date of preparation, date published).

6. **Performing Organization Code.** Leave blank.

7. **Author(s).** Give name(s) in conventional order (e.g., John R. Doe, or J.Robert Doe). List author's affiliation if it differs from the performing organization.

8. **Performing Organization Report Number.** Insert if performing organization wishes to assign this number.

9. **Performing Organization Name and Mailing Address.** Give name, street, city, state, and zip code. List no more than two levels of an organizational hierarchy. Display the name of the organization exactly as it should appear in Government indexes such as Government Reports Index (GRI).

10. **Project/Task/Work Unit Number.** Use the project, task and work unit numbers under which the report was prepared.

11. **Contract/Grant Number.** Insert contract or grant number under which report was prepared.

12. **Sponsoring Agency Name and Mailing Address.** Include zip code. Cite main sponsors.

13. **Type of Report and Period Covered.** State interim, final, etc., and, if applicable, inclusive dates.

14. **Sponsoring Agency Code.** Leave blank.

15. **Supplementary Notes.** Enter information not included elsewhere but useful, such as: Prepared in cooperation with . . . Translation of . . . Presented at conference of . . . To be published in . . . Supersedes . . . Supplements . . . Cite availability of related parts, volumes, phases, etc. with report number.

16. **Abstract.** Include a brief (200 words or less) factual summary of the most significant information contained in the report. If the report contains a significant bibliography or literature survey, mention it here.

17. **Key Words and Document Analysis. (a). Descriptors.** Select from the Thesaurus of Engineering and Scientific Terms the proper authorized terms that identify the major concept of the research and are sufficiently specific and precise to be used as index entries for cataloging.
    (b). Identifiers and Open-Ended Terms. Use identifiers for project names, code names, equipment designators, etc. Use open-ended terms written in descriptor form for those subjects for which no descriptor exists.
    (c). COSATI Field/Group. Field and Group assignments are to be taken from the 1964 COSATI Subject Category List. Since the majority of documents are multidisciplinary in nature, the primary Field/Group assignment(s) will be the specific discipline, area of human endeavor, or type of physical object. The application(s) will be cross-referenced with secondary Field/Group assignments that will follow the primary posting(s).

18. **Distribution Statement.** Denote public releasability, for example "Release unlimited", or limitation for reasons other than security. Cite any availability to the public, other than NTIS, with address, order number and price, if known.

19 & 20. **Security Classification.** Do not submit classified reports to the National Technical Information Service.

21. **Number of Pages.** Insert the total number of pages, including introductory pages, but excluding distribution list, if any.

22. **NTIS Price.** Leave blank.

BIBLIOGRAPHIC DATA SHEET	1. Report No.	2.	3. Recipient's Accession No.
4. Title and Subtitle Experiments on Transitional Oscillatory Pipe Flow IIHR Report No. 221			5. Report Date August 1979 6.
7. Author(s) B.R. Ramaprian and S.W. Tu			8. Performing Organization Rept. No.
9. Performing Organization Name and Address			10. Project/Task/Work Unit No. 11. Contract/Grant No.
12. Sponsoring Organization Name and Address U.S. Army Research			13. Type of Report & Period Covered 14.

15. Supplementary Notes

16. Abstracts

Fully developed oil flow in a smooth circular pipe at a mean Reynolds number of about 2100 was subjected to a nominally sinusiodal flow modulation at frequencies ranging from 0.05 - 1.75 Hz. It was observed that flow oscillation increased the critical Reynolds number and, under certain conditions, even brought about linearization of the flow, which would be intermittently turbulent at the mean Reynolds number under quasi-steady (infinitely small oscillation frequency) conditions. The occurrence and extent of laminarization was, however, found to depend on factors such as the intermittency of turbulent puffs in the mean quasi-steady flow, frequency of oscillation, etc. Two series of experiments were performed. In one series, the oscillatory flow was fully turbulent. In both the cases, instantaneous velocities in the flow were measured using Laser Doppler anemometry. The instantaneous velocity was decomposed into time-mean periodic and random components employing ensemble averaging techniques. The experiments indicated that the laminarized oscillatory flow behaves (continued in book)

17. Key Words and Document Analysis. 17a. Descriptors

17b. Identifiers/Open-Ended Terms

17c. COSATI Field/Group

18. Availability Statement	19. Security Class (This Report) UNCLASSIFIED	21. No. of Pages 125
	20. Security Class (This Page) UNCLASSIFIED	22. Price

FORM NTIS-35 (REV. 10-73) ENDORSED BY ANSI AND UNESCO. THIS FORM MAY BE REPRODUCED USCOMM-DC 8265-P74

EXPERIMENTS ON TRANSITIONAL OSCILLATORY PIPE FLOW

by

B. R. Ramaprian and S. W. Tu

IIHR Report No. 221

Iowa Institute of Hydraulic Research
The University of Iowa
Iowa City, Iowa 52242

August 1979

TABLE OF CONTENTS

LIST OF FIGURES

LIST OF FIGURES (continued)

LIST OF FIGURES (continued)

LIST OF SYMBOLS

A	area of cross-section of the pipe
A_e	exit area
C_D	coefficient of discharge of the slot
D	diameter of pipe
F	factor in equation 3
f	frequency of oscillation
f_t	characteristic frequency of turbulence
H	constant head
h_t	frictional head loss
K	factor in equation 4
L	length of pipe
M	number of cycles sampled
N	number of samples in a cycle
P	static pressure at any point
P_A	static pressure at an upstream reference point
ΔP^*	non-dimensional pressure drop (Equation 17)
R_e	Reynolds number
r	local radius
S	Strouhal number
ΔT	sampling time interval
t	time
U	instantaneous longitudinal velocity
U^+	non-dimensional velocity in wall layer
u	turbulent velocity component in x-direction

LIST OF SYMBOLS (continued)

u_*	friction velocity
V	instantaneous radial velocity
v	turbulent velocity component in radial direction
x	longitudinal coordinate
x^*	non-dimensional x-coordinate = x/D
Y^+	non-dimensional radial coordinate in the wall layer
β	pressure gradient parameter (Equation 23)
λ	friction factor
η	non-dimensional radial coordinate = 1-2r/D
Ω	frequency parameter, $[D/2 \sqrt{\frac{2\pi f}{\nu}}]$
ρ	fluid density
ν	kinematic viscosity of the fluid
τ	shear stress
τ_w	wall shear stress

Subscripts:

m	cross-sectional average
p	periodic component
q	quasi-steady
max	maximum value
overbar	time average
< >	ensemble (phase) average

ACKNOWLEDGEMENTS

This study was made possible initially by a Grant from the Graduate College of The University of Iowa under the Biomedical Research Grants Program. Subsequently, the project has been supported internally by the Institute of Hydraulic Research and the Division of Energy Engineering. The final stages of the study and the preparation of this report have been supported in part by the United States Army Research Office Grant No. DAAG29-79-G-0017.

The authors gratefully acknowledge the support from all these sources. The authors wish to thank Professor V.C. Patel for many useful discussions and Mr. Dale Harris and his workshop staff for their support in the construction of the experimental apparatus.

ABSTRACT

Fully developed oil flow in a smooth circular pipe at a mean Reynolds number of about 2100 was subjected to a nominally sinusoidal flow modulation at frequencies ranging from 0.05 - 1.75 Hz. It was observed that flow oscillation increased the critical Reynolds number and, under certain conditions, even brought about laminarization of the flow, which would be intermittently turbulent at the mean Reynolds number under quasi-steady (infinitely small oscillation frequency) conditions. The occurrence and extent of laminarization was, however, found to depend on factors such as the intermittency of turbulent puffs in the mean quasi-steady flow, frequency of oscillation, etc. Two series of experiments were performed. In one series, the oscillatory flow was almost completely laminarized. In the other series, the oscillatory flow was fully turbulent. In both the cases, instantaneous velocities in the flow were measured using Laser Doppler anemometry. The instantaneous velocity was decomposed into time-mean, periodic and random components employing ensemble averaging techniques. The experiments indicated that the laminarized oscillatory flow behaves very similar to laminar oscillatory flow at either end of the Strouhal number range studied. The oscillatory turbulent flow was found to depend on both the Strouhal number and the ratio of the oscillation frequency (f) to some characteristic frequency (f_t) of turbulence in the flow. The design of the present experimental facility made it possible to study the flow at $f/f_t \approx 1$, a condition that could not be attained in most previous investigations. It was found, that at this frequency of oscillation, the Reynolds stresses generally remained frozen at an average state during the entire oscillation cycle. The turbulent structure showed significant departures from equilibrium at all times during the oscillation cycle. As a result, there was a net change in the time-mean velocity profile near the wall and a net increase in the time-mean wall shear stress and power loss due to friction. The data also indicated that the direct interaction between oscillation and the turbulent structure was essentially confined to the Stokes layer.

The study suggests that quasi-steady turbulence models may not be adequate to describe unsteady flows when the time scale of unsteadiness is comparable to that of dominant turbulent eddies.

I. INTRODUCTION

The study of unsteady shear flows is relevant to many areas of application such as aerodynamics, ship hydrodynamics, biofluid mechanics and wind engineering. Much of the study reported in the literature on unsteady flows, however, concerns laminar flows. Exact solutions are available for relatively simple unsteady laminar flow situations in the classical literature [(see Rosenhead 1963)]. Laminar flows in pipes due to periodic pressure gradients have been studied by Richardson and Tyler (1929), and Uchida (1956) and others. The situation with regard to unsteady transitional and turbulent flows is, however, less satisfactory. While there have been some attempts to analyze the problem of stability in periodic flows (e.g., Kerczek and Davis 1974, 1975, Hino and Sawamoto 1975, Hino et al 1976), much remains to be studied in this area. Of the laboratory experiments on periodic pipe channel flow that have been reported in the literature, most pertain to high Reynolds number turbulent flows. The earliest of such experiments were reported by Schulz-Grunow (1940). More recent experiments in this category are those performed by Hirose and Oka (1969), Lu et al, (1973), and Acharya and Reynolds (1975). In all these experiments fully developed turbulent pipe flow was perturbed by imposing a periodic modulation in discharge at a prescribed frequency. Of these, the work of Acharya and Reynolds involved the most detailed measurements such as Reynolds shear stress, though the amplitude of flow modulation in their experiments was less than 5 per cent of the mean. These experiments suggested that even at that amplitude, the structure of turbulence can be significantly affected in the Stokes layer near the wall. Their measurements in this layer were very limited because of the thinness of the layer. Lu et al experienced considerable difficulty in the use of hot film anemometry as well as in analog data processing in their experiments on oscillatory flow of water in a circular pipe. Their measurements of mean and turbulent velocities did not lead to any significant conclusions.

One would intuitively expect that the effects of unsteadiness on the flow structure will be stronger on flows in the neighborhood of transition than on flows at very large Reynolds numbers. This is because

transition process can be sensitive to the strong acceleration/deceleration in the unsteady flow. The experience with steady flows subjected to spatial pressure gradients has confirmed that pressure gradients have a significant effect on the critical Reynolds number. Strong effects of periodic flow modulation on the flow characteristics at transitional Reynolds numbers have, indeed, been observed in the experiments of Sarpkaya (1966) and in the more recent studies of Gerrard (1971) and Hino and Sawamoto (1975). From a study of the growth of disturbances in sinusoidally modulated pipe flow in the mean flow Reynolds number range of 2000-5000, Sarpkaya concluded that flow pulsation increases the critical Reynolds number. Gerrard's experiments related to periodic pipe flow at a mean Reynolds number of 3700 while the experiments of Hino and Sawamoto pertaineed to purely oscillatory pipe flow (i.e., at a mean Reynolds number of zero). These latter two studies were mainly qualitative but they indicated that, in general, turbulence is inhibited during the acceleration part of the modulation cycle and enhanced during the retardation part. In fact, the flow, under certain circumstances, appeared to remain laminar during the acceleration part of the cycle. Indications of inhibition of turbulence or delayed transition have also been observed in some of the in-vivo studies of pulsatile blood flow in the aorta of mamals (e.g., Falsetti et al 1972, Kiser et al 1976). However, the instrumentation and data reduction techniques used in the blood flow studies, as well as in the other laboratory studies mentioned above, were not sufficiently sophisticated to yield detailed quantitative information on the flow structure.

There is one class of unsteady turbulent flows, however, that has been studied in fair detail using moderate to highly sophisticated data reduction techniques. This is the unsteady turbulent boundary layer in a periodic free stream. Most of these studies (Karlsson 1959, Houdeville et al 1976, Cousteix et al 1977, and Patel 1977) pertain to zero pressure gradient boundary layers though some experiments on adverse pressure gradient flows have been reported recently (Kenison 1977, Houdeville and Cousteix 1978). The experiments on the zero pressure gradient boundary layers have, generally, lead to the conclusion that flow modulation has no effect on the average behavior of the flow and that the turbulent structure can still be

described by quasi-steady turbulence models. A careful study of these investigations, however, reveals that in all these experiments, the frequency of flow modulation was small compared with the characteristic frequency of turbulence in the boundary layer. One can expect to find a significant effect of flow modulation on the average flow structure only when the modulation frequency is comparable to the characteristic turbulent frequency in the flow. The very recent report of Houdeville and Cousteix (1978) on the unsteady boundary layer in the neighborhood of separation (where this condition is satisfied) does indicate strong effects of flow modulation on the flow structure. Hence, the behavior of an unsteady turbulent flow is not only determined by the Strouhal number (ratio of the time scale of mean flow to the time scale of unsteadiness), but also by the ratio of the time scale of unsteadiness to the characteristic time scale of turbulence. Further, since most of the interaction between the impressed oscillation and the turbulence structure is likely to occur within the Stokes layer, it is necessary to design the experiment carefully so as to get a thick enough Stokes layer and yet keep the modulation frequency at a value comparable to the characteristic turbulent frequency.

The present study was directed towards obtaining experimental data on fully developed oscillatory pipe flow at transitional Reynolds numbers. The nature of the periodic flow was found to depend strongly on the nature of the steady flow at the mean Reynolds number. It was found that if the steady mean flow was fully turbulent (with an intermittency of unity), the flow would remain fully turbulent when the Reynolds number was modulated at a frequency large enough to approach the characteristic turbulent frequency. On the other hand, if the steady mean flow was not turbulent but contained turbulent puffs at a low intermittency, the flow would tend to laminarize on periodic oscillation. Both these flow situations were studied in detail using Laser Doppler anemometry (LDA) together with a digital phase averaging technique. Important features of the present experiments, particularly with regard to the turbulent unsteady flow are (i) the oscillation frequency was comparable to the characteristic turbulence frequency in the flow and (ii) the viscous sublayer (2 mm) and Stokes sublayer (6 mm) were thick enough to permit detailed measurements in a region where the interaction of flow oscillation and turbulence have been found to be very strong.

II. EXPERIMENTAL PROGRAM

A. General. A test facility for producing sinusoidally oscillating pipe flow at transitional Reynolds numbers was designed and built for the present study. This facility used Eureka oil (of kinematic viscosity, $\nu = 1.384 \times 10^{-5}$ m^2/s at 26°C) and consisted of a long pipe of 50 mm diameter in which the oscillating flow was maintained. The flow oscillation was produced by varying the flow exit area sinusoidally by a rotating sleeve situated at the exit end of the pipe. The design of the rotating sleeve was very similar to that used in the classical experiments of Schultz-Grunow (1940). The exit area was kept small in comparison with the pipe area so that most of the head loss in the system occurred at the exit. Under such conditions, it is possible to obtain a discharge rate nearly proportional to the exit area. Velocity measurements were made using a single channel LDA. The data was acquired and processed using the IIHR IBM/1800 Data Acquisition System and a data processing technique developed by Mueller and Ramaprian (1977) for the analysis of unsteady turbulent flows. The details are described in the following sections

B. Description of the Apparatus. The experimental apparatus is shown schematically in figure 1. Oil is pumped by the circulating pump from the sump tank to the constant level overhead tank. The overhead tank is a cylindrical reservoir of 0.5 m diameter × 0.75 m height. The head is maintained constant (about 4 m above the ground level) by providing a 50 mm diameter overflow pipe which returns the extra oil to the sump tank. Oil from the constant head tank flows down through the 100 mm diameter inlet pipe and then through the 200 mm diameter curved pipe. A set of turning vanes is provided in the curved pipe to distribute the flow uniformly in the pipe. The horizontal section of the 200 mm pipe acts as a calming chamber. This section is followed by a bell-shaped contraction nozzle of 50 mm exit diameter. The test pipe is made of copper and has a nominal inlet diameter of 50 mm. It has a total length of 8.8 m, (i.e., L/D = 176) which ensures full development of flow even under laminar flow conditions. The pipe has been assembled from sections. The joints between the different sections

have been matched with special care insuring that there are no irregularities in the surface. Twenty-eight wall static pressure taps of 1 mm diameter have been provided at regular intervals along the pipe for the measurement of pressure loss through pipe. These pressure taps have been provided along the bottom of the tube in order to prevent air bubbles from accumulating near the holes. Provision has also been made for flush mounting pressure transducers at three locations along the pipe. The first one is at a point 1.3 m from the contraction exit. The second one is at a point 50 mm upstream from the measurement location and the third at 1.3 m upstream of the second. Pressure transducers mounted at locations 2 and 3 can be used to obtain the pressure gradient in the pipe. The test section where velocity measurements were made is a plexiglass tube, 0.3 m long and 50 mm in internal diameter. The upstream end of the tube is machined and matched with the copper pipe. The other end is connected to a 50 mm diameter × 300 mm long copper tube whose downstream end is closed. Two longitudinal rectangular slots, 50 mm × 3.2 mm, milled on the surface of this tube along two generators 180 degrees apart from each other, provide the exit for the oil. The oil falls into a rectangular plexiglass collection chamber (vented adequately to the atmosphere) from where it flows into a weigh tank. The weigh tank rests on a platform weighing machine and is used for measuring the mass rate of flow of the oil. The oil from the weigh tank can be drained via a valve into the sump tank.

The technique used for producing discharge oscillation is similar to that used by Schultz-Grunow. The device consists of a hollow copper cylindrical sleeve rotating over the slotted copper tube mentioned above. One end of the sleeve is profiled on a milling machine in such a way as to form, on development, two cycles of a sine wave of amplitude 12 mm. The other end of the sleeve is closed and is attached to a 13 mm diameter shaft. The shaft is connected to a variable speed motor, by means of a coupling that permits adjustment of the longitudinal position of the sleeve relative to the slots. The shaft is supported by a bearing housed in the wall of the plexiglass collection chamber. The motor is mounted independently on a bracket secured to the framework supporting the apparatus. The motor is manufactured by Bodine Electric and is a geared D.C. motor having an output speed range of 1.2-55 rpm. Its speed is regulated electronically by

controlling the motor voltage via a feed-back circuit. The regulator maintains the speed of the motor within 1% of the preset speed, which is continuously selectable within the range mentioned above. When the sleeve rotates, the area of opening of the pair of slots is continuously varied by the profiled sleeve. It is seen that the exit area variation will be a sinusoidal function of time with the variation going through two cycles during each revolution of the sleeve. The mean exit area can be adjusted within limits by changing the axial location of the sleeve relative to the slots. In the present study, this location has been chosen (after several trial runs) such that the mean flow Reynolds number would be about 2100. The sleeve profile was initially designed for an estimated discharge modulation amplitude of 0.35 × mean discharge. Later tests showed that the actual discharge modulation at infinitely low frequencies (i.e., quasi-steady state), was in fact, quite close to this calue. With the present design, it is possible to produce fully laminar flow at the minimum slot opening and fully turbulent flow at the maximum slot opening (under steady flow conditions). At higher frequencies, the amplitude is reduced. This aspect is discussed next in greater detail.

C. Performance of the Apparatus

1. Quasi-steady performance. If H is the gross head available (about 2.7 m), h_f the overall head loss in the system, V_e the exit velocity, V the test section velocity, A_e the exit area, A the cross sectional area of the test section and C_D the discharge coefficient (assumed constant), we have, for quasi-steady flow,

$$H - h_f = V_e^2/2g - V^2/2g \doteq \frac{V_e^2}{2g} \text{ (Since V is very much smaller than } V_e) \qquad (1)$$

$$AV = C_D A_e V_e$$

or

$$V = C_D \frac{A_e}{A} \sqrt{2g(H - h_f)} \qquad (2)$$

If $h_f = K\, V^2/2g$, where K is a constant for the system, one finally gets

$$V = \sqrt{2gH}\ (C_D A_e/A)\ [1/\{1 + K(C_D A_e/A)^2\}^{\frac{1}{2}}] \qquad (3)$$

$$= \sqrt{2gH}\ C_D\ (A_e/A) F$$

where

$$F = [1/\{1 + K(C_D A_e/A)^2\}]^{\frac{1}{2}}$$

Since C_D is assumed constant, V is proportional to A_e, if F is constant; i.e., if $K(A_e/A)^2 << 1$. The frictional loss in the various components of the system can be estimated using standard handbook data. These estimates yield a value of $K \doteqdot 2$ for the present system. The ratio A_e/A has a maximum value of 0.1 in the present case (for fully "open" position). Substituting these values, one gets, for the fully "open" sleeve position,

$$K(A_e/A)^2 = 0.02 \tag{4}$$

This means that F varies from 1.0 to 0.98 from the fully closed to fully open sleeve positions. Thus an almost sinusoidal discharge rate (or velocity) can be expected. The quasi-steady discharge variation with the rotation of the sleeve is shown in figure 2. It is seen that the modulation is very nearly sinusoidal. It is possible to improve the wave shape of modulation by departing slightly from an exact sinusoidal sleeve profile. The required sleeve profile can then, be calculated from Eq. (3). This requires a knowledge of the precise values of K and C_D as functions of quasi-steady discharge. These can be obtained after the steady flow operation. In the present design, however, this procedure was not followed.

2. Unsteady performance. The performance of the system will be described by Eq. (3) only when the exit area is constant or varied infinitely slowly (i.e., under quasi-steady conditions). At finite frequencies of area variation, the flow in the system will be governed by the appropriate unsteady euations of motion. Specifically, the dynamic response of the system will be affected by the inertia of the fluid. As a consequence, as the frequency of oscillation is increased the amplitude of the flow modulation will decrease, the modulation will be distorted from the sinusoidal shape and the pressure at any point in the system will oscillate. Further, the discharge and pressure oscillations will generally be out of phase with the exit area variation. Some of these effects are seen from figure 2 showing the shape of the discharge (or cross sectional average velocity, U_m) vs. time curve, at two different oscillation frequencies; 0.057 Hz and 1.75 Hz. In

this figure, the distribution of U_m is normalized with respect to the quasi-steady cross sectional average velocity at the mid slot opening. The quasi-steady velocity distribution (U_q) as well as an exact sinusoidal distribution are also shown in the figure. The reduction in amplitude and the phase shift of discharge modulation, as well as the distortion in the shape of the modulation curve can be easily seen from the figure. It is seen that at the lower frequency, these effects are very small while at the higher frequency, they are perceptible. We, however, regard the distortion from the sinusoidal shape to be still small enough to be ignored for the purpose of the present study. Likewise, the reduction in amplitude at the higher frequency is no cause for concern, since it is still large enough (20% of the mean) to allow useful and meaningful measurements to be made at this frequency.

D. Instrumentation

1. Pressure measurement. Wall static pressure distribution along the pipe in steady flow was measured using the static pressure taps and an inverted U-tube oil manometer. The most upstream static pressure hole was connected to one of the limbs of the manometer. The other limb could be connected to any static pressure hole via a manifold with which all the static pressure holes were in communication through individual stop cocks. The manometer thus measured the pressure drop from the first hole.

In the unsteady flow experiments, pressure was measured using a pressure transducer mounted flush with the inner surface of the pipe. Pressure measurements were made at only one position viz. at station 2 in Fig. 1. Unsteady pressure drop measurements were, however, not made due to instrumentation problems. The pressure transducer used was an ENDEVCO 8510 semiconductor type, of range 0-15 psi, with a sensitivity of 9.5 mv/psi at an excitation voltage of 5 volts. An IIHR-built straingage balance and 5-volt-power supply was used with the transducer. The unbalanced voltage output from the bridge was amplified by a PRESTON D.C. amplifier. The instantaneous amplified output which was proportional to the static pressure was measured using the data acquisition technique described later.

2. Discharge measurements. The time averaged flow rate was measured using the weigh tank. The flow rate was measured by clocking the time required for a preset weight of oil to flow into the weigh tank. Unfortunately, due to the small capacity of the tank, it was necessary to limit the duration of oil collection to 15-20 s only. This resulted in some inaccuracy in the estimate of the flow rate, especially in the unsteady flow experiments. These measurements of flow rate were, however, neither critical nor extremely important in the present study. In fact, the flow rate could be more accurately determined in specific cases by integrating the velocity distribution across the pipe obtained from LDA measurements.

3. Velocity measurements. Velocity measurements in unsteady flow studies reported so far in the literature have been made using either pitot-tubes or hot-wire/film anemometry. These probes have two important disadvantages; (i) they disturb the flow and (ii) they do not allow reversals in velocity to be detected or measured. In addition, the Pitot tube has the added limitations that it cannot measure turbulent intensity nor can it even by used in any except very slowly oscillating flows. One of the most important features of the present study is the use of LDA, a technique that can measure instantaneous flow velocities without disturbing the flow. The LDA has also the additional advantages that its signal is proportional to the velocity and that it does not require calibration against other standards. One can, thus, avoid the calibration drift problems associated with hot-film anemometry in liquids. Reversal of flow can be detected and measured using LDA if a "frequency shift" technique is used. The LDA system used in the present studies used a frequency-shift feature though flow reversal did not actually occur in the range of flows studied. The single channel LDA system of IIHR and the details of the traverse system are described in appendix A.

4. Reference time signal. In the present report, the time history of the flow during the oscillation cycle was studied using the instant of maximum slot opening as the reference ($t = 0$) point in the cycle. As will be seen later, the Data Acquisition System was designed to use this point as the instant at which data sampling should begin. For this purpose

an electromagnetic device was used to produce a voltage pulse at the instant of maximum slot opening once during each revolution of the profile sleeve. (Note that this corresponds to once in every two oscillation cycles). The device included an electromagnetic pick up (1.5 mm) diameter) mounted on the support frame and a thin steel rod (1.5 mm diameter) attached to the motor shaft. The position of the rod was carefully adjusted such that during its rotation the tip passed within 1 mm of the pick up, cutting the magnetic field. The voltage induced in the pick up was used as the reference time signal. The intensity and duration of the pulse would depend upon the diameter of the rod and its rotational speed. The diameter of the rod (1.5 mm) was determined from the requirement that a signal of sufficient strength to drive the Data Acquisition System was to be produced at the lowest speed studied. With this diameter and with the radius of rotation of the rod of about 150 mm, the pulse duration was found to vary from about 2.5 degrees, at the lowest speed, to about 3.5 degrees at the highest speed of rotation. This corresponds to the range 5-7 degrees when referred to an oscillation cycle and represents the overall uncertainty in the reference time signal. The phase angle measurements reported in this study are all subjected to this uncertainty. The angular position of the rod was adjusted such that the rod was aligned with the pick up in the maximum slot opening position. A 360-degree graduated protractor fixed to the plexiglass collection chamber and a pointer attached to the shaft enabled setting up the sleeve at any desired position (θ) relative to the maximum slot opening position ($t = 0$ or $\theta = 0$) in steady flow experiments.

E. Experimental Details

1. General. As already mentioned, two series of experiments were carried out. In both the series, the steady flow had a Reynolds number of about 2900 at maximum slot opening (θ=0°) and a Reynolds number of about 1300 at minimum slot opening (θ=180°). The mean steady flow Reynolds number was about 2100 and this occured at $\theta \cong 90°$. However, in the first series, the steady flow at θ=90° was found to be fully turbulent at all times. In fact, the intermittency of turbulence remained at unity for $\theta \lesssim 100°$. When this flow was oscillated at the highest possible frequency

of 1.75 Hz, the flow remained fully turbulent. Instantaneous velocity measurements were obtained across the pipe for this situation (Run 13). A rough estimate of the turbulent burst frequency in this flow using the criterion of Rao et al, (1971) indicates a value of about 2 Hz. Thus the oscillation frequency can be expected to interact significantly with the turbulent structure in this flow. In the second series of experiments, while the steady flow at the maximum and minimum slot opening behaved exactly as in the first series, the mean flow at $\theta=90°$ exhibited an intermittent turbulent structure. The structure strongly resembled the puff type transitional structure studied by Wygnanski and Champagne (1973). In fact, the steady flow became fully turbulent only at values of $\theta \lesssim 60°$. When this flow was oscillated (at whatever frequency) it was found to laminarize with the intermittency of puffs dropping almost to zero. This is clearly seen from figure 3 where a photograph of the storage oscilloscope traces corresponding to the center line velocity signals obtained from the LDA under three different conditions are shown superimposed on one another. These are: i) steady flow at $\theta=0°$, Re = 2872 (fully turbulent), ii) steady flow at $\theta=180°$, Re = 1278 (fully laminar) and (iii) oscillatory flow at 0.057 Hz between the above two Reynolds numbers (laminarized). The peak velocity in the oscillatory flow is different from the velocity in steady turbulent flow because the steady flow is laminar and hence has a different velocity distribution. Velocity measurements were made in this laminarized unsteady flow at oscillation frequencies of 1.75 Hz (Run 23) and 0.057 Hz (Run 24). These frequencies correspond to Strouhal numbers S (defined as $\frac{2\pi fD}{\bar{U}_m}$) of 1.0 and 0.032 respectively.

In both the series, measurements of velocity distribution in the pipe were made for the steady flows at $\theta=0$ and $\theta=180°$. In addition, steady flow axial pressure drop data were obtained for several (fixed) angular positions, θ of the sleeve. These steady flow experiments can be considered to approximate closely to quasi-steady experiments. They are used as a reference in the study of the unsteady flow behavior. The use of these data instead of steady flow data from other sources is both necessary and desirable in view of the very low Reynolds numbers and transitional nature of the flow.

2. Quasi-steady measurements. One of the features of the present design is that it allows one to make measurements at steady flow conditions corresponding to any desired point on the oscillation cycle. These measurements closely approximate to quasi-steady flow measurements, i.e., measurements obtained in unsteady flow oscillating at infinitesimally low frequencies. These quasi-steady measurements form the basis for studying the effect of flow oscillation at finite frequencies. Quasi-steady measurements were made in both series of experiments. These included:

(1) discharge

(2) pressure drop and

(3) velocity distribution across the pipe.

The discharge measurements were made using the weigh tank and have been already referred to earlier in Section D.2. As mentioned previously, it was found that due to the small collection time used, there was some inaccuracy introduced into the discharge measurements. The discharge data obtained from the weigh tank measurements were compared with the more accurate values obtained from the integration of velocity profiles in the test section and a correction factor for the former was arrived at. This was used for the rest of the discharge data from the weigh tank. These discharge measurements were made for several fixed slot openings (i.e., for several fixed values of θ) in both the experimental series.

The distribution of static pressure along the pipe was measured only in series 2. Pressure drop measurements were made for several values of θ. These pressure measurements were made using the inverted oil manometer mentioned earlier.

The velocity measurements were made in both series. However, they were made only for two values of θ; θ=90° and θ=0° (Runs 11, 12; 21, 22). Further, the velocity profiles were measured at 16 points across the pipe in series 1. In series 2, velocities were measured at a fewer number of points. Since these measurements appeared to reproduce closely the first series of measurements, it was felt unnecessary to obtain data at finer intervals. The velocity measurements were made using the IIHR Data Acquisition System, as described in Section F. Measurements at θ=90° (i.e., in laminar flow) served to check the accuracy of measurement as

well as the quality of flow (axisymmetry) in the pipe by comparing the observation with the theoretical parabolic profile. Measurements in fully turbulent flow ($\theta=0°$) provided the basis for studying the effect of flow oscillation. The turbulent velocity distribution in the pipe at low Reynolds numbers is strongly dependent on the Reynolds number and possibly on the characteristics of the specific experimental apparatus. It is thus necessary to use the quasi-steady measurements in the same apparatus at similar Reynolds numbers in order to make any comparisons with unsteady flow measurements.

3. Unsteady flow measurements. The flow was oscillated at the desired frequency by setting the voltage control of the motor at the appropriate position. The rotational speed (equal to twice the oscillation frequency) was measured by clocking the time taken for 50 revolutions of the sleeve. Several minutes were allowed to elapse after starting the oscillations before the measurements were made. As in the case of quasi-steady flow, velocity measurements were made at 16 points across the pipe. The instantaneous velocity signal from the LDA, was read on to he IIHR Data Acquisition System and processed using the procedure described in section F. The reference time signal from the magnetic pick-up was used as the synchronizing signal in the data acquisition process.

An oscillation frequency of 1.75 Hz was studied in series 1. (Run 13). As already mentioned, the flow was observed to be fully turbulent in this case. At lower frequencies (say <1 Hz), the flow was found to switch intermittently between laminar and turbulent regimes. This was accompanied by large variations in the "mean" velocity of the flow. Hence, it was not possible to make any quantitative velocity measurements under these conditions. In the second series of experiments, the flow remained laminar or nearly laminar at 1.75 Hz (Run 23) as well as at a very low frequency, viz. 0.057 Hz (Run 24). Detailed velocity profiles were obtained at these two frequencies.

4. Intermittency measurements. A careful and extended study did reveal that even in the second series of experiments, the flow did not remain

fully laminar at all oscillation frequencies. It became turbulent intermittently and this intermittency was found to depend on the oscillation frequency. In order to study this aspect in some detail, the velocity signal from the LDA was recorded on a strip chart recorder for a duration long enough to allow one to estimate the intermittency of turbulence from the record. This duration corresponded approximately to 300 cycles or 5 minutes whichever was larger. Such records were obtained for several oscillation frequencies in the range of 0.05 Hz - 1.75 Hz and for two points in the pipe, viz., $r = 0$ mm, and $r = 18.4$ mm.

F. Data Acquisition and Processing. The procedure used in the present study for the analysis of unsteady turbulent flows is based on that used by Nakato (1974) and is essentially similar to that used by many recent investigators of oscillatory turbulent boundary layers. The author considers it to be superior and more informative than the analog procedures used by previous investigators of pulsating flows in arteries or rigid walled-tubes. The analysis can be used in a degenerate form for unsteady laminar flows, steady turbulent and steady laminar flows also. The analysis is briefly described below.

Let the instantaneous velocity $U(y, ,t)$ be written as:

$$U(r,\theta,t) = \bar{U}(r) + U_p(r,\theta) + u(r,\theta,t) = < U(r,\theta) > + u(r,\theta,t) \quad (8)$$

where $\bar{U}$ is the time mean velocity, u is the turbulent (random) velocity, and $<U>$ is the deterministic velocity. The deterministic velocity can be obtained by a process of ensemble averaging. In the present periodic flow, ensemble averaging is equivalent to phase averaging i.e., averaging over the values obtained at identical values of r and θ in a large number of cycles. Thus,

$$< U(r,\theta) > = \frac{1}{N} \sum_{i=1}^{N} U_i(r,\theta,t) \quad (9)$$

where N is the total number of cycles being averaged and U_i is the velocity in the ith cycle. The time mean value $\bar{U}(r)$ is obtained by long time averaging or equivalently by averaging $<U>(r,\theta)$ over a cycle. Thus,

$$\bar{U}(r) = \frac{1}{2\pi} \int_0^2 <U \quad (r,\theta)> d\theta \quad (10)$$

If M descrete samples are taken during a cycle, we can write

$$\bar{U}(r) = \frac{1}{M} \sum_{j=1}^{M} \langle U_j(r,\theta_j) \rangle \tag{11}$$

The random velocity component u is obtained as

$$u(r,\theta,t) = U(r,\theta,t) - \langle U(r,\theta) \rangle \tag{12}$$

The ensemble average value of turbulent velocity u_p' defined by

$$u_p'(r,\theta) = \sqrt{\langle u^2(r,\theta,t) \rangle} \tag{13}$$

is obtained from the process

$$u_p'(r,\theta) = \sqrt{[\frac{1}{N} \sum_{i=1}^{N} u^2{}_i(r,\theta,t)]} \tag{14}$$

and the rms value of turbulent velocity u'(y), defined by

$$u'(r) = \sqrt{\overline{u_p'^2(r,\theta)}} \tag{15}$$

is obtained from the process

$$u'(r) = \sqrt{\frac{1}{M} \sum_{j=1}^{M} u_p'^2(r,\theta_j)} \tag{16}$$

In the present experiments, the Data Acquisition System was programmed to sample the LDA output once at the end of each sampling interval (ΔT), starting from the instant when the synchronizing signal (reference time signal) was received. ΔT was so chosen that 100 $\Delta T \gtrsim$ the period of oscillation. This would ensure that 100 samples could be taken per cycle. However, only 96 samples were taken, no samples being taken at the end of 97th, 98th, 99th, and 100th time intervals. These "holes" in the data were required in order to allow for the fact that the period of oscillation might not be exactly equal to but less than 100 ΔT. It may be noted that with the present program, data would be acquired actually from two consecutive oscillation cycles, the first cycle yielding 50 (No. 1 - No. 50) samples and the second cycle yielding 47 (No. 50 - No. 96) samples. A total of 100 revolutions were used for phase averaging (N = 100) at the higher oscillation frequency. At the lower frequency, 25 revolutions were used. From the sampled data, the various velocities $\bar{U}$, U_p, u', etc were computed according to Eqs (8) through (12). In most cases, the experiments were repeated thrice and the results averaged over the three experiments. If the results in consecutive experiments differed significantly from one

another, the experiments were repeated till three consecutive experiments gave nearly the same results. (Such repititions were, however, rarely necessary). The value of $\bar{U}$ varied insignificantly among consecutive repititions, while the scatter in $\langle U \rangle$ was within 1% and the scatter in u' within 5%. The computer programs in Assembler Language used in the present experiments for both the acquisition and the subsequent processing of the data were developed by Mueller (see Mueller and Ramaprian 1977) from an earlier version developed by Nakato (1974). A listing of the program package used in the present experiments is given in Appendix C. One of the important features of the present program was that it would detect the LDA signal drop-out and reject the samples taken during such a cycle. Data acquisition would then proceed until N valid revolutions were sampled. However, with the use of frequency shift technique, there was virtually no "signal dropout" problem and this feature in the program was never made use of.

The above program package was also used for processing unsteady laminar flows, the value of u' in this case being used as a measure of the noise in the optics and electronics. It was found that u' ranged from 2-5 parts per 1000 in these cases, indicating the acceptability of the experimental procedure. The program package was also used for processing steady flow (laminar and turbulent) data, the quantities $\bar{U}$ and u' being the only quantities sought for in these cases. While experimenting with steady flows, a fictitious synchronizing signal was provided from a square wave generator with a period of approximately 3 seconds. With 100 "cycles" of sampling, this would result in an overall averaging time of 5 minutes.

The unsteady data acquisition program package was also used for the unsteady pressure measurements referred to in section D.1.

III. RESULTS AND DISCUSSION

A. Steady Flow Measurements

1. Axial pressure drop. The nondimensional pressure drop ΔP^* defined by

$$\Delta P^* = (P_A - P)/(1/2\ \rho \bar{U}_{qm}^{\ 2}) \tag{17}$$

is shown in figure 4 for various values of θ (i.e., for various Reynolds

numbers). P_A is the static pressure at an upstream reference point, x=0 (see figure 1). P is the static pressure at a longitudinal location x and ρ is the fluid density. The values shown are from the second series of experiments. The figure shows that mean flow has attained full development at all Reynolds numbers for $x^* = x/D \geq 70$. The quasi-steady friction factor, λ_q is defined in the usual way as

$$\lambda_q(\theta) = -\left[\frac{dP}{dx}(\theta)\ D\right]/\left[1/2\ \rho\bar{U}_{qm}{}^2\right] = \frac{d(\Delta P^*)}{dx^*} \tag{18}$$

and thus, is given by the slope of the lines in figure 4. The values of λ_q at different Reynolds numbers are shown in figure 5. Also shown for comparison are the laminar relation, $\lambda = 64/Re$ and the Blasius relation for low Reynolds number turbulent flows, $\lambda = 0.3165\ Re^{-1/4}$ (Schlichting 1968). The value of $\bar{U}_{qm}$ used in figures 4 and 5 were obtained from discharge measurements made using the measuring tank. Figure 5 is presented to show that the apparatus was functioning as expected and that the flow was transitional.

2. Velocity distribution. The results of velocity measurement at θ=180° (minimum slot opening) and θ=0° (maximum slot opening) are shown in figure 6. In each case, data obtained in both the series of experiments are shown even though fewer points are shown for series 2. This is considered adequate in view of the excellent repeatability observed between the two series of steady flow experiments. In the case of laminar flow (θ=180°), the data are seen to agree well with the theoretical parabolic profile. This good agreement, however, has been obtained, as already mentioned, by applying a constant "zero correction" to the apparent location of the measurement point. The adjustment is justified by the fact that a constant zero correction brings the measured profile in agreement with the parabolic profile. The same correction was applied to the turbulent flow (θ=0°) measurements also. It is seen from the figure that the mean velocity profiles in turbulent flow obtained from the two series of experiments also indicate agreement with each other. The agreement between the two sets of data obtained with a gap of several months in between establishes the accuracy of the measurement procedure. It also confirms that the behavior of the

quasi-steady flow at both the maximum and minimum end of the oscillation cycle did not change even though the transitional character at intermediate Reynolds numbers had changed.

The velocity profile for the turbulent flow at $\theta=0°$ is shown in figure 7 in the usual wall layer coordinate U^+ $(=\bar{U}/u_*)$ vs. $Y^+[=(D/2-r)u_*/\nu]$ u_* being the shear velocity, $\sqrt{\tau_w/\rho}$ where τ_w is the wall shear stress. The value of u_* was obtained from the quasi-steady pressure drop and discharge data for $\theta=0°$ using the relation,

$$\lambda_q = \frac{1}{8}\frac{u_*^2}{U_{qm}^2} \tag{19}$$

The measured velocity distribution is compared with the universal law of the wall, namely $U^+ = Y^+$ in the viscous sub-layer and $U^+ = 5.75 \log Y^+ + 5.5$ in the fully turbulent region. The deviation of the experimental data from the universal log law is to be expected in view of the very low Reynolds number of the flow. On the other hand, the fact that the first data point near the wall falls on the linear $U^+ = Y^+$ curve indicates not only that this point is in the viscous sub-layer but also that the value of u_* and r are accurate.

3. Turbulence intensity distribution. Figure 6 introduced earlier, also shows the distribution of the rms intensity, u' of the longitudinal turbulent velocity fluctuations in the steady turbulent flow at $\theta=0$. The distribution is normalized using the velocity and length scales, u_* and D/2 respectively. Consequently, the distribution can be expected to show Reynolds number dependence in the inner region. This is, in fact, the case as is seen from the comparison with the data of Laufer (1954) obtained at a Reynolds number of 5×10^5. The distribution in the region $0.5 < (1-2r/D) < 1$ seen to coincide reasonably well with Laufer's data while in the region $(1-2r/D) < 0.5$, a strong Reynolds number effect is observed. In fact, the large viscous region in the present case allows one to observe the gradual decrease of u' from a maximum towards zero at the wall, a feature which is usually difficult to observe in higher Reynolds number laboratory flows. The purpose of presenting the steady flow

turbulence distribution in figure 6 is to provide a basis for the comparison with the unsteady turbulent flow data. It is clear that it is very important to make comparisons in approximately the same Reynolds number range in order to arrive at reliable conclusions.

B. Velocity Distribution in Unsteady Flow. Figure 8 shows the distribution of the time-averaged velocity $\bar{U}$ across the pipe in the three runs 13, 23, and 24. The velocities, in each case, are normalized with respect to the corresponding velocity at the pipe axis ($\bar{U}_{max}$). The distributions are compared with the quasi-steady velocity distributions corresponding to θ=180° and θ=0°. It is seen from the figure that the unsteady flows in run 23 and run 24 that appeared to be laminar were, indeed, very nearly laminar i.e., they exhibit nearly parabolic velocity distributions. In fully developed oscillatory laminar pipe flow of a Newtonian fluid, the time-mean velocity distribution should be identical to that of the steady Poiseuille flow since the velocity field is determined from the linear equation

$$\frac{\partial U}{\partial t} = -\frac{1}{\rho}\frac{\partial P}{\partial x} + \nu\left[\frac{\partial^2 U}{\partial r^2} + \frac{1}{r}\frac{\partial U}{\partial r}\right] \qquad (20)$$

It is seen that, in the high frequency run 23, in which the intermittency of turbulent puffs was negligibly small (see figure 23), the time-mean unsteady flow behaves almost exactly like laminar flow. The deviation of the experimental data of run 24 from the parabolic profile has been caused by the flow becoming turbulent with a larger intermittency than in run 23. It is, however, important to observe from figure 8 that the effect of flow oscillation on the time-mean velocity gradient and hence the wall shear stress, is negligible in both these runs.

When the oscillatory flow is turbulent, the total shear stress (τ) distribution in the pipe is given by the linear equation

$$\frac{\partial U}{\partial t} = -\frac{1}{\rho}\frac{\partial P}{\partial x} + \frac{1}{\rho r}\frac{\partial(\tau r)}{\partial r} \qquad (21)$$

and hence the distribution of time averaged shear stress, $\bar{\tau}$ is now given by

$$\bar{\tau}/\rho = \nu\frac{\partial \bar{U}}{\partial r} - \overline{uv} \qquad (22)$$

(where u and v are the turbulent velocity fluctuations in the x and r

directions, respectively), the velocity field is not determined by a linear equation. The time averaged velocity distribution, and hence the time averaged wall shear stress need not, therefore, be necessarily the same as in the steady flow at the mean Reynolds number. It is, in fact, seen from figure that the time-mean velocity distribution in the unsteady turbulent flow of run 13 exhibits a point of inflection near the wall and thus differs from the steady state turbulent velocity profile. The time mean velocity gradient at the wall is slightly larger than in the steady case resulting in a larger time-mean wall shear stress. This observation differs from those reported by previous investigators of oscillatory turbulent boundary layers, who concluded that unsteadiness has no effect on the time-mean properties (or even the turbulent structure) of the flow. However, as already mentioned, a significant difference between the present experiment and the earlier experiments is that the oscillation frequency in the present case is comparable to the characteristic turbulent frequency.

Figure 9 presents the variation of the periodic component U_p of the velocity through the oscillation cycle at a few typical points across the pipe. The velocity is normalized with respect to the amplitude $(U_{qmp})_{max}$ of the quasi-steady cross sectional average periodic velocity. The variations are shown only for 700 degrees of oscillation cycle, short record gaps being present (for reasons mentioned earlier) from 0 - 7.2° and 698.4 - 720°, i.e., a total of 4 sampling periods. For run 13, the data are shown only for 600 degrees of oscillation cycle, due to some difficulties encountered during data acquisition. These difficulties were subsequently removed before the second series of experiments were started. However, since data over only 360 degrees of oscillation cycle are sufficient for the purpose of analysis, the loss of redundant data is not serious. In each of the figures 9 (a), (b), (c), the distributions of the unsteady cross sectional average periodic velocity, U_{mp} and quasi-steady cross sectional average periodic velocity, U_{qmp} (proportional to the effective modulation in exit area) are also shown for comparison. The latter curve is the same as the periodic part of the velocity distribution shown in figure 2. A comparison of the laminar flow data for runs 23 and 24 shows that the phase-wise variations are strongly dependent on the oscillation frequency. The variations

appear to be very nearly sinusoidal at the lower frequency while significant distortion in the wave shape can be observed at the higher oscillation frequency. The distortion at the higher frequency is, as mentioned earlier, due to nonlinear effects.

It is also clear from the figures 9 (a), and 9 (b), that at the higher oscillation frequency, there is a significant phase shift between the velocity variation and the exit area opening. Most of this phase shift is brought about by the global dynamics of the system and is observable as the phase shift of unsteady cross sectional average flow. However, there is also a relative phase shift between the local velocity and the cross sectional average velocity. The flow in the wall region leads the cross sectional average flow while the flow in the core region lags behind the average flow. Unfortunately, owing to the uncertainty in phase angle measurement ($\pm 3.5°$) and the distortion in the modulation profile, it is not possible to make a precise quantification of the phase differences nor is it possible to look for differences between the laminar and turbulent flow.

Figures 10 (a), (b), and (c) show cross plots of the distribution of the periodic velocity, U_p across the pipe for a few typical fixed phase angles in the oscillation cycle. It is seen that at the higher oscillation frequency, the variations in U_p are confined essentially to $\eta = (1-2r/D) \leq 0.25$ (i.e., the Stokes layer), the rest of the flow oscillating virtually as one solid mass at all times. At the lower frequency, U_p varies across the entire pipe at all times. The responses of turbulent and laminar flows appear to be qualitatively similar.

Figure 11 shows the distribution of the "amplitude", $(U_p)_{max}$ of the periodic velocity across the pipe for the three experiments. Since the velocity modulation is distorted from a sine wave especially at the higher frequency, it is not strictly appropriate to use the term "amplitude" without making a formal harmonic analysis. However, in the present case, $(U_p)_{max}$ denotes one half of the peak to peak variation in the periodic velocity U_p. In the figure $(U_p)_{max}$ is normalized with respect to the amplitude $(U_{mp})_{max}$ of the cross sectional average periodic velocity. It is more clearly seen from this figure that at the higher frequency, the amplitude variations are confined to a small region($\eta \lesssim 0.25$) near the wall while at the lower frequency the variations extend over the entire pipe cross section.

Also, it is seen that an overshoot occurs in the amplitude distribution. The dominant effect of oscillation frequency is clearly seen from this figure. At the same time, it is possible to notice, in this figure, a difference between the responses of laminar and turbulent flow in the near-wall region. The turbulent flow data of run 13 exhibit a larger overshoot than the laminar flow data of run 23. Also shown in the figure are the results computed from the exact solution of Uchida (1956) for fully developed laminar periodic flow in a pipe under the influence of a pressure gradient sinusoidally varying with time. The pressure gradient variation in the present experiments at the higher frequency differs significantly from that assumed in Uchida's analysis. The experiment at the lower frequency, however, approximates closely to the theoretical case. The data for this experiment are seen to agree reasonably well with the exact solution, any apparent discrepancy being possibly due to the intermittency effects mentioned earlier.

Lastly, the distribution of the ensemble average velocity $\langle U \rangle$ at prescribed phase angles are shown in figures 12 a, b, and c, for a few typical points in the oscillation cycle, for each of the runs. The distribution of the time-mean velocity, $\bar{U}$ is also shown, in each case, for comparison. The velocities are normalized with respect to the time-mean velocity at the center line ($\bar{U}_{max}$) corresponding to each run. The distributions at the higher frequency indicate simple displacement but very little distortion from the shape of the time-mean profile in the core region. Near the wall, (in the Stokes layer) however, the profiles cross over and suffer some distortion. However, no reverse flows were observed in the present experimrnts. At the lower frequency, the different profiles of $\langle U \rangle$ show distortion with respect to the time mean profile across the entire pipe because of the variation of both the amplitude and phase angle of the periodic velocity continuously across the pipe.

C. Effect of Flow Modulation on Turbulence and Transition

1. General. The data obtained in the two series of present experiments provide some insight into the effects of impressed unsteadiness on the structure of turbulence and transition in pipe flow. For convenience, the two series of experiments will be discussed one by one.

2. Results of Series 1 experiments (turbulent unsteady flow): The distribution of the rms turbulent intensity u', normalized with respect to $\bar{u}_*$[1] is shown in figure 13. Comparison with the steady flow data for $\theta=0$ shows that in the oscillatory flow there is a slight decrease in the maximum turbulence intensity near the wall, while the turbulence intensity farther away from the wall is not affected. The near-wall region where the turbulent intensity is affected extends approximately over 25 per cent of the pipe radius and this region coincides with the Stokes layer where significant effects of flow oscillation are observed on the time-mean and periodic structures of the flow also. This result is in agreement with the conclusions of Acharya and Reynolds (1975) that the structure of turbulence is primarily affected within the Stokes layer. The distributions of the ensemble averaged turbulence intensity $u'_p(\theta)$ normalized with respect to the corresponding shear velocity $u_{*p}(\theta)$ are also shown in figure 13 for a few typical fixed phase angles of the oscillation cycle. Large variations in the distributions from one another and from the distribution of $u'/\bar{u}_*$ indicate that the turbulence structure is highly disturbed from equilibrium. The variations in the relative turbulent intensity (u'_p/u_{*p}) with time are shown in figure 14 for two typical locations across the pipe. These figures suggest that the flow was undergoing rapid structural distortion in time. Actually, the wall shear stress (u_{*p}) could nearly follow the changes through the discharge cycle while the turbulent u-fluctuations could not. This is seen clearly from figure 14 which also shows the variation of u_{*p} and the variation of u'_p (not normalized) at these two typical points in the pipe. It is seen that u_{*p} oscillates with a slight phase lead with respect to the cross sectional average periodic velocity U_{mp}, while u'_p remains

---

[1] The shear velocity $u_{*p}(\theta)$ in unsteady flow was obtained from the ensemble average velocity gradient at the wall. The velocity gradient at the wall was calculated from the measured $\langle U(\theta)\rangle$ at the first point near the wall assuming a linear velocity distribution in the viscous sublayer at all instants. This procedure was found to be generally satisfactory as verified from checks made in steady laminar and turbulent flow. In these cases, the wall shear stress obtained by this method compared well (within 3%) with the value obtained from pressure drop measurements. From the ensemble averaged value u_{*p}, the time averaged value $\bar{u}_*$ was obtained from the discrete analog of the relation,

$$\bar{u}_*^2 = \frac{1}{2\pi}\int_0^{2\pi} u_{*p}^2 \, d\theta$$

practically constant throughout the oscillation cycle. Such a freezing of the turbulent normal stress can be expected to occur when the flow is subjected to rapid strain rates, i.e., when changes occur at time scales comparable to some important characteristic time scale of turbulence. In a wall-bounded flow, we can regard the turbulent burst frequency, f_t to determine such a characteristic time scale (at least near the wall). In the present case the estimated burst frequency is about 2.3 Hz, (using the criterion $\frac{U_m}{f_t D} \cong 5$ of Rao et al 1971). The estimate is rough but is sufficient to indicate that one can expect to find interaction between the external oscillation and the internal turbulence structure when the flow pulsates at a frequency of 1.75 Hz. Stress-freezing is well documented in rapidly accelerated steady flows but studies of rapidly decelerated steady flows are difficult to perform, since the flow in such cases would separate very quickly. One of the interesting features of the present experiments is that the flow experiences large pressure gradients of alternating sign but yet does not actually separate. An estimate of the severity of the pressure gradient in the present case can be made by calculating the value of the Clauser pressure gradient parameter β defined by (neglecting the shear effects),

$$\beta = \frac{D}{2\rho u_*^2} \frac{\partial P}{\partial x} \approx \frac{D}{2u_*^2} \frac{dU_m}{dt} \tag{23}$$

Such a calculation shows that β varies from about -40 to about +40 during a cycle. The magnitudes of β attained during the cycle are comparable with the values for some of the severe adverse pressure gradient steady flows reported in the Proceedings of the Stanford Conference (Coles and Hirst 1978). Not only are the pressure gradients very large but they vary rapidly, the value of $d\beta/dt$ being of the order of 100 sec^{-1}, (based on a variation in β from 40 to -40 in half the period of oscillation). It is thus clear that the turbulent structure will be in a highly disturbed state. Hence, quasi-steady turbulence models based on local equilibrium assumption cannot be expected to describe the flow at such oscillation frequencies.

The quantity which is of greater value than u' in understanding the structure of turbulence is the Reynolds shear stress $- \rho \overline{uv}$. Unfortunately,

on account of instrumentation limitations, it was not possible to make direct measurements of the Reynolds shear stress. However, it is possible to compute it, perhaps with some loss of accuracy, from the measured wall shear stress and velocity distribution. For this purpose, we write the instantaneous x-momentum equation for pipe flow as

$$\rho \frac{\partial U}{\partial t} + \rho U \frac{\partial U}{\partial x} + \rho V \frac{\partial U}{\partial r} = - \frac{\partial P}{\partial x} + \frac{1}{r} \frac{\partial(\tau r)}{\partial r} \qquad (24)$$

where V is the instantaneous velocity in the radial direction. Performing an ensemble average on this equation, one gets, for fully developed unsteady turbulent flow,

$$\rho \frac{\partial \langle U \rangle}{\partial t} = - \frac{\partial \langle P \rangle}{\partial x} + \frac{1}{r} \frac{\partial \langle (\tau r) \rangle}{\partial r} \qquad (25)$$

$$\text{where } \langle \tau \rangle = \tau_{laminar} - \rho \langle uv \rangle \qquad (26)$$

We define $- \rho\langle uv \rangle$ as the ensemble averaged Reynolds shear stress. Mutliplying both sides of the equation (25) by $2\pi r$ and integrating across the pipe, one gets (after inserting the phase average notations introduced earlier)

$$\rho \frac{\partial U_m(\theta)}{\partial t} = - \frac{\partial \langle P \rangle}{\partial x}(\theta) + \frac{4\tau_w(\theta)}{D} \qquad (27)$$

Eliminating $\frac{\partial P}{\partial x}$ between equations (25) and (27) one gets

$$\frac{\tau}{\rho}(r,\theta) = \frac{1}{r} \int_0^r \frac{\partial}{\partial t} [\langle U(r,\theta) \rangle - U_m(\theta)] \cdot r \, dr + \frac{2\tau_w(\theta) r}{D} \qquad (28)$$

and

$$-\langle uv \rangle (r,\theta) = \frac{\tau}{\rho} (r,\theta) - \nu \frac{\partial \langle U(r,\theta) \rangle}{\partial r} \qquad (29)$$

The ensemble (phase) averaged Reynolds shear stress $-\langle uv \rangle$ was obtained from Equations (28) and (29) using measured velocity and wall shear stress data. The process required differentiation with respect to time and integration across the pipe both of which were performed numerically on a computer. The velocity-time data were smoothed in order to reduce the numerical noise in differentiation. The procedure was found to work reasonably well because the velocity values were available at very close time intervals (50 values per cycle), velocity gradients in the radial direction were not severe (due to the low Reynolds number of the flow), sufficient cycles were used for phase averaging (effectively 300) and lastly, the three terms in equation (28) were all of similar order of magnitude.

Variation of the ensemble averaged Reynolds shear stress during the cycle is shown in figures 15 a, b, c for three typical locations in the pipe, viz; 1, 2 and 10 mm from the wall. Although there is some scatter in the data, the results are still good enough to allow one to arrive at meaningful conclusions especially in the region of flow where the Reynolds shear stress is significant. Very near the wall, $\langle uv \rangle$ shows a cylical variation but lags behind U_m (and hence behind u_{*p} also). As the distance from the wall increases, the amplitude of variation of $\langle uv \rangle$ decreases until it becomes almost indistinguishable from scatter beyond the Stokes layer (as seen from figure 15c). The well-defined cylical variation of $\langle uv \rangle$ in the inner layer (figures 15 a, b) is in contrast to the frozen structure of u'_p. This suggests that the modulation in $\langle uv \rangle$ might have originated from modulations in the ensemble averaged intensity, v'_p. This is possible since the v-fluctuations are likely to be of finer scale than the u-fluctuations (by a factor of nearly 5 as observed by Ramaprian, 1975) and hence can respond more readily to the impressed oscillations. Since the time scale gets larger as the distance from the wall increases, the response of $\langle uv \rangle$ must be expected to diminish eventually in the core region. The nearly frozen structure of $\langle uv \rangle$ in the core region (figure 15c) thus indicates rapid strain rates. The departure from local equilibrium is again seen from the variations in $\langle uv \rangle/u_{*p}^2$ during the oscillation cycle.

Figure 16 a, b, c, and d are cross plots of the above data and show some typical distributions of the total, laminar and ensemble averaged Reynolds shear stresses, across the pipe for fixed phase angles during the cycle. The distributions are normalized using the relevant inner layer scales of velocity, (u_{*p}) and length, (ν/u_{*p}). The large variations in the distribution of the stresses from one point in the cycle to the other (seen more clearly from these figures) again indicate that the turbulence structure is far from equilibrium and hence cannot be described by quasi-steady models. Figure 17 shows the time averaged distributions of each of the above stresses using $\bar{u}_*$ as the scaling velocity. These distributions were obtained by averaging the computed distributions at 50 phase positions in the cycle. It is seen that except for a slight discrepancy near the wall, the time-averaged total shear stress $\bar{\tau}$ shows the expected

linear distribution. This indicates that there were no significant errors in the numerical procedure used for calculating the shear stresses from the experimental data. Some of the important features pertaining to figures 16 and 17 that require comments are:

(i) The laminar shear stress is significant upto a considerable distance from the wall. This is to be expected in view of the low Reynolds number of the flow.

(ii) The time averaged turbulent shear stress reaches a maximum at about 6 mm (η=0.25) from the wall i.e., at about the same location where u' reaches a maximum. It is important to note that this is within the Stokes layer.

(iii) The time averaged laminar shear stress distribution exhibits a local minimum near the wall. This is due to the presence of a point of inflection in the time-mean velocity profile.

(iv) The distribution of the time-mean Reynolds shear stress also exhibits a kink within the Stokes layer. Also, it is observed that, in the region very close to the wall, the time-mean Reynolds shear stress attains a value larger than in steady flow.

(v) The time-mean distributions of the stresses are not significantly different from the corresponding distributions in steady flow, in the region beyond the Stokes layer. However, by affecting the distributions within the Stokes layer, the imposed unsteadiness produces an increase in the time-mean velocity gradient at the wall and hence increases the wall shear stress. This is seen from figures 14 a, b, where the quasi-steady time-mean value, u_{*qm} (obtained from pressure drop measurements at the mean Reynolds number of 2100) is shown as a horizontal dashed line against the distribution of u_{*p} in unsteady flow. The time-mean value of u_{*p} is clearly larger than the quasi-steady mean value of u_*.

Figure 18 shows a few typical distributions of the ensemble average velocity <U> in the inner layer co-ordinates $\langle U\rangle/u_{*p}$ vs $(D/2-r)u_{*p}/\nu$. The time-mean distribution $\bar{U}/\bar{u}_*$ vs $(D/2-r)\bar{u}_*/\nu$ is also shown in the figure.

The data display exactly the trend that one would expect to see. In the region very close to the wall $y^+ < 10$, the ensemble average velocity scales with the corresponding u_{*p} but at larger distances from the wall, the flow structure does not keep in step with u_{*p} and hence the data at different phase angles exhibit different distributions. It is also important to note that there is a net difference between time averaged velocity distribution in the unsteady flow (shown by open circles) and the velocity distribution in steady flow (shown by the full line). This difference is seen more clearly in this figure than in figure 8, discussed earlier.

The quantity, $E_p = \int_0^R \{<\tau> \frac{\partial <U>}{\partial r}\} 2\pi\, r\, dr$ represent the rate of work done per unit length of pipe by the shear stress and hence its average value over an oscillation cycle represents the power loss in the pipe. The term E_p normalized with respect to $(\rho \bar{U}^3_{qm} \pi D/4)$ is shown in figure 19 as a function of the phase angle. The corresponding power loss in a hypothetical quasi-steady turbulent flow can be obtained for the same Reynolds number modulation using the Blasius relation, $\lambda = 0.3165\, Re^{-\frac{1}{4}}$. Also, for the actual transitional quasi-steady flow, the power loss for the same Reynolds number can be obtained from the quasi-steady pressure drop data of figure 4 (or alternately the friction factor data of figure 5). Both these distributions are also shown in figure 19. It is seen that flow oscillation in run 13 at a high frequency results in an increase in average power loss when compared with the quasi-steady transitional flow. This is, however, to be expected since the unsteady flow is fully turbulent during the entire cycle, whereas the quasi-steady flow is not. However, it is interesting to observe that the unsteady flow has a slightly higher average power loss when compared to the hypothetical fully turbulent quasi-steady flow also.

3. Results of Series 2 experiments (laminarized unsteady flow)

During the second series of experiments, the unsteady flow remained nearly laminar. Since this was a very significant observation, it was carefully verified to insure that the laminarization was not due to any obvious reasons such as an increase in fluid viscosity, reduction in flow velocity, etc. Starting from a fully turbulent flow at the fully open slot position, the flow could be laminarized by just rotating the sleeve at the lowest possible speed (0.057 Hz). The photographs in figure 20 show a few typical

oscilloscope traces obtained from the LDA at several oscillation frequencies and include data from two radial locations, r = 0 and r = 18.4 mm. In each photograph, three traces are shown: (i) fully turbulent steady flow at θ=0 corresponding to a Reynolds number of about 2900, (ii) fully turbulent laminar flow at θ=180°, and (iii) fully or partially laminarized oscillatory flow. The photographs generally confirm that the oscillatory flow had a strong tendency towards laminarization under the operating conditions of the series 2 experiments.

A careful study of the traces at several oscillation frequencies indicated that laminarization was not always complete, and that the oscillatory flow did, in fact, become turbulent at times (as seen in some of the photographs in figure 20). The intermittency of this occurence depended on the oscillation frequency. In order to make a more detailed study of this phenomenon, several long-time records of the LDA signal were obtanined using a strip chart recorder. The record length in all the cases was equal to 300 cycles or 5 minutes whichever was longer. Records were obtained for r = 0 and r = 18.4 mm. Similar records were obtained in quasi-steady flow for comparison. A few typical records are shown in figures 21 and 22. It is seen that the flow does become turbulent several times during the duration of the record. Estimating the intermittency of turbulence from such records is no doubt difficult and subjective; particularly when turbulent and oscillation frequencies are not well separated. The following procedure was arbitrarily selected for making a rough estimate of the intermittency. The procedure is based on the observation (and assumption) that whenever the flow became turbulent, its velocity level would jump upwards or downward from the laminar value depending on whether the point under consideration was in the wall region or on the centerline. In both the cases, a distortion would be observed in the velocity signal recorded on the strip chart. The dynamic response of the recorder (5 Hz) was adequate for indicating this distortion. A short length of the laminar record traced out on a transparent sheet would be moved over the record and portions of the record that did not coincide with the laminar record would be marked out as turbulent intervals. The intervals marked T in the photographs of figure 22 correspond to typical turbulent intervals. The intermittency factor, γ was defined as the ratio of the total turbulent interval to the

total record length. In the case of steady flow, the turbulent intervals could be easily recognized without much ambiguity.

The intermittency factor is plotted in figure 23 for quasi-steady flow as a function of quasi-steady Reynolds number. It is seen that the mean quasi-steady flow (θ=90°, i.e., Re $\cong$ 2100) has an intermittency of about 0.2. The intermittency factor for oscillatory flow is shown in figure 24 as a function of oscillation frequency. A parameter often used in characterizing laminar oscillatory pipe flows is Ω defined as $[D/2\sqrt{\frac{2\pi f}{\nu}}]$. It is seen that Ω is proportional to the ratio of the pipe radius, to the thickness of the Stokes layer. The values of Ω are also shown in figure 24. The data for unsteady transitional flow show some interesting trends. The intermittency is very low at either end of the frequency range studied (Ω=4-22). However, it increases fairly significantly and appears to reach a maximum around an oscillation frequency of about 0.4 Hz ($\Omega \cong 12$). This maximum intermittency factor attained, is not very small, and, at r=18.4 mm, is indeed comparable to that of the mean quasi-steady flow. Lastly, the data indicate different values for intermittency near the wall and at the center. It is interesting to note that Yellin (1966) also observed that when transition occurred in pulsatile flows, the disturbances were typically restricted to the core. However, the authors have no explanation at this time for this behavior of the flow. The other aspects of transition in oscillatory flows are examined in some detail below.

Wygnanski and Champagne (1973) have reported detailed study of the steady transitional pipe flow. They divide intermittent transitional turbulence into two categories - the "puff" type and the "slug" type. Puffs are caused by large disturbances at the inlet region of the pipe and are actually remnants of a partial relaminarization process. Slugs, on the other hand, originate from the instability of the boundary layer and represent various stages of amplification of these disturbances. The puffs usually occur in the Reynolds number range of 2000-2700 while the slugs appear generally at very much larger Reynolds numbers. The intermittency measurements in steady flow in the present case are compared in figure 23 with the puff flow data from Wyganski and Champagne. The qualitative agreement between the two sets of data suggests that the present transitional flow can be regarded as a 'puff' type flow. This is further borne out by the

fact that the turbulent puffs are of approximately the same intensity near the wall as at the center line (as seen from the strip chart record), unlike a slug type flow which is known to exhibit an increase in intensity from the centerline to the wall. It may be noted also that the flow is fully turbulent at about Re = 2700.

The development of turbulence through a puff-type transition process does not depend on shear layer instability near the pipe wall since the disturbance is provided by the inlet conditions but depends on the existence of a Reynolds number above a critical value so that the initial turbulence can be sustained. This threshold critical value is about 2000 and transition to turbulence can not occur below this Reynolds number. In a flow subjected to a favorable pressure gradient, this critical Reynolds number is known to increase. But, in an adverse pressure gradient, it will not decrease significantly below the threshold value. Hence, if the Reynolds number of flow oscillates around 2000, the net effect would be an increase in the critical Reynolds number and hence a partial or complete laminarization of the initial turbulent puffs. The increase in the critical Reynolds number will be larger at larger favorable pressure gradients and hence one would expect to find a greater degree of laminarization as the oscillation frequency increases. This is, exactly what is observed in figure 24 as a decrease in the intermittency in the range of 0.4 Hz - 1.75 Hz (Ω=12-22) with the flow being almost completely laminar at 1.75 Hz. The existence of a maximum intermittency (almost equal to the intermittency in the mean steady flow) at about 0.4 Hz ($\Omega \cong 12$) appears somewhat to contradict the above argument. It is, however, important to note that at low frequencies, (0 - 0.4 Hz), (Ω = 0-12) the favorable pressure gradients are very small (at the amplitude of modulation employed) and consequently, the effect on the critical Reynolds number is negligibly small at these frequencies. On the other hand, the extent of laminarization of the puffs depends not only on the critical Reynolds number but also on the length of time in a cycle the puffs are exposed to a Reynolds number lower than the critical Reynolds number. At low frequencies the latter effect becomes dominant and since the residence time of the puffs below the critical Reynolds number increases as the oscillation frequency is reduced, the intermittency of puffs would

decrease with frequency in this range. The results in this range agree qualitatively with those of Sarpkaya (1966) whose experiments extended over the range Ω = 4-7.8. He found that at small amplitudes of modulation (λ = 0.2 - 0.3) there was only a slight increase in critical Reynolds number above the steady state value and that increase in the oscillation frequency in this range reduced the rise in critical Reynolds number. Sarpkaya noticed negligible effect of oscillation on the transition characteristics at Ω = 7.8 (which, incidentally, he regarded as 'rapid' oscillation). It is interesting to note that at about 0.4 Hz corresponding to $\Omega \cong 12$ the present unsteady flow exhibits the maximum intermittency. The present observations are thus in qualitative agreement with those of Sarpkaya. There is, however, quantitative disagreement between the present data and those of Sarpkaya with respect to the actual magnitudes of the critical Reynolds number at the various values of Ω. This is due largely to the difference between the definitions of critical Reynolds number used in the two cases. In the present case, the critical Reynolds number is taken to be the Reynolds number at which the puffs (external disturbances) disappear whereas Sarpkaya defined it as the Reynolds number at which the external disturbances cease to amplify. It is thus clear that the present definition describes the lower bound for the puff-type transition process.

The major difficulty with studies connected with puff-type transition is that the process is very sensitive to the nature of external disturbances and other ambient conditions. It is thus very difficult to find repeatability in observations over a period of time. This is especially true when an additional factor, namely flow oscillation, is introduced. This has been clearly demonstrated by the two series of experiments reported in this paper. The two series gave entirely different results under what apparently appeared to be identical conditions. It is worth examining the reasons for this at least in a qualitative way. As mentioned already, the mean steady flow (θ=90°) was fully turbulent in the Series 1 experiments. In fact, it was fully turbulent even at θ=100° (corresponding to Re$\cong$2000). Unfortunately, intermittency measurements were not made in these series. However, one can visualize (without much error) the intermittency variation with Reynolds number to be as shown in figure 23. It is very clear that

in this flow, transition occurred within a very narrow range of Reynolds numbers, unlike in the second series of experiments in which it was spread over a much wider range of Reynolds numbers. The reason for this is not known with certainty but a reasonable guess is as follows. The first weries of experiments were conducted in summer during which time, the laboratory temperature was about 30°C while the fluid temperature remained at about 26°C. Since the pipe was not insulated, there was heat transfer from the ambient to the fluid. This would aid the process of transition. On the other hand, the second series of experiments were conducted in winter when the laboratory temperature was around 20°C while the fluid temperature still remained at 26°C. There was, thus, a heat transfer from the fluid to the surroundings. This loss of energy to the surroundings would reduce the energy available for producing and completing the transition and hence would tend to stabilize the flow.

The two intermittency distributions shown in figure 23 for the two series can be used to explain qualitatively the observed difference in response of the flow to oscillate at a high frequency in the two cases. Flow oscillation at a high frequency would raise the critical Reynolds number from its value of about 2000 at quasi-steady state by an amount, say, ΔRe. This is equivalent to moving the operating line, i.e., mean flow Reynolds number of the unsteady flow to the left by ΔRe in figure 23. It is seen that in the series 2 experiments, the new operating line corresponds to a laminarized flow (of very small intermittency) while in the series 1 experiments, it corresponds to fully turbulent flow (of intermittency 1). It is to be mentioned here that laminarized oscillatory flow can be observed only under very restricted conditions. These include puff-type transition (i.e., transition brought about by inlet disturbances), a relatively small intermittency of puffs at the mean Reynolds number and either strong pressure gradient fluctuations (high frequency, large amplitude oscillation) or large puff-residence time (long enough pipe). These conditions are often found in the pulsatile flow of blood in the mammalian aorta and hence laminarization of the flow can be expected to occur in such cases. This is, in fact, corroborated by some of the recent in-vivo aorta experiments mentioned at the beginning of this paper.

IV. CONCLUSIONS

The present study has lead to the following conclusions:

(i) Periodic oscillation of discharge tends to increase the critical Reynolds number of puff-type transitional pipe flow. Under certain conditions, the transitional flow may be laminarized on periodic oscillation. For a given amplitude of flow modulation the extent of laminarization depends on factors such as the intermittency of puffs in the quasi-steady mean flow, the oscillation frequency and the residence time of the puffs in the pipe.

(ii) The laminarized periodic flow behaves very much like laminar periodic flow. For example, the time-mean flow properties remain unchanged from those of quasi-steady mean flow and the phase lag and amplitude of the periodic velocity component depend strongly on the Strouhal number.

(iii) When the oscillatory flow is fully turbulent, its time mean and periodic structure qualitatively resemble those of oscillatory laminar flow at the same Strouhal number. However, the behavior of the oscillatory turbulent flow is also influenced by an additional parameter, namely the ratio of the oscillation frequency to some characteristic frequency of turbulence. When this ratio is of the order unity, the oscillations interact with the turbulent structure. Important differences can be observed between laminar and turbulent flows at such oscillation frequencies. For example, the time-mean velocity profile in the oscillatory flow exhibits a point of inflection near the wall, and the time mean wall shear stress and power loss increase from their quasi-steady values. Also, the periodic velocity component exhibits an overshoot in the Stokes layer, the magnitude of the overshoot being larger than in laminar oscillatory flows at the same Strouhal number.

(iv) At the interactive frequency of scillation, mentioned above, the ensemble averaged turbulence intensity is frozen everywhere in the pipe. The ensemble averaged Reynolds shear stress is able to follow the oscillation cycle (with some lag) only very close to the wall. However, beyond the Stokes layer, it is also frozen at some average value. The stress freezing

is brought about by the large and rapidly varying strain rates. The ensemble averaged Reynolds stresses as well as the ensemble averaged velocity do not scale with the corresponding ensemble averaged wall shear stress indicating significant departures from local structural equilibrium.

REFERENCES

Acharya, M. and Reynolds, W.C. (1975). Measurements and predictions of a fully developed turbulent channel flow with imposed controlled oscillations. Stanford University Thermosciences Division, Tech. Report No. TF-8.

Cousteix, J., Desopper, A., and Houdeville, R. (1977).. Structure and development of a turbulent boundary layer in an oscillatory external flow," Proceedings of Symposium on Turbulent Shear Flows, Penn State University, University Park, Pa.

Falsetti, H.L., Kiser, K.M., Francis, J.P., and Belmore, E.R. (1972). Sequential velocity development in the ascending aorta of the dog. Cir. Research 31, pp. 328-338.

Gerrard, J.H. (1971). An experimental investigation of the pulsating turbulent flow in a water tube. Journal of Fluid Mechanics, 46, Pt. 1, pp. 43-64.

Hino, M., and Sawamoto, M. (1975). Linear stability analysis of an oscillatory flow between parallel plates. Proceedings of the Seventh Symposium on Turbulence (ed. Sato, H., and Ohji, M.) Institute of Space and Aeronautics, University of Tokyo, pp. 1-7.

Hino, M., Sawamoto, M., and Takasu, S. (1976). Experiments on transition to turbulence in oscillatory pipe flow. Journal of Fluid Mechanics, 75, Pt. 2, pp. 193-207.

Houdeville, R. and Cousteix, J. (1978) "Premiers Resultats d'une etude sur les couches limites turbulentes en ecoulement pulse avec gradient de pression moyen defavorable", 15e Colloque D'Aerodynamique Appliquee, Marseille, November 7-8.

Lu, S.Z., Nunge, R.J., Erian, F.F. and Mohajery, M. (1973). Measurements of pulsating turbulent water flow in a tube. Proceedings of the Third Symposium on Turbulence in Liquids, University of Missouri, Rolla, pp. 375-392.

Mueller, A. and Ramaprian, B.R. (1977). Velocity measurements in a transitional oscillatory boundary layer. Proc. of 2nd Annual ASCE EMB Specialty Conference, Raleigh, N.C.

Nakato, T. 1974. Wave-induced sediment entrainment from rippled beds, Ph.D. Thesis, Mechanics and Hydraulics Program, University of Iowa, Iowa City.

Patel, M.H. (1977). On turbulent boundary layers in oscillatory flow. Proceedings of the Royal Society of London. A353, pp. 121-144.

Ramaprian, B.R. (1975). Turbulence measurements in an 'equilibrium' axisymmetric wall jet. Journal of Fluid Mechanics, 71, Pt. 2, pp. 317-338.

Rao, K.N., Narasimha, R. and Badri Narayanan, M.A. (1971). The 'bursting' phenomena in a turbulent boundary layer. Journal of Fluid Mechanics, 48, pp. 339-352.

Richardson, E.G., and Tyler, E. (1929). The transverse velocity gradient near the mouthes of pipes in which an alternating or continuous flow of air is established. Proceedings of Physical Society of London, 43, pp. 1-15.

Rosenhead, L. (1963). (ed). Laminar Boundary Layers, Oxford Univ. Press, London.

Sarpkaya, T. (1966). Experimental determination of the critical Reynolds number for pulsating Poiseuille flow. Journal of Basic Engineering, Trans. ASME 88, pp. 589-598.

Schlichting, H. (1968). Boundary Layer Theory. McGraw-Hill, New York.

Schulz-Grunow, (1940). Pulsierender Durchfluss durch Rohre, Forschung 11, 4, pp. 170-187. Translated as "Pulsation Flow Through Pipes", NASA Technical Translation, NASA-TT-F-14881, 1973, 50 p.

Tu, S.W. (1978). An experimental study of oscillatory pipe flow at transitional Reynolds numbers, M.S. Thesis, Mechanics and Hydraulics Program, The University of Iowa, Iowa City, Iowa.

Coles, D.A. and Hirst, E.A. (1968). (ed.) Proceedings of the 1968 Stanford Conference on Boundary Layers.

Uchida, S. (1956). The pulsating viscous flow superposed on the steady motion of incompressible fluid in a circular pipe. ZAMP, 7, pp. 403-421.

Wygnanski, I.J., and Champagne, F.H. (1973). On transition in a pipe. Part I, The origin of puffs and slugs and the flow in a turbulent slug. Journal of Fluid Mechanics, 59, Pt. 2, pp. 281-336.

Yellin, E.L. (1966). Laminar turbulent transition process in pulsatile flow. Circ. Res. 19; pp. 791-804.

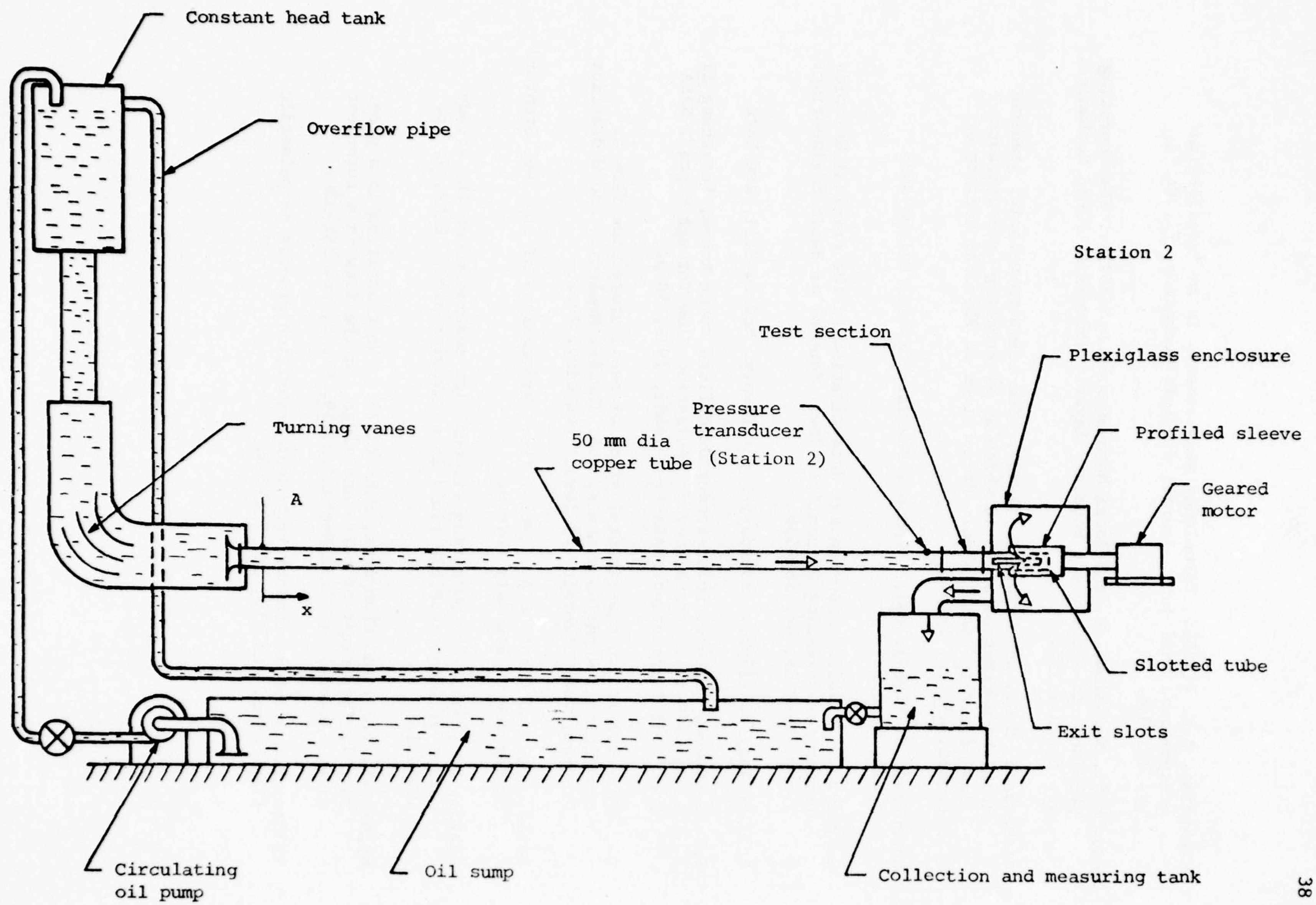

Figure 1. Schematic layout of the experimental apparatus

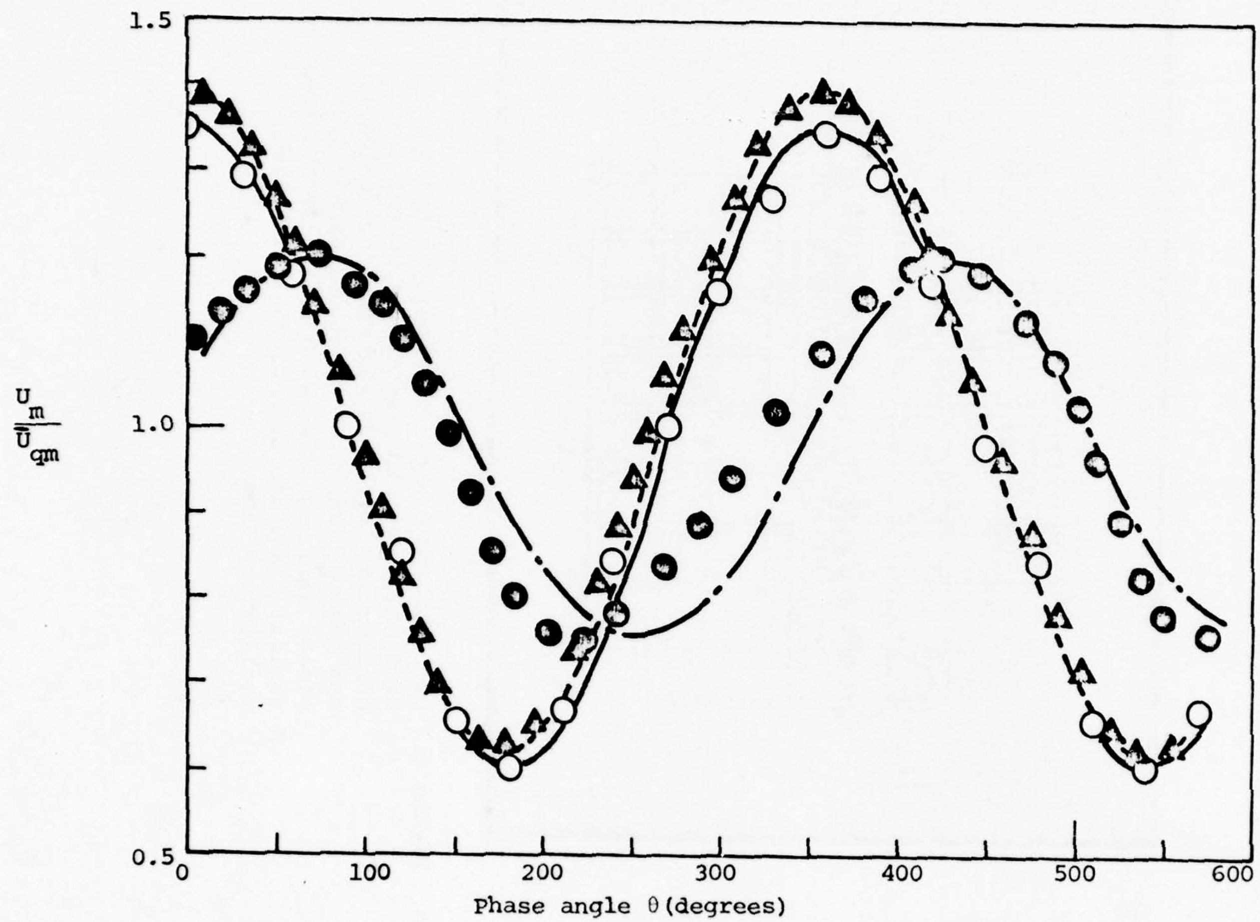

Figure 2. Variation of the cross sectional average velocity during a cycle. O, quasi-steady; ▲, oscillatory flow at 0.057 Hz (Run 24); ●, oscillatory flow at 1.75 Hz (Run 13); Lines denote exact sine waves with corresponding amplitude; ——, quasi-steady; ---, 0.057 Hz; — · —, 1.75 Hz

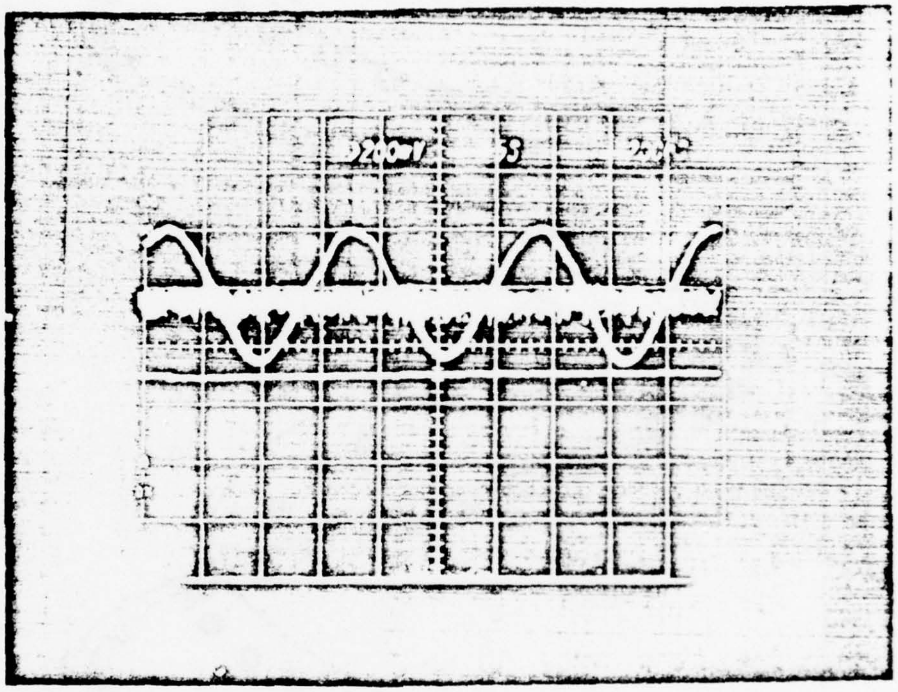

Figure 3. Oscilloscope traces of velocity signals From LDA ($r = 0$). The smooth horizontal trace corresponds to steady laminar flow ($\theta = 180°$); the hashed horizontal trace corresponds to steady turbulent flow ($\theta = 0°$); the smooth sinusoidal trace corresponds to laminarized oscillatory flow

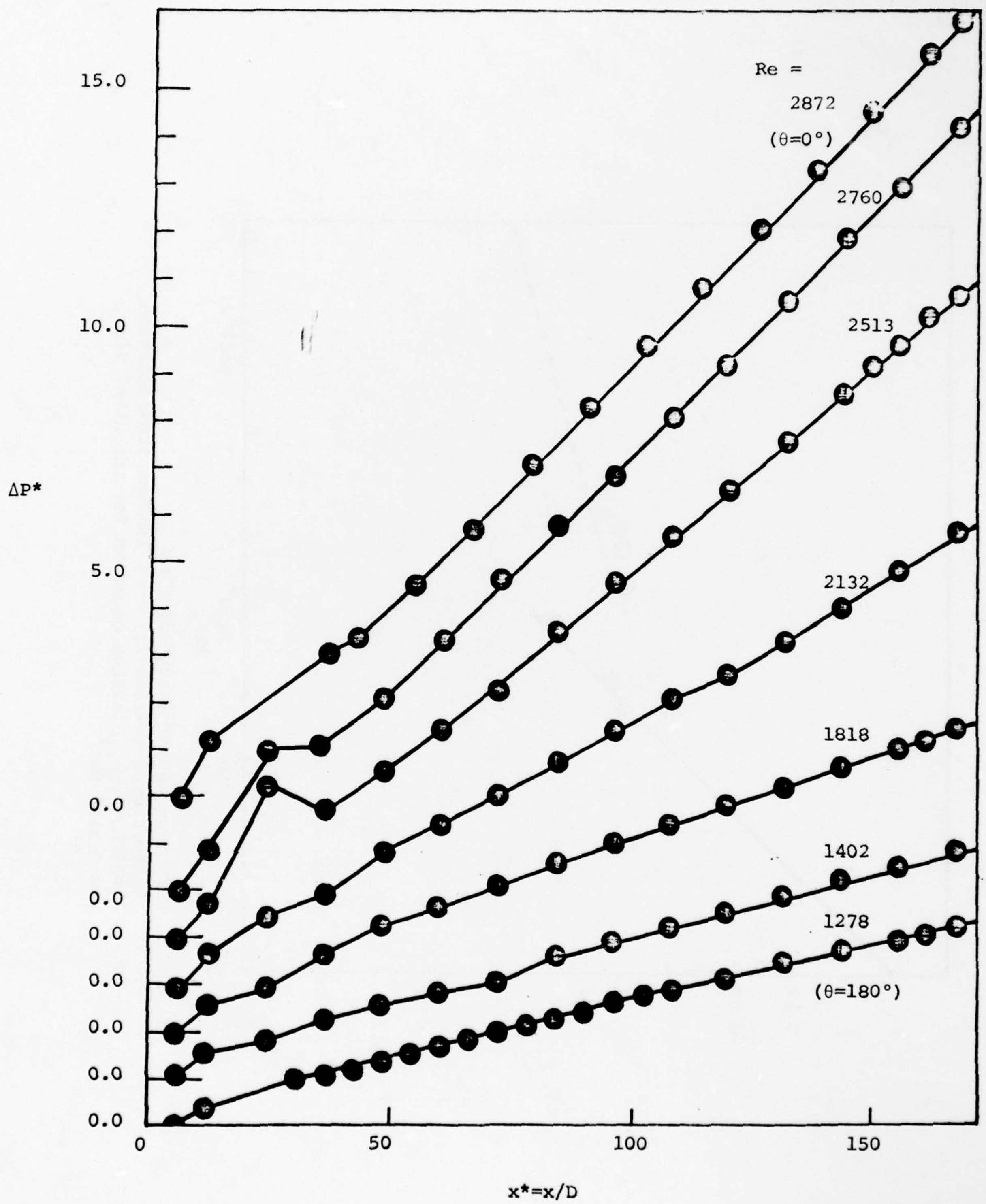

Figure 4. Static pressure drop along the pipe in steady flow; results from experiments of series 2.

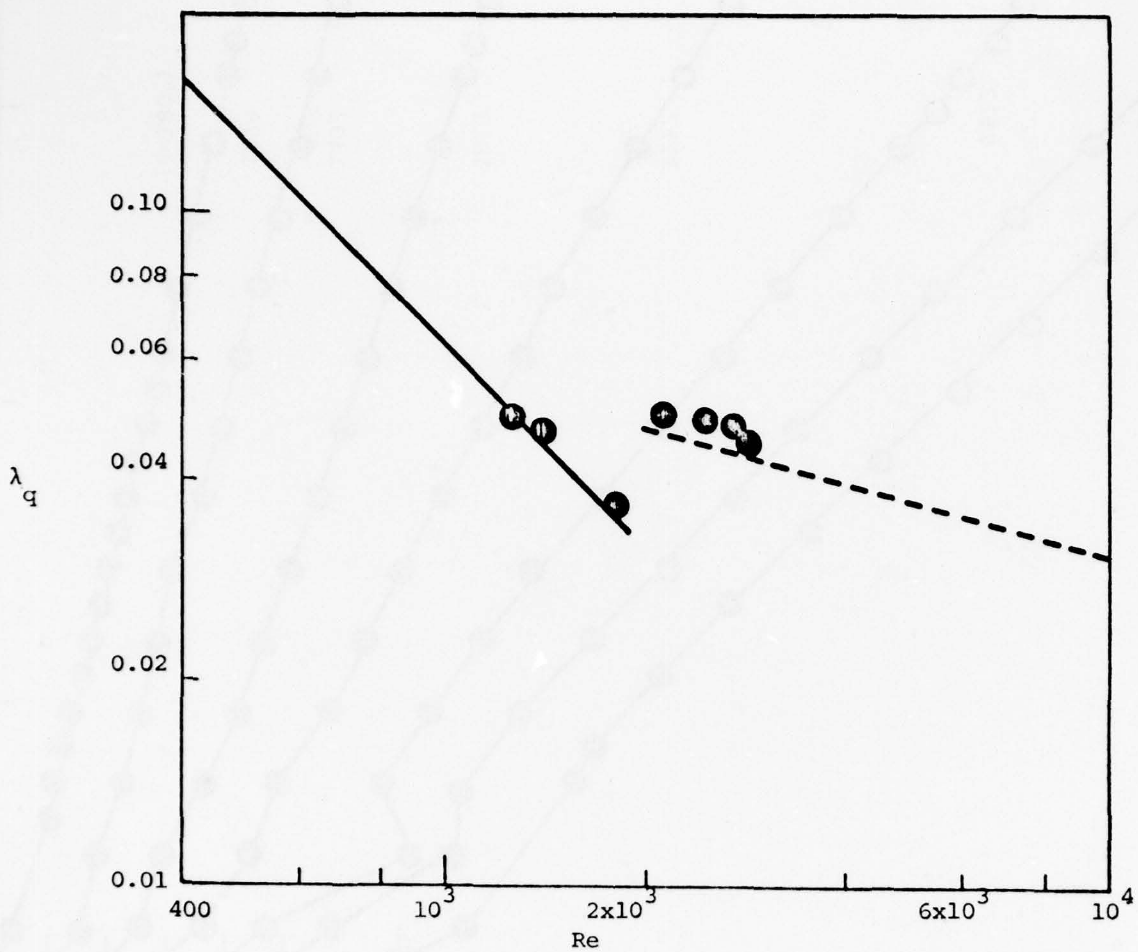

Figure 5. Friction factor in steady flow
● Experiment (series 2); ——, laminar flow relation $\lambda=64/Re$; ---, Blassius equation for turbulent flow, $\lambda= 0.3165\ Re^{-\frac{1}{4}}$

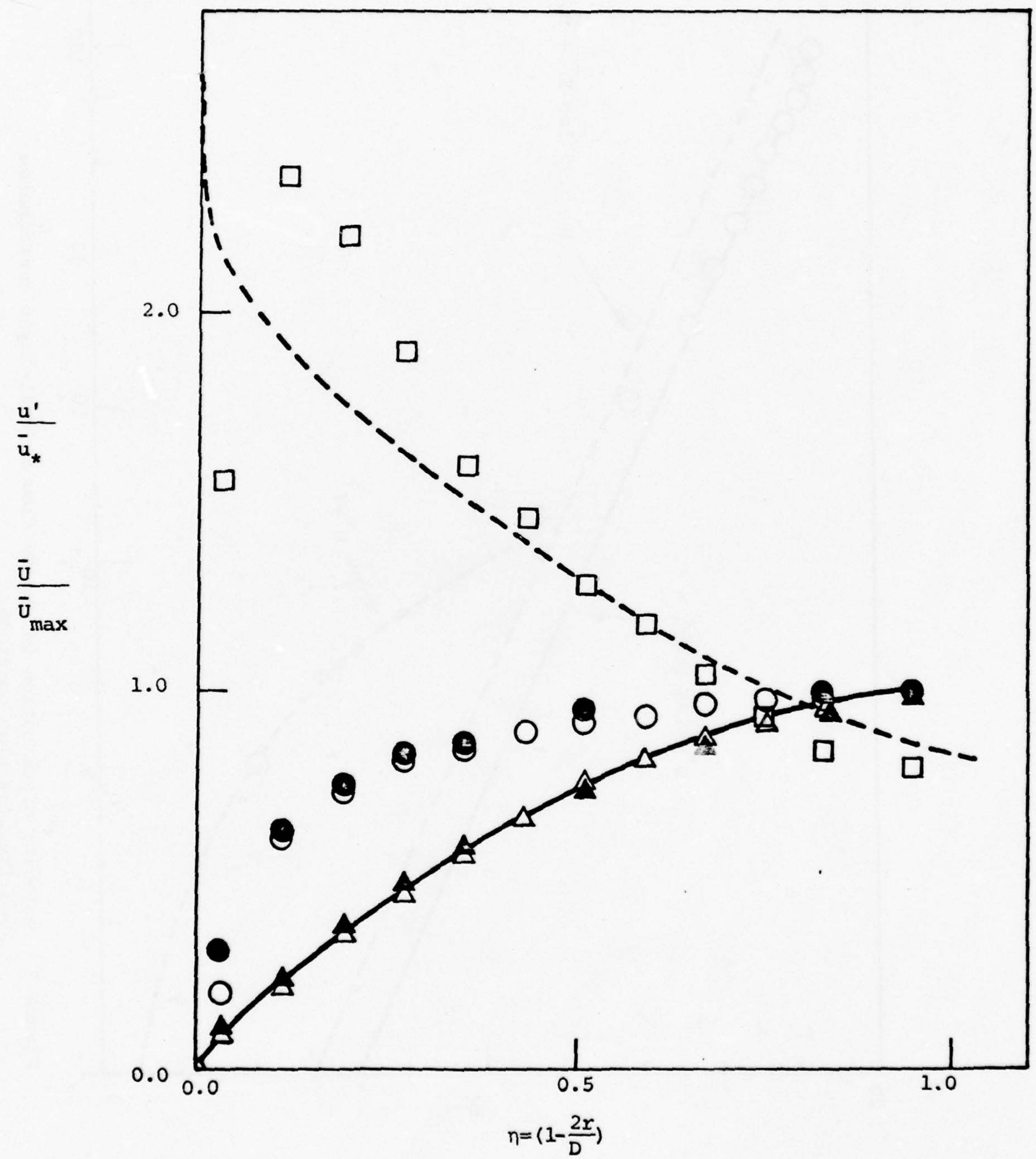

Figure 6. Distributions of mean and turbulent velocities in steady flow.
mean velocity {Δ, Run 11; ▲, Run 21 Laminar flow at θ=180° (Re=1278)
{O, Run 12; ●, Run 22 Turbulent flow at θ=0° (Re=2870
——, theoretical parabolic profile for laminar flow
Turbulent intensity: □, Run 12;---data from Laufer (1954) for Re=5x10^5

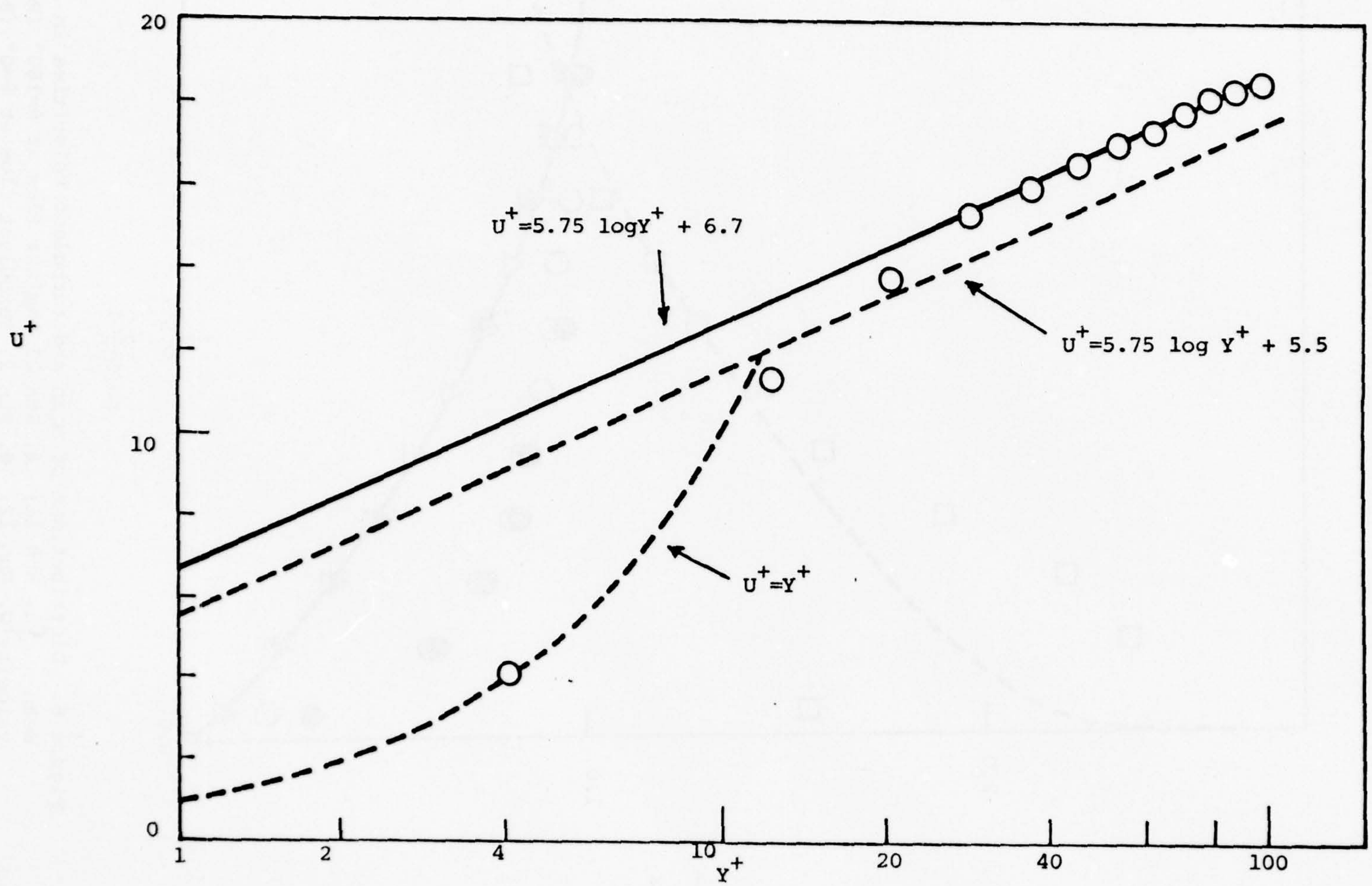

Figure 7. Velocity distribution in steady flow in wall-layer coordinates $\theta=0$ (Maximum slot opening)

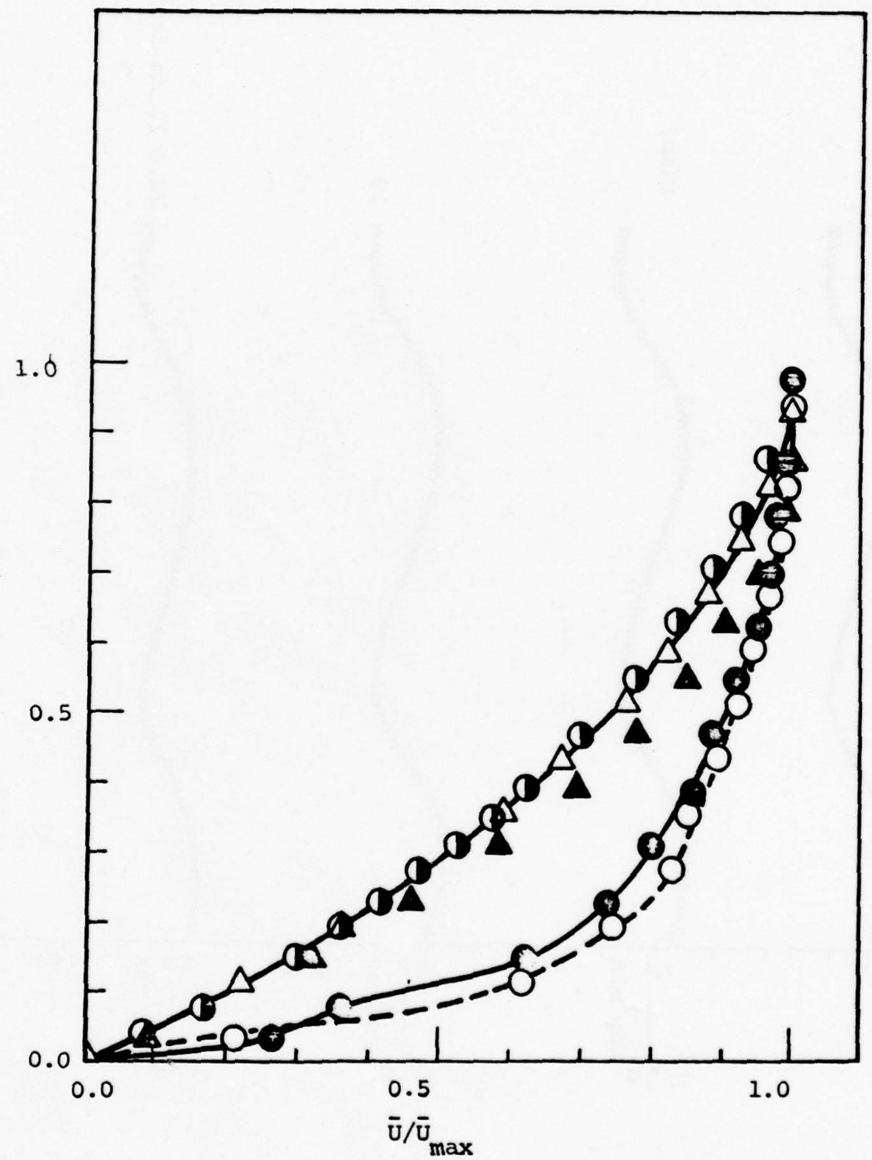

Figure 8. Distribution of the time-mean velocity across the pipe in unsteady flow.

Δ, steady laminar flow (θ=180°); -θ-, steady turbulent flow (θ=0°),
-●-, unsteady turbulent flow at f=1.75 Hz (Run 13);
◐, unsteady laminarized flow at f=1.75 Hz (Run 23),
▲, unsteady laminarized flow at f=0.057 Hz (Run 24);
——, theoretical parabolic profile for laminar flow

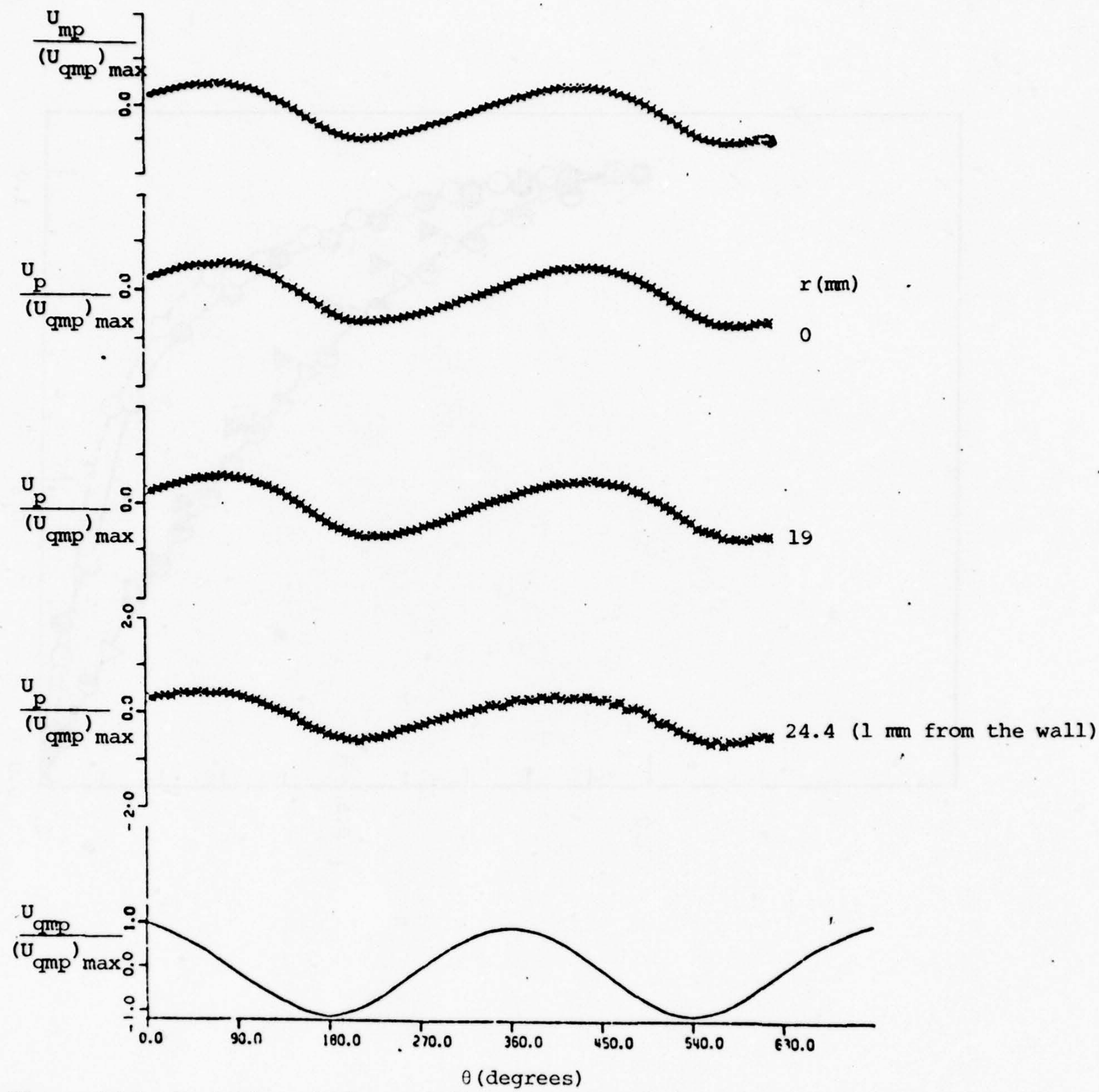

Figure 9(a). Variation of the periodic component of the velocity with phase angle (Run 13).

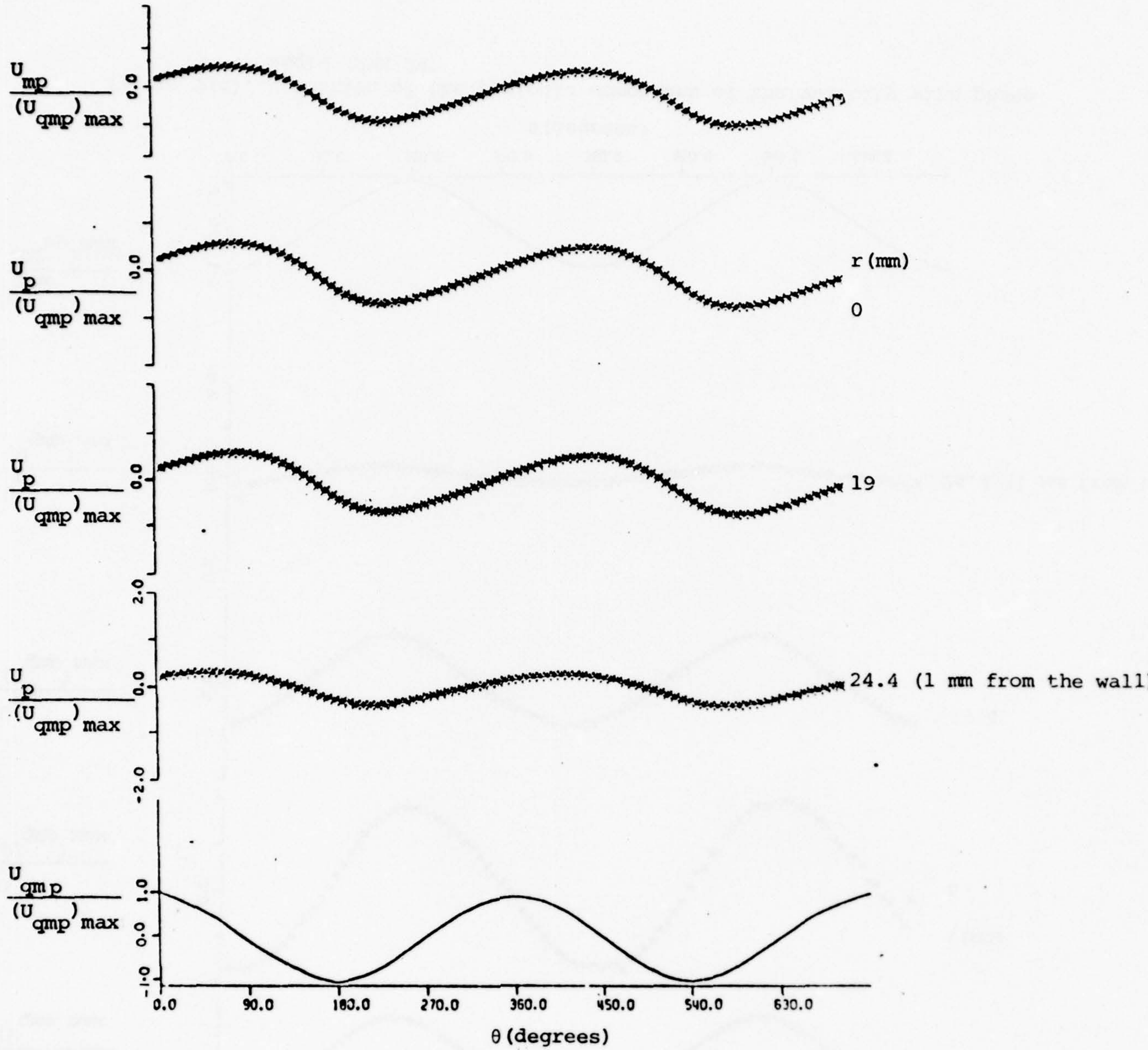

Figure 9(b). Variation of the periodic component of the velocity with phase angle (Run 23).

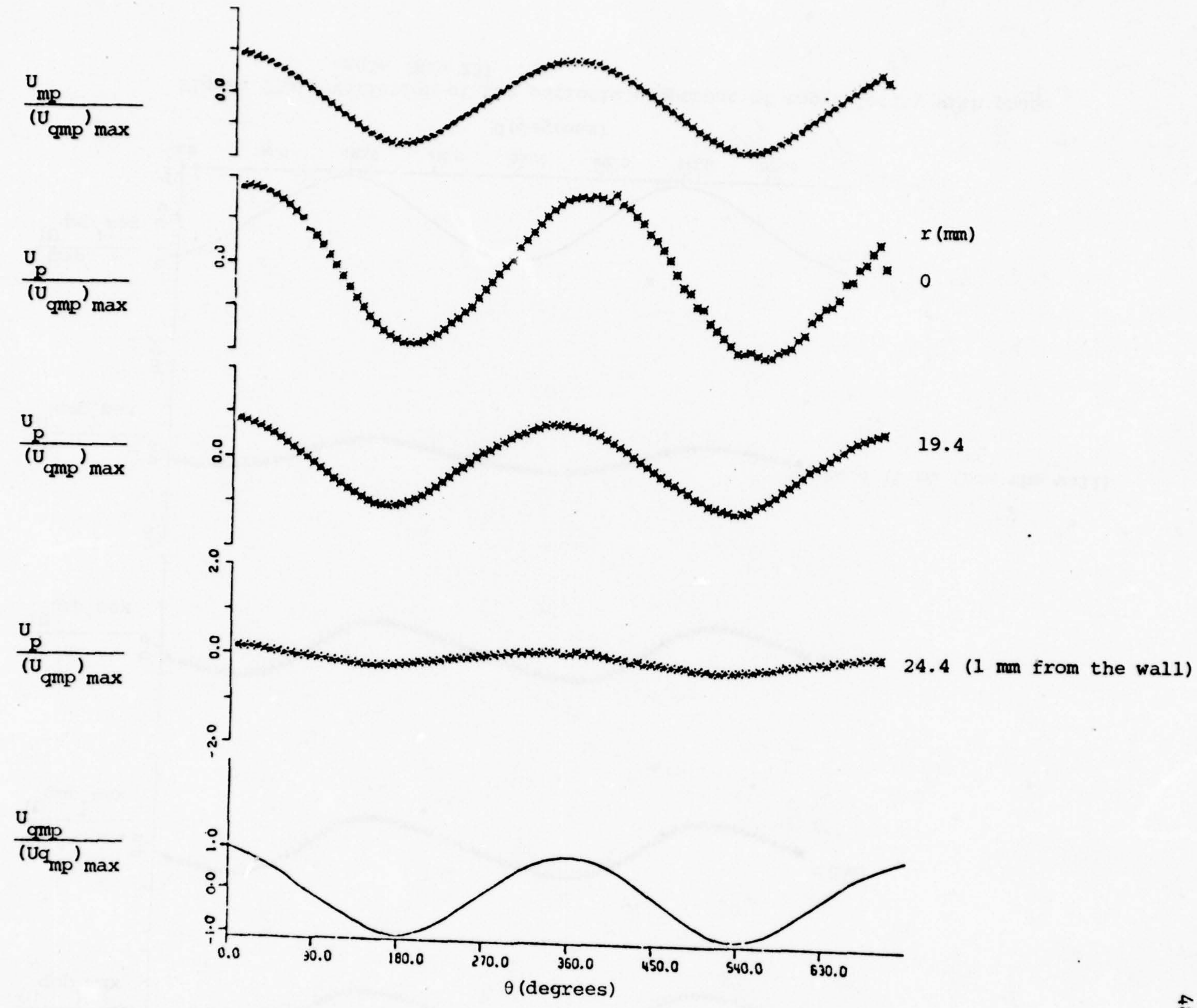

Figure 9(c). Variation of the periodic component of the velocity with phase angle (Run 24)

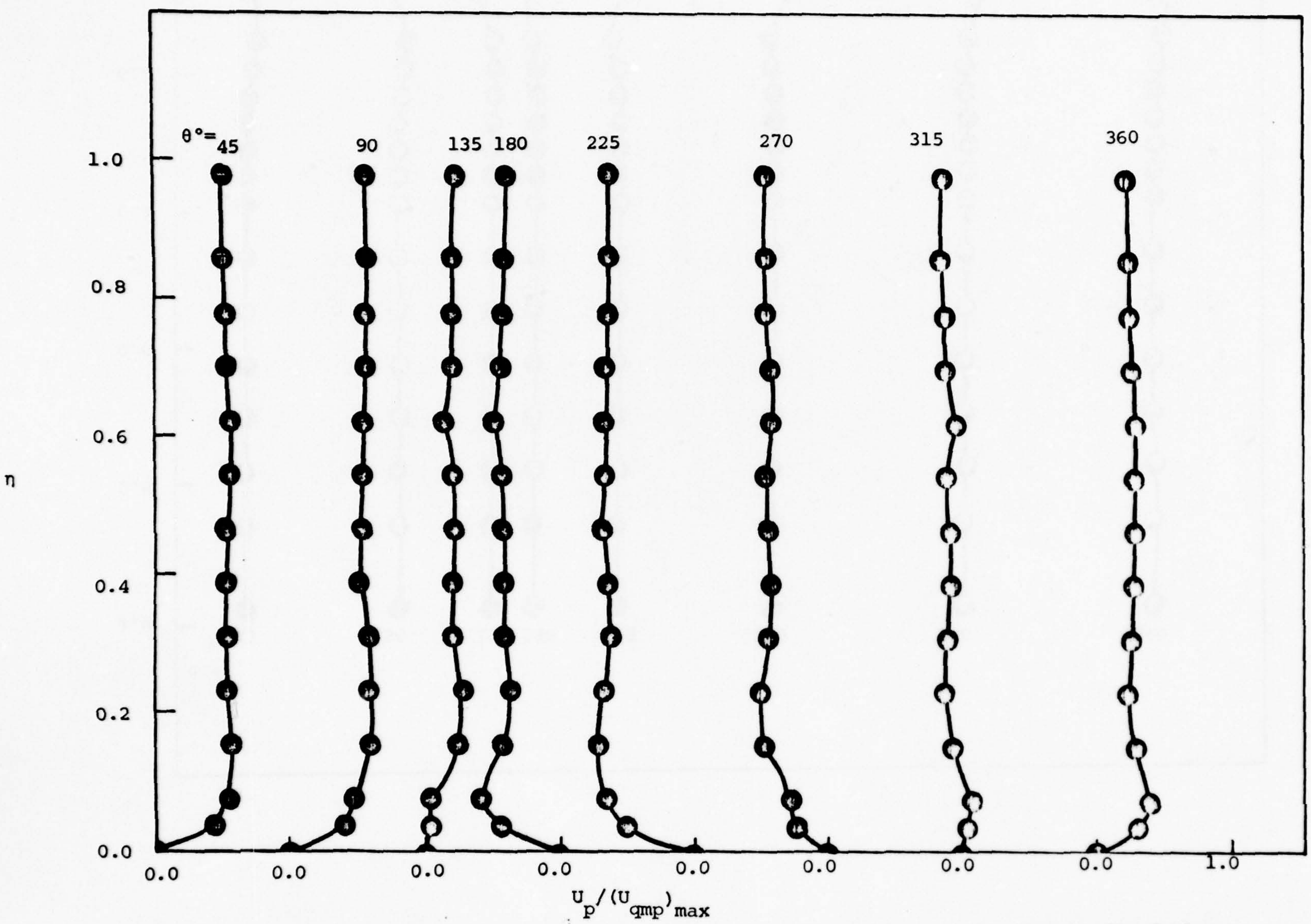

Figure 10(ã) Distribution of the periodic component of the velocity across the pipe at fixed phase angle in oscillating turbulent flow; f=1.75 Hz (Run 13).

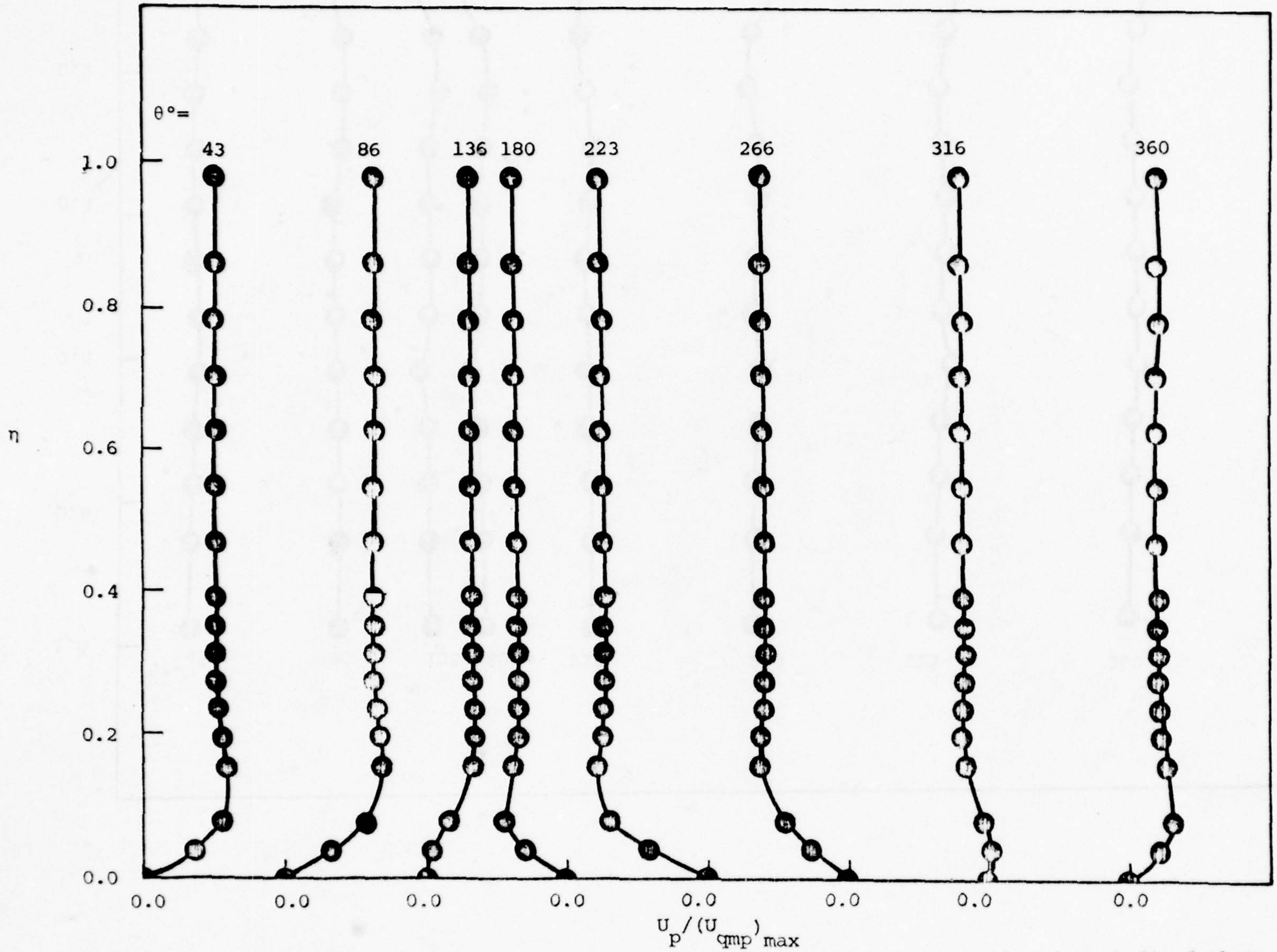

Figure 10(b). Distribution of the periodic component of the velocity across the pipe at fixed phase angle in oscillating laminar flow; f=1.75 Hz (Run 23)

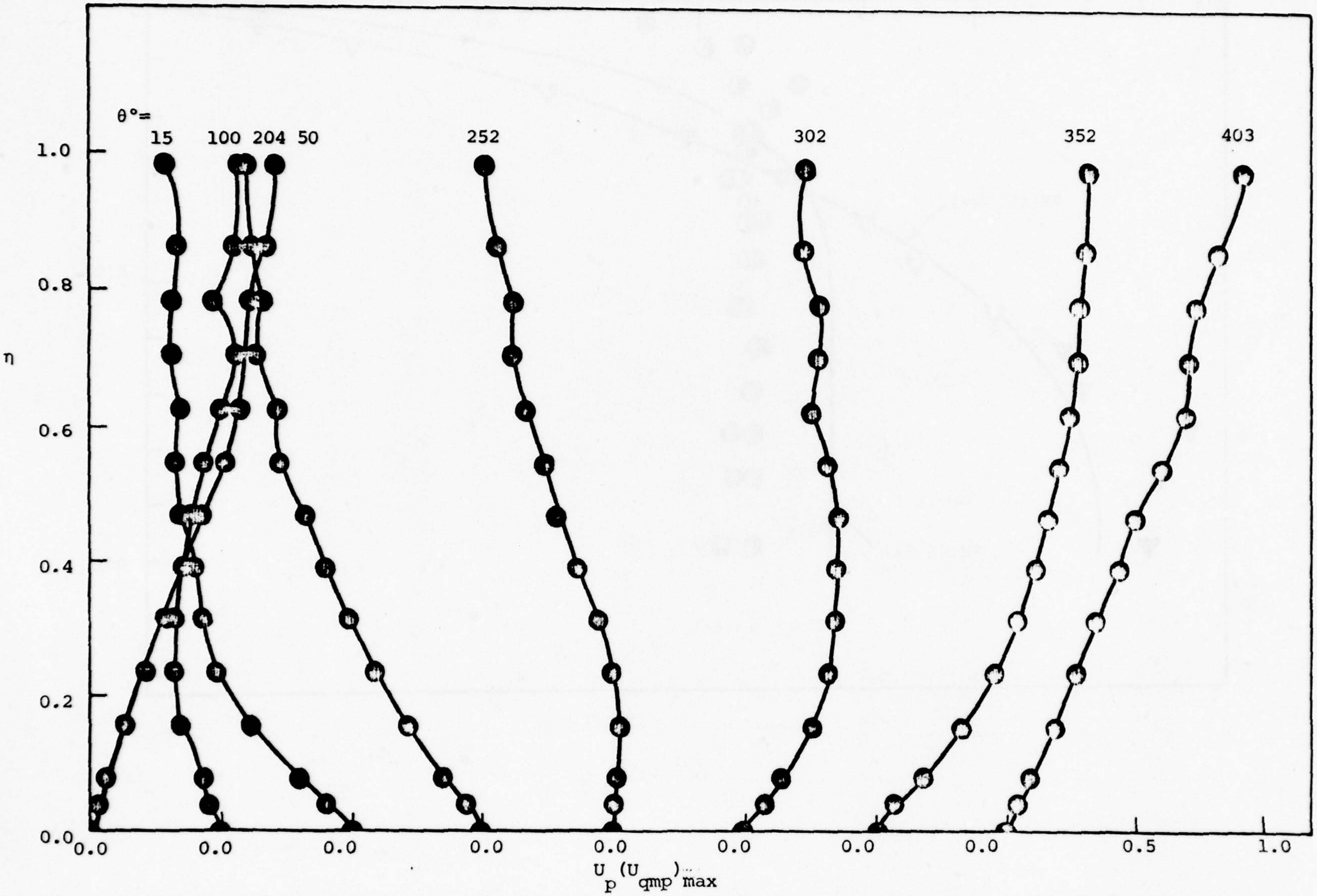

Figure 10(c). Distribution of the periodic component of the velocity across the pipe at fixed phase angle in oscillating laminar flow; f=0.057 Hz (Run 24)

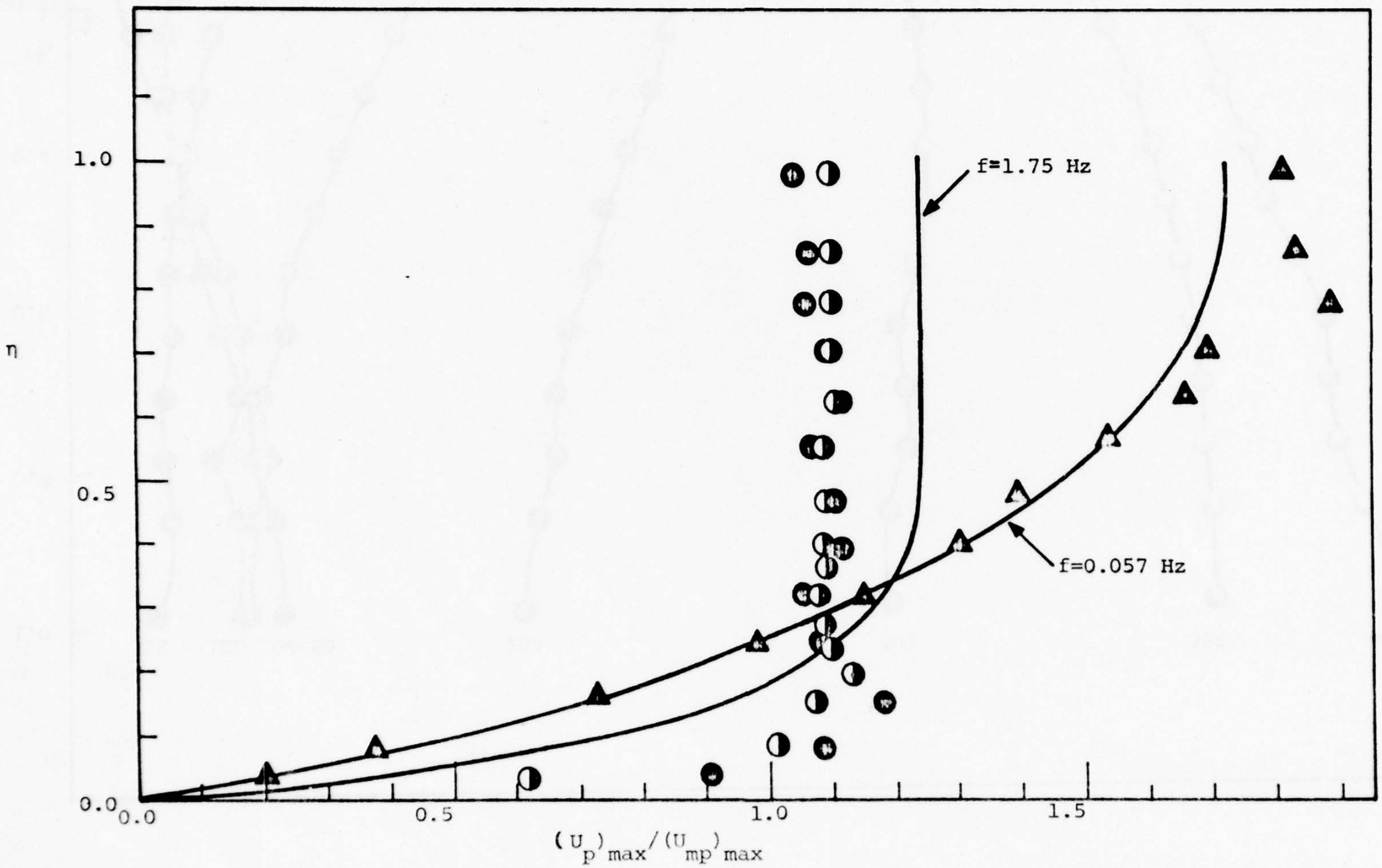

Figure 11. Distribution of the amplitude of the periodic component of velocity across the pipe.
●, Run 13; (f=1.75 Hz) ◑, Run 23; (f=1.75 Hz) ▲, Run 24; (f=0.057 Hz) ——, Laminar theory from Uchida (1956)

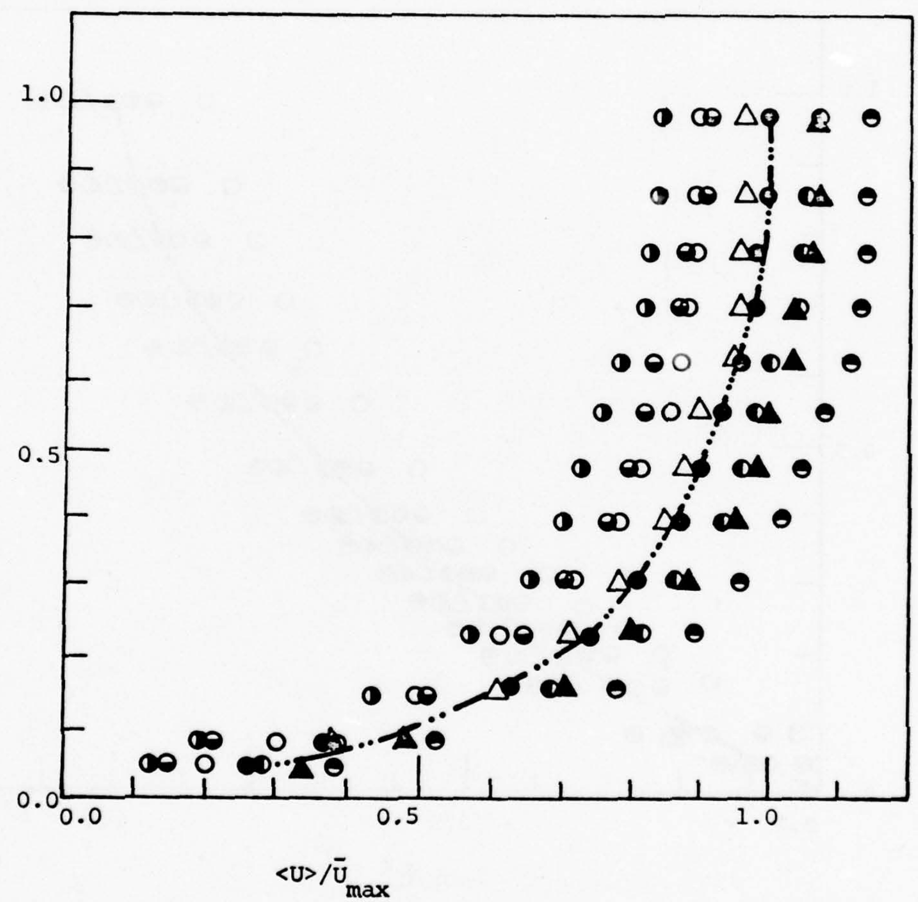

Figure 12(a). Distribution of the ensemble average velocity across the pipe in oscillatory turbulent flow, f=1.75 Hz (Run 13)

symbol, phase angle θ(degrees): ◐, 45°; ◐, 135°; ⊖, 180°; ◑, 225°; O, 270°; Δ, 315°, ▲, 360°; time-mean velocity

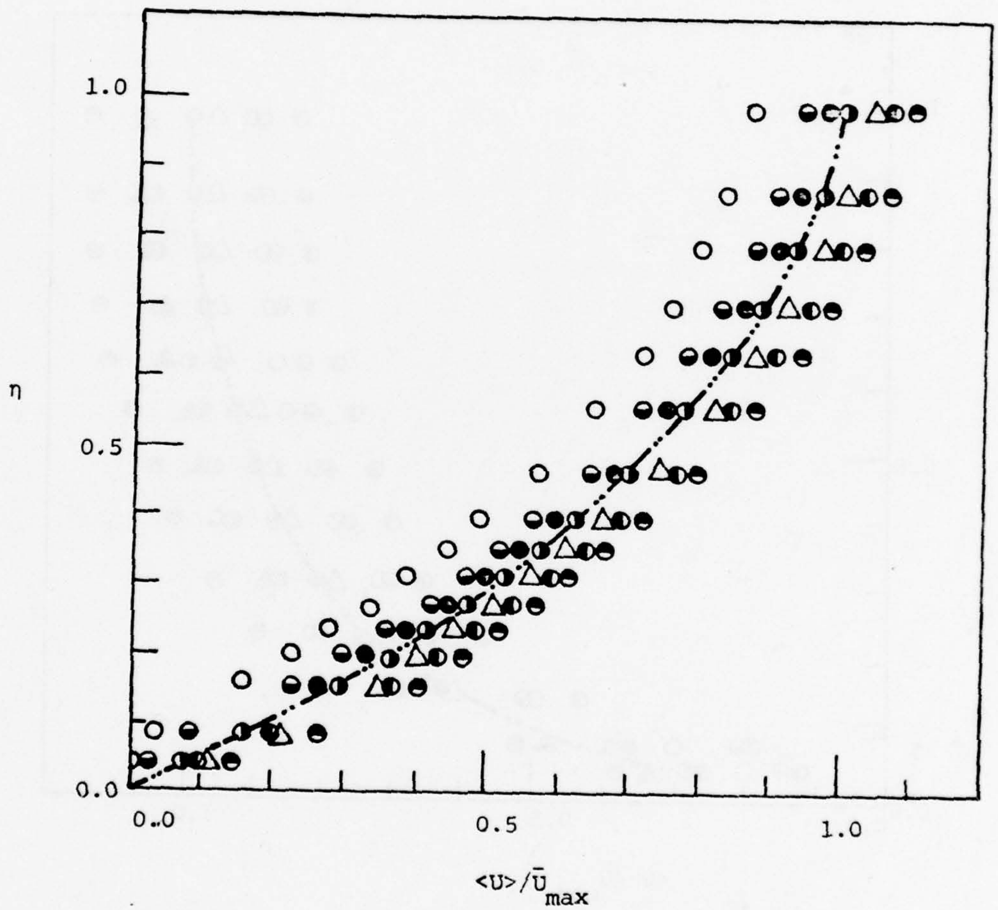

Figure 12(b). Distribution of the ensemble average velocity across the pipe in oscillatory laminarized flow, f=1.75 Hz (Run 23) symbol, phase angle θ(degrees): ◐, 45°; ◐, 135°; ◓, 180°; O, 225°; ●, 315°; Δ, 360°; —··—◐—··— ; time-mean velocity

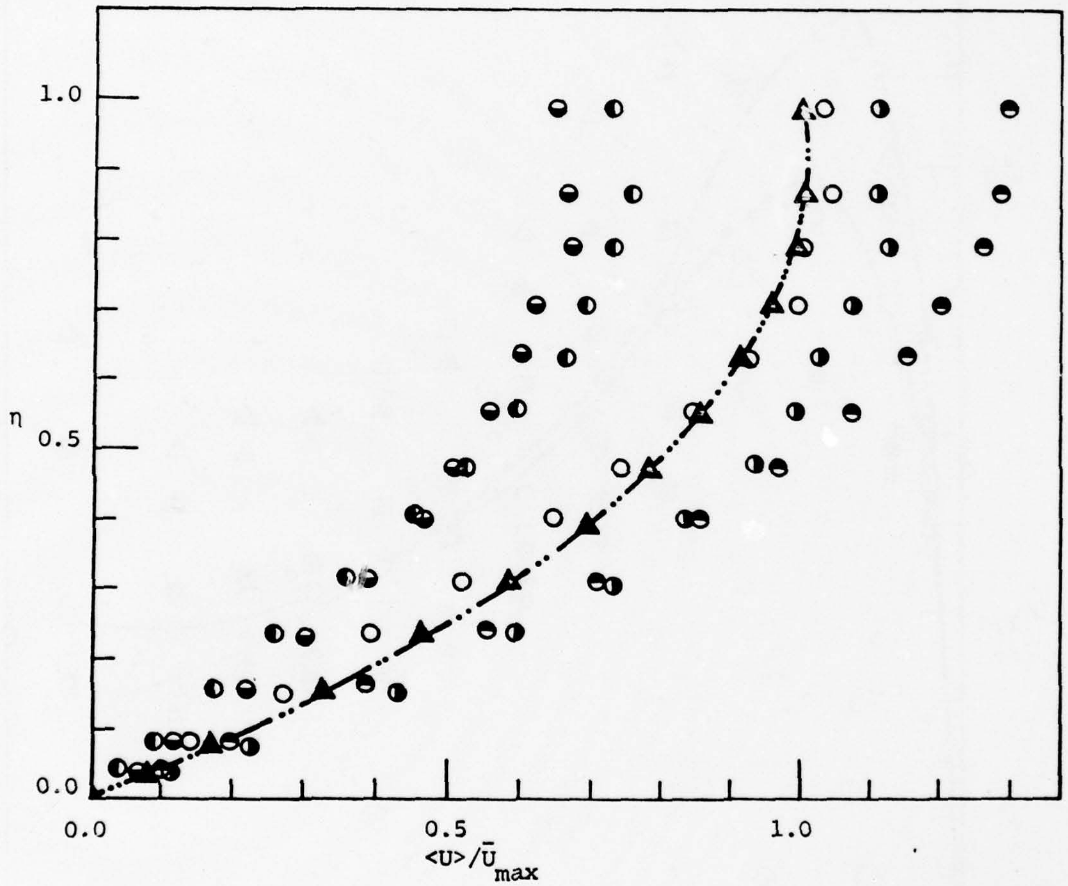

Figure 12(c). Distribution of the ensemble average velocity across the pipe in oscillatory laminarized flow, f=0.057 Hz (Run 24). symbol, phase angle θ(degrees) ⊖, 50°; ◐, 100°; ⊖, 150°; ◑, 200°; O, 300°; —··▲··—, time-mean velocity

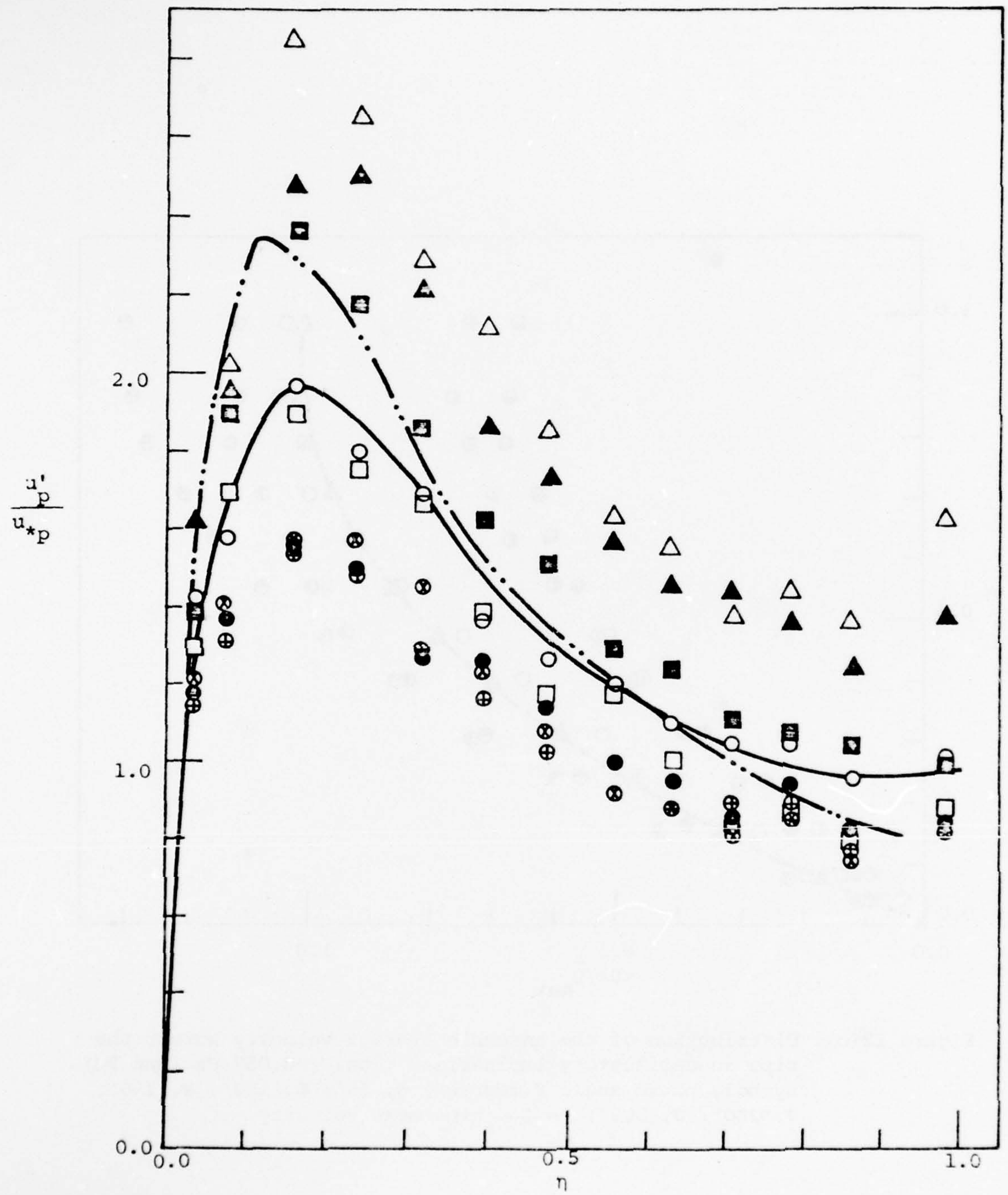

Figure 13. Distribution of the turbulent intensity across the pipe in run 13 (f=1.75 Hz)
——, time averaged turbulent intensity $u'/\bar{u}_*$ in oscillatory flow;
—··—, u'/u_* in quasi-steady flow at θ=0°
Data points denote the ensemble average turbulent intensity u'_p/u_{*p}
symbol, phase angle: ⊗, 6°; ⊕, 45°; ●, 90°; O, 135°; ▲, 180°;
Δ, 225°; ■, 270°; □, 315°

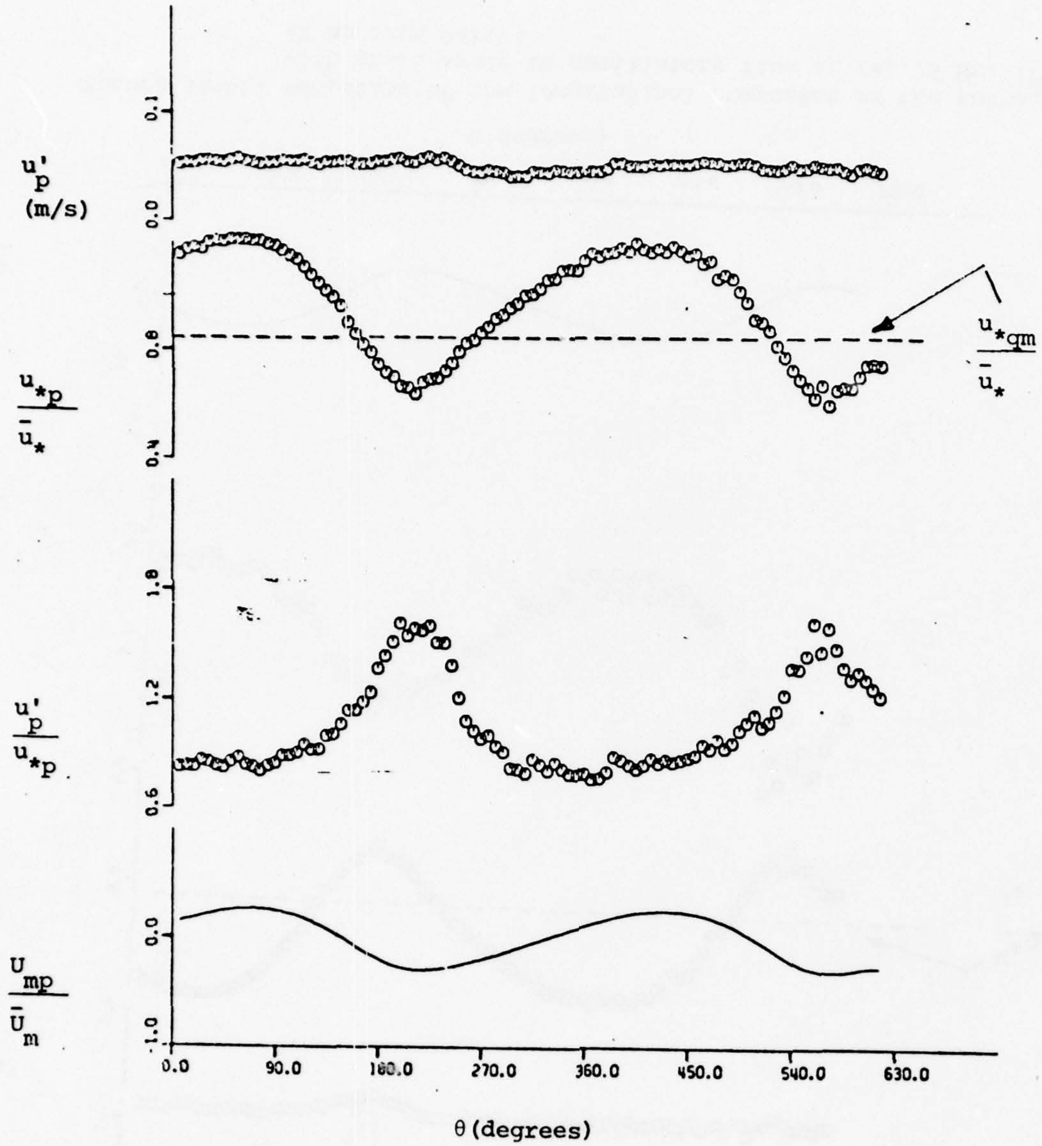

Figure 14 (a). Variation of the longitudinal component of the turbulent velocity with phase angle in oscillatory flow at f=1.75 Hz (r=0)

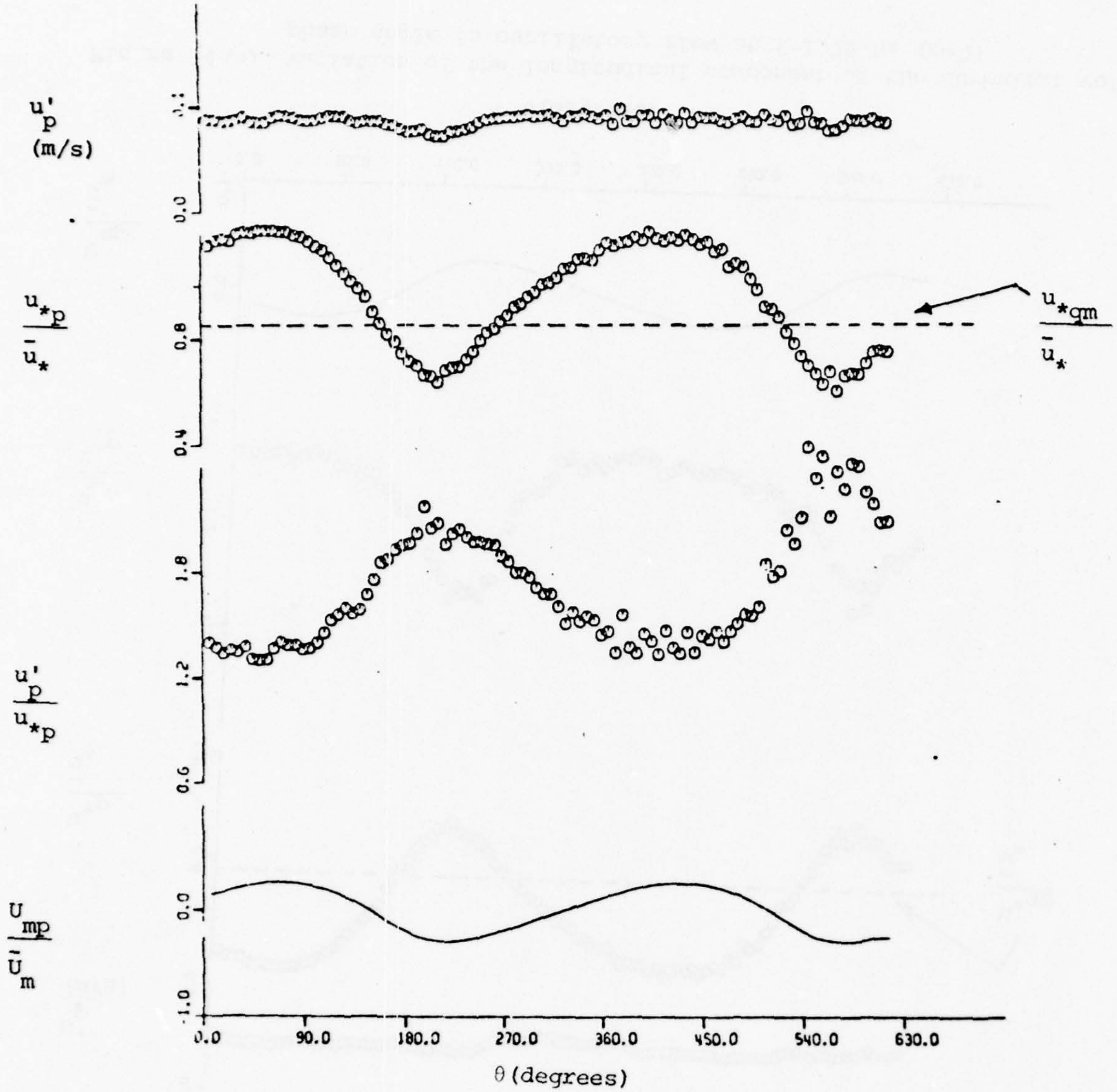

Figure 14(b). Variation of the longitudinal component of the turbulent velocity with phase angle in oscillatory flow at f=1.75 Hz. [r=23.4 mm (2 mm from wall)]

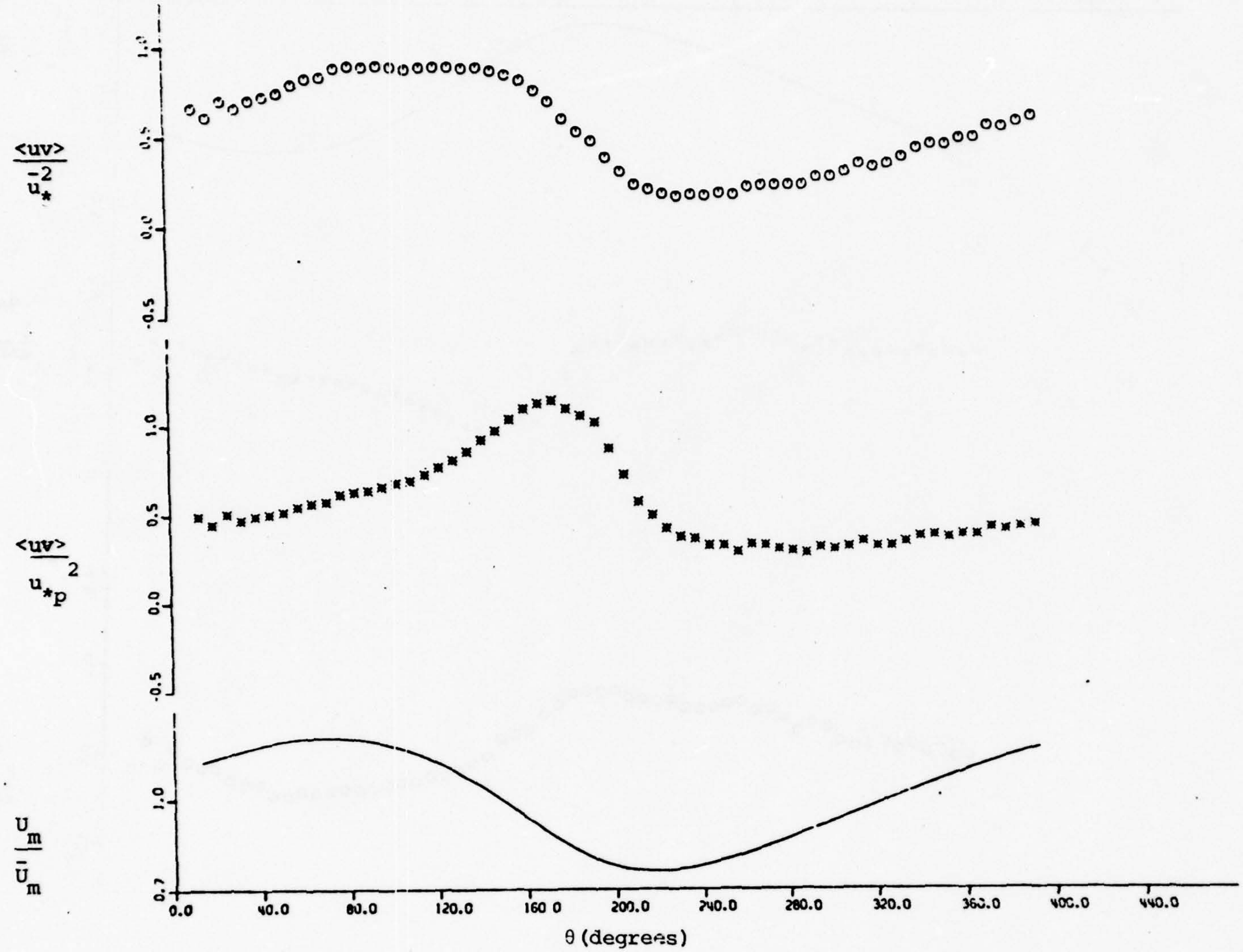

Figure 15(a). Variation of the Reynolds shear stress with phase angle in oscillatory flow. distance: 1 mm from the wall; f=1.75 Hz (Run 13)

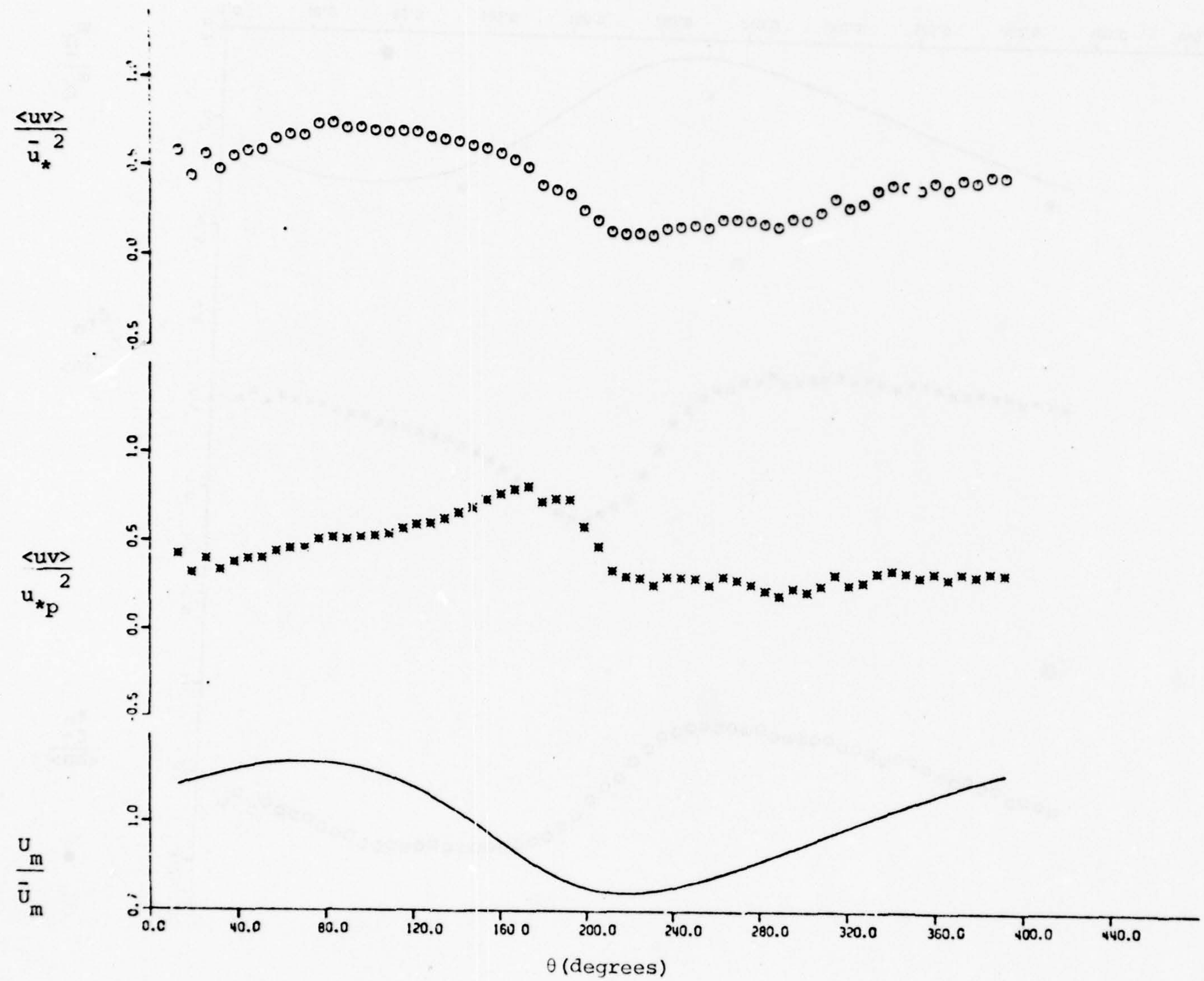

Figure 15(b). Variation of the Reynolds shear stress with phase angle in oscillatory flow. distance: 2 mm from the wall; f=1.75 Hz (Run 13)

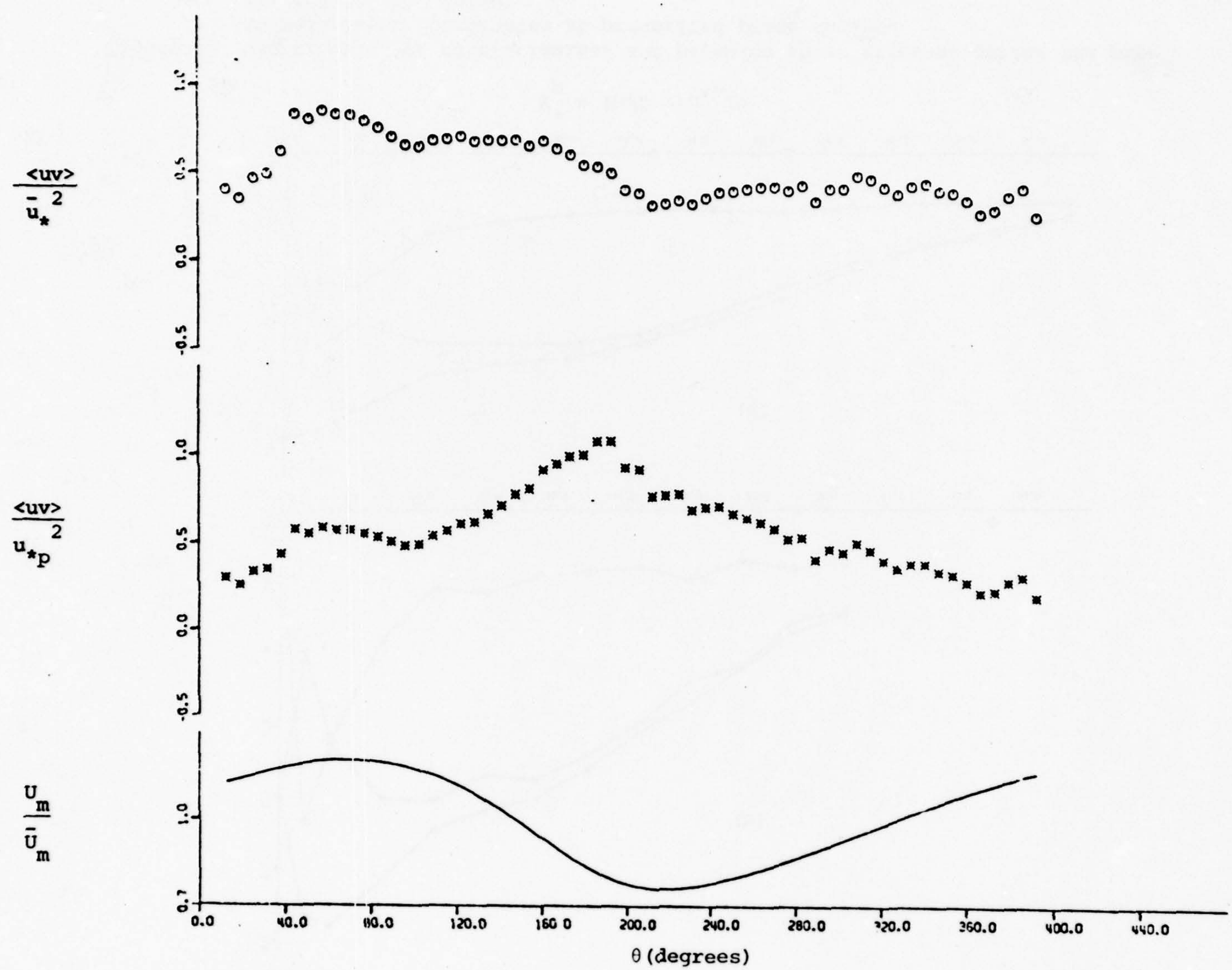

Figure 15(c). Time variation of the Reynolds shear stress with phase angle in oscillatory flow. distance: 10 mm from the wall; f=1.75 Hz (Run 13)

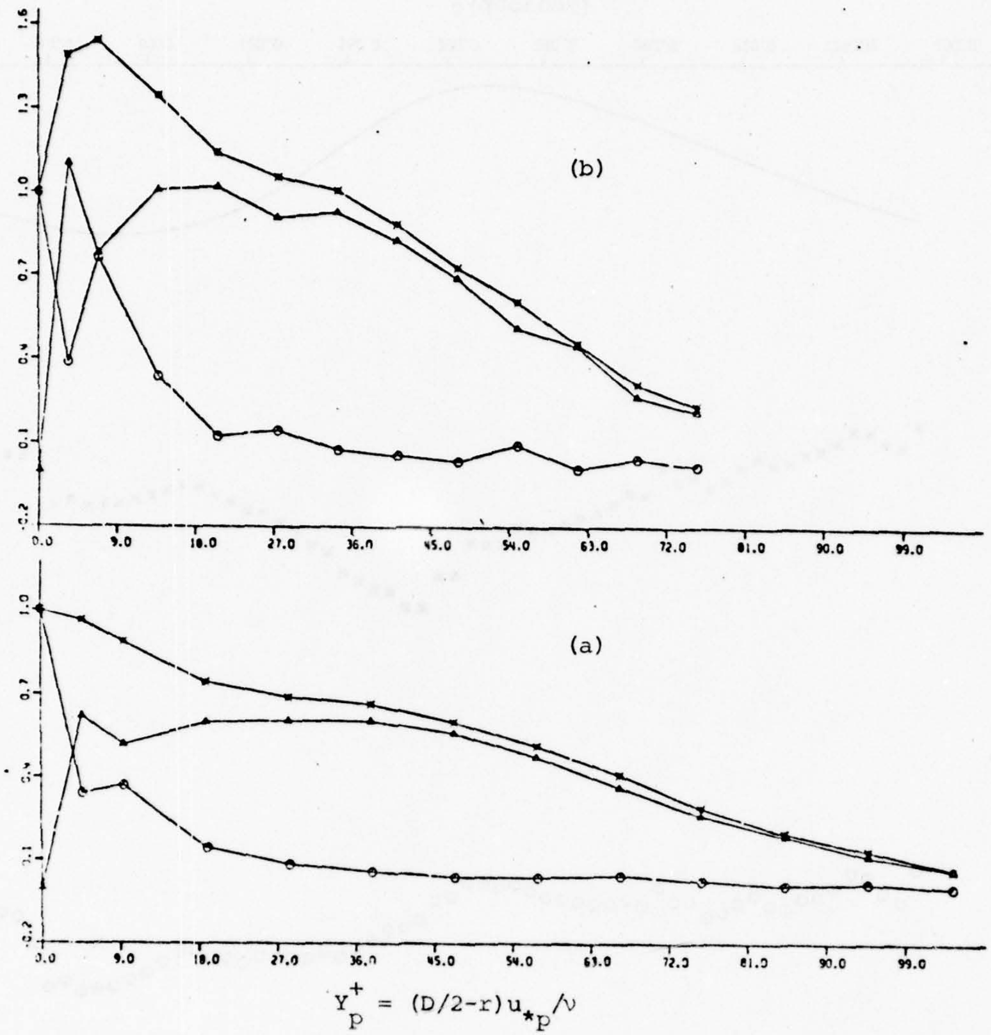

Figure 16. Distribution of total, laminar and Reynolds shear stresses across the pipe in wall-layer coordinates at prescribed phase angles.
(a) $\theta=77°$ (b) $\theta=160°$
—*—, total shear stress; —O—, laminar shear stress; —▲—, Reynolds shear stress. The stresses are normalized with respect to the wall shear stress at the corresponding phase angle.

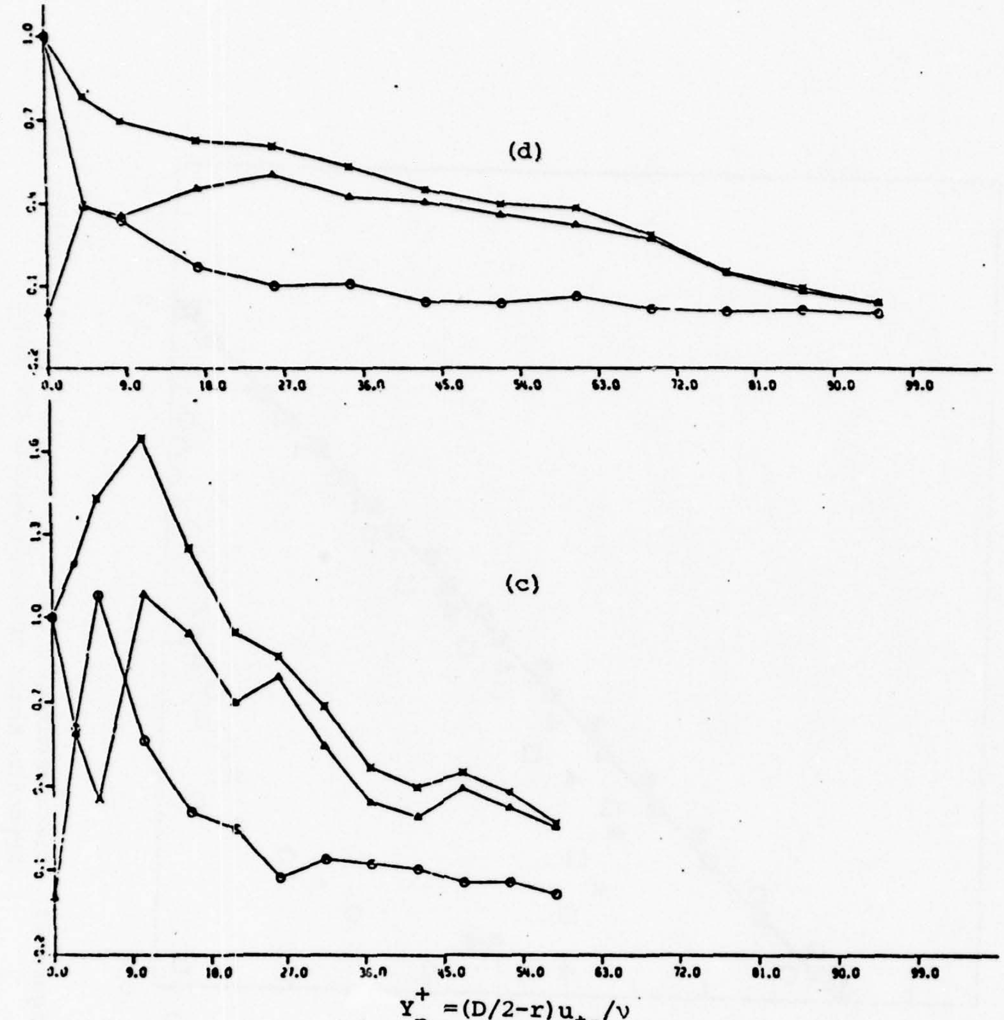

Figure 16. Distribution of total, laminar and Reynolds shear stresses across the pipe in wall-layer coordinates at prescribed phase angles
(c) θ=212° (d) θ=340°
—*—, total shear stress; —O—, laminar shear stress; —▲—, Reynolds shear stress. The stresses are normalized with respect to the wall shear stress at the corresponding phase angle

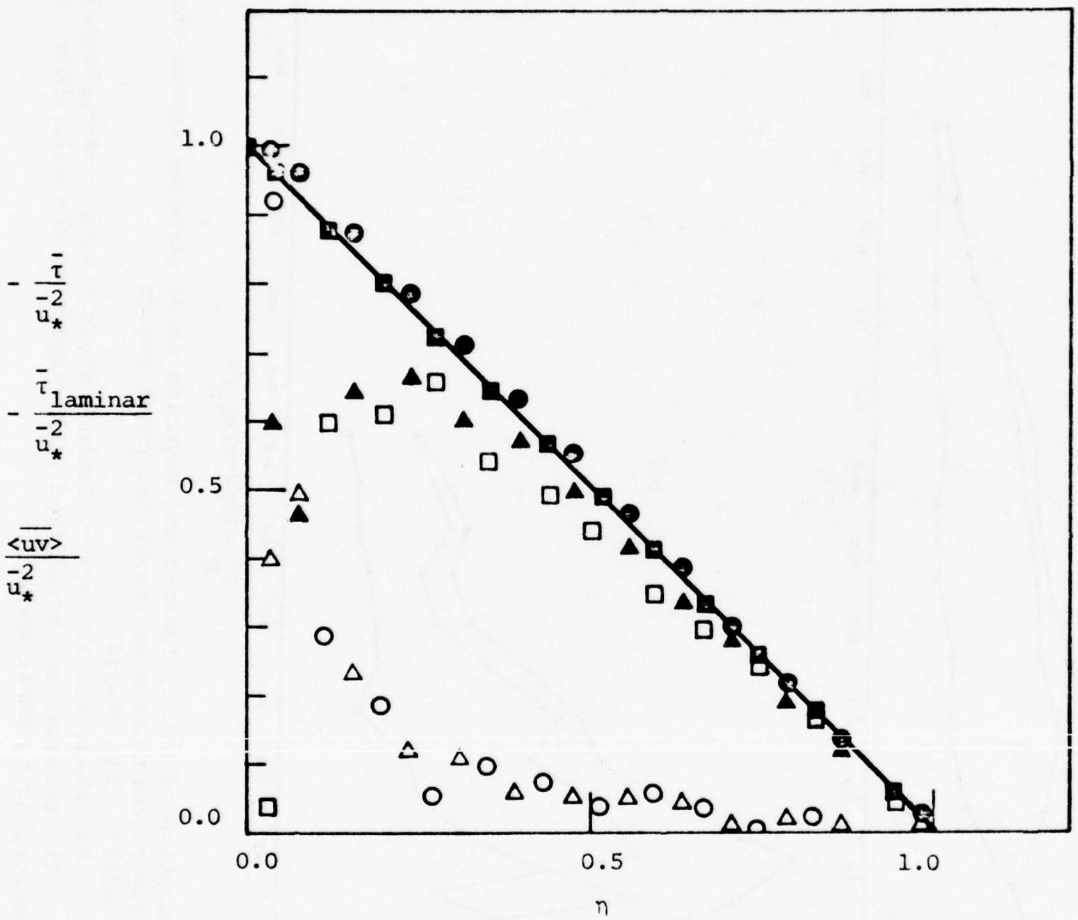

Figure 17. Distribution of the time-averaged total, laminar and Reynolds shear stresses across the pipe.

Steady turbulent flow at a Reynolds number of 2870 (θ=0°)
■ , total shear stress; □ , Reynolds shear stress;
O, laminar shear stress
Unsteady turbulent flow, f=1.75 Hz (Run 13)
●, total shear stress; ▲, Reynolds shear stress;
Δ, laminar shear stress

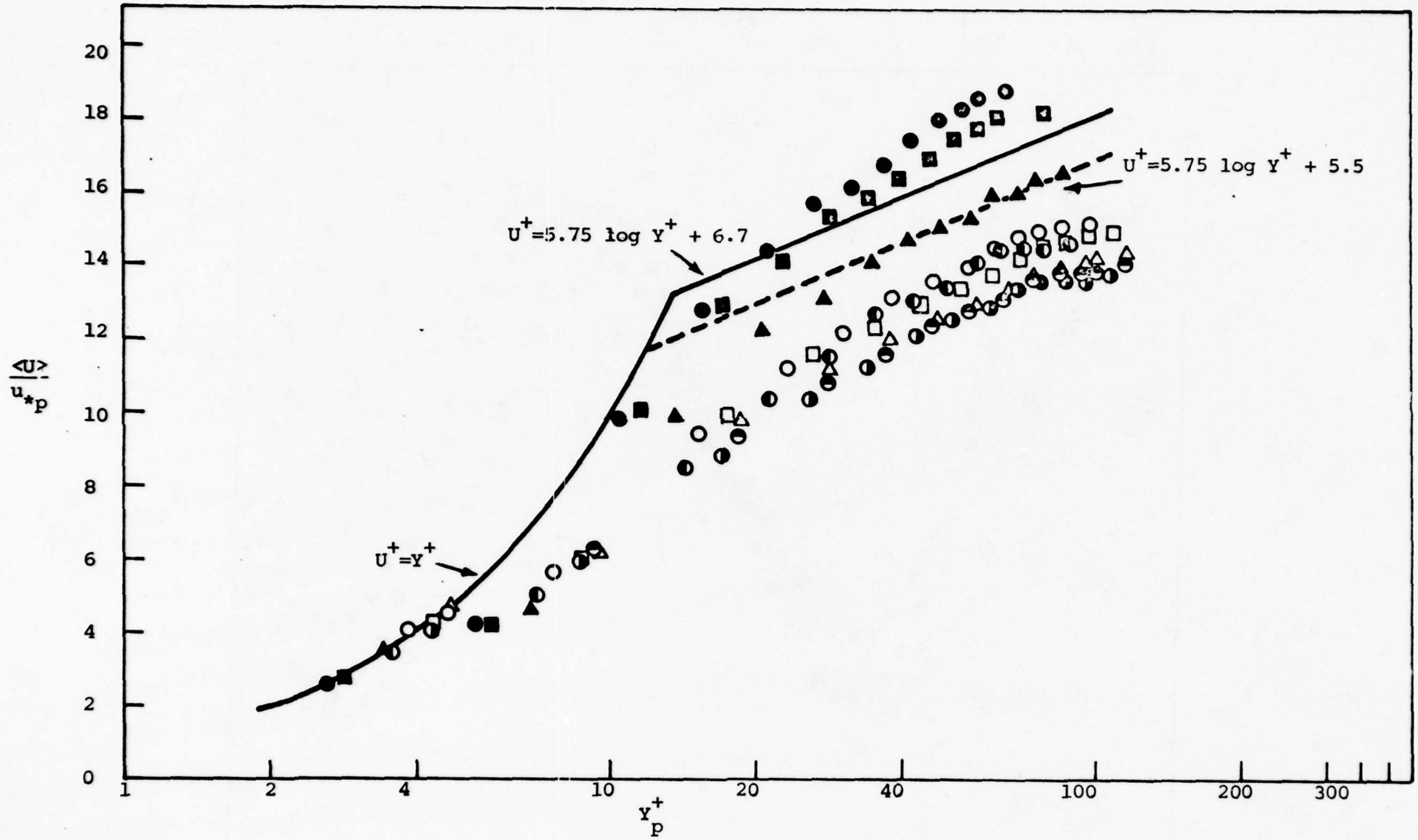

Figure 18. Velocity distribution in unsteady flow in wall-layer coordinates. symbol, phase angle θ(degrees): △, 77°; □, 115°; ▲, 160°; ■, 185°; ●, 212°, ◐, 276°; O, time-mean distribution $\bar{U}/\bar{u}_*$ Vs $(D/2-r)\bar{u}_*/\nu$; ◑, 340°; ⊖, 385°; ——, steady flow (θ=0°); --- universal log law

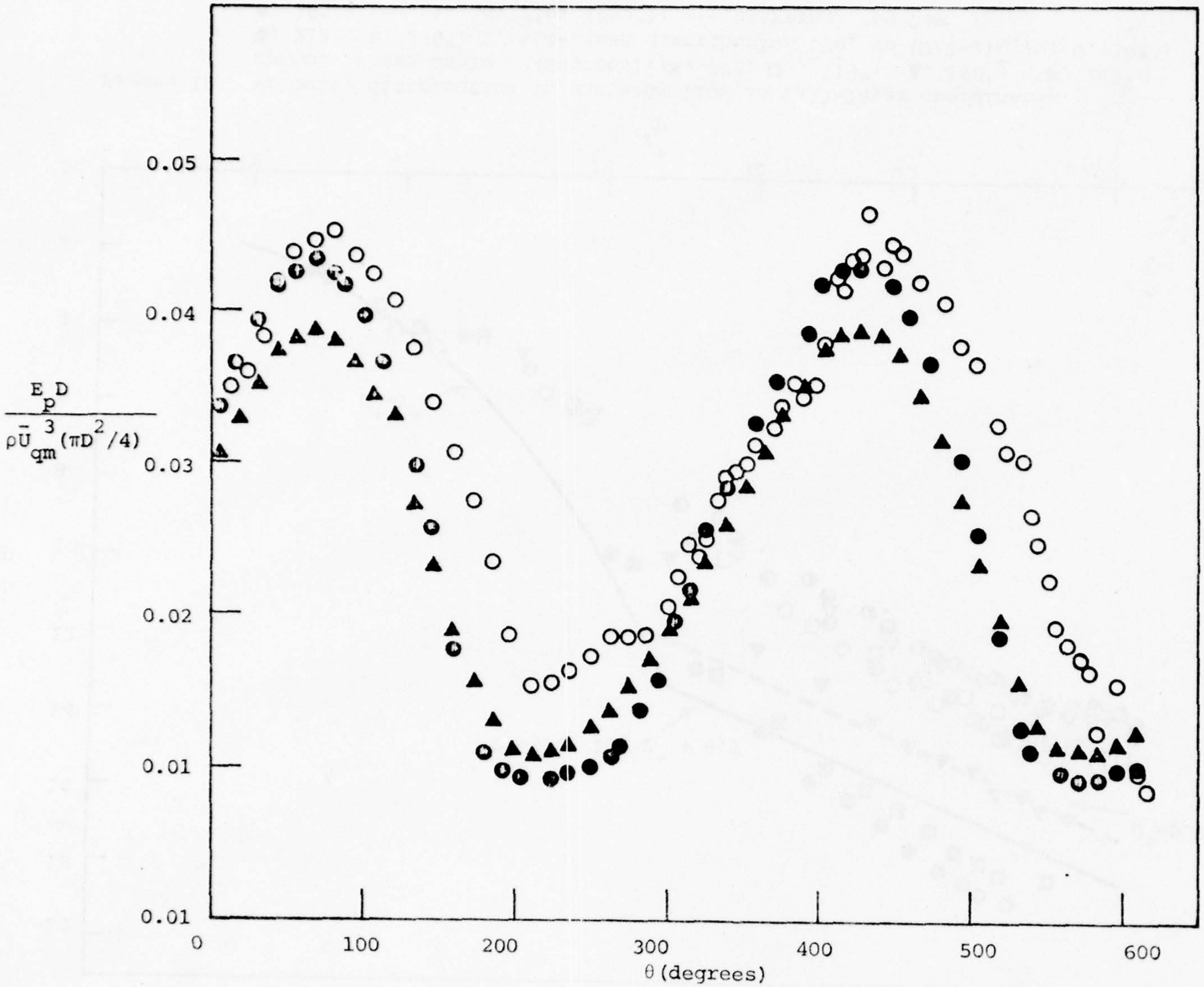

Figure 19. Variation of the rate of shear work with the phase angle. O, data from unsteady turbulent flow, f=1.75 Hz (Run 13); ▲, based on quasi-steady Blasius relation, $\lambda = 0.3165\ Re^{-\frac{1}{4}}$; ●, based on quasi-steady pressure drop measurements in actual transitional flow

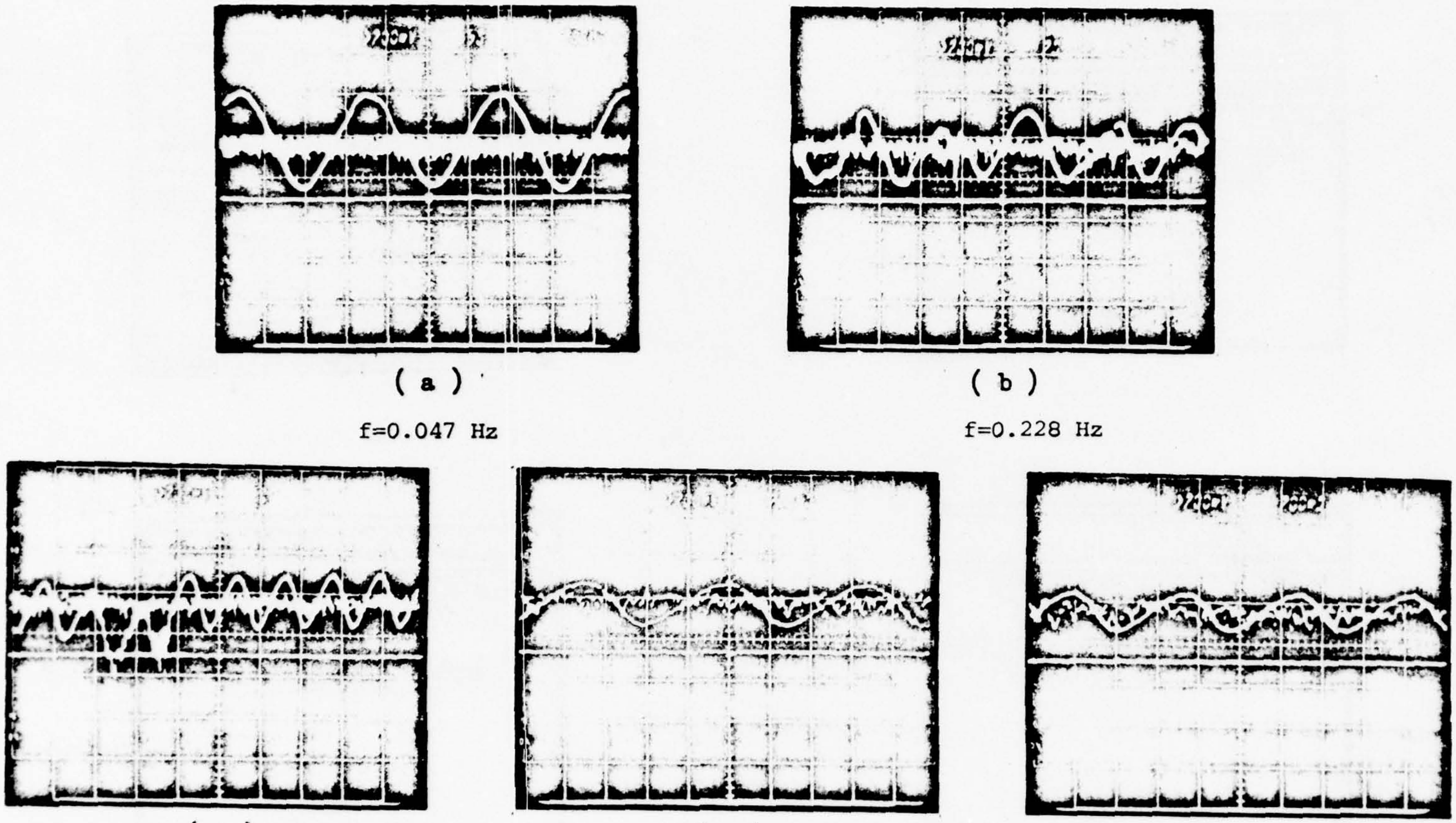

(a)

f=0.047 Hz

(b)

f=0.228 Hz

(c)

f=0.926 Hz

(d)

f=1.37 Hz

(e)

f=1.75 Hz

Figure 20. Oscilloscope traces of velocity signals from LDA from experiment series 2. r=0

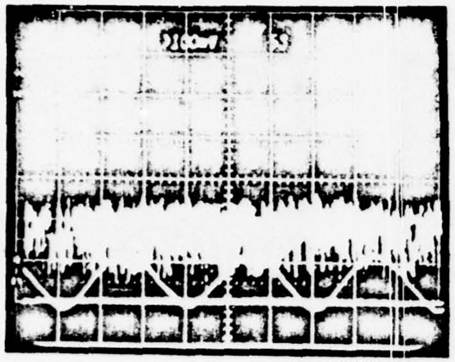

(a)

f=0.047 Hz

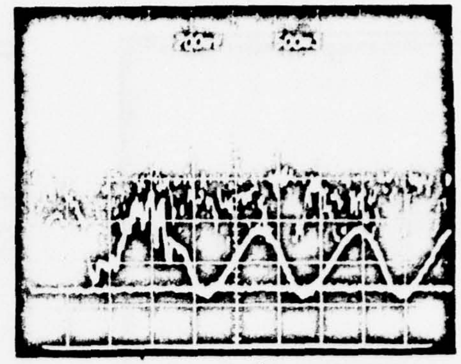

(b)

f= 0.926 Hz

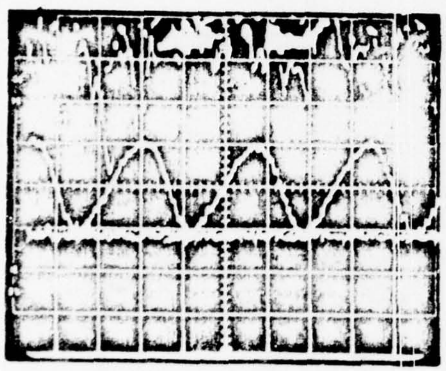

(c)

f=1.37 Hz

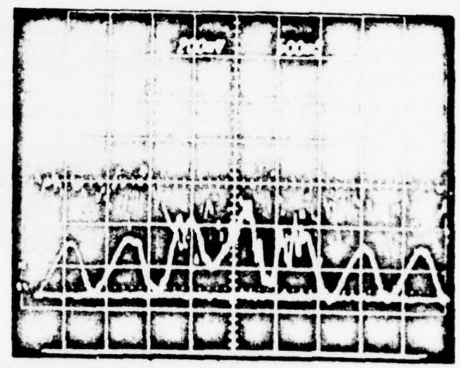

(d)

f=1.75 Hz

Figure 20. Oscilloscope traces of velocity signals from LDA from experiment series 2. r=18.4 mm

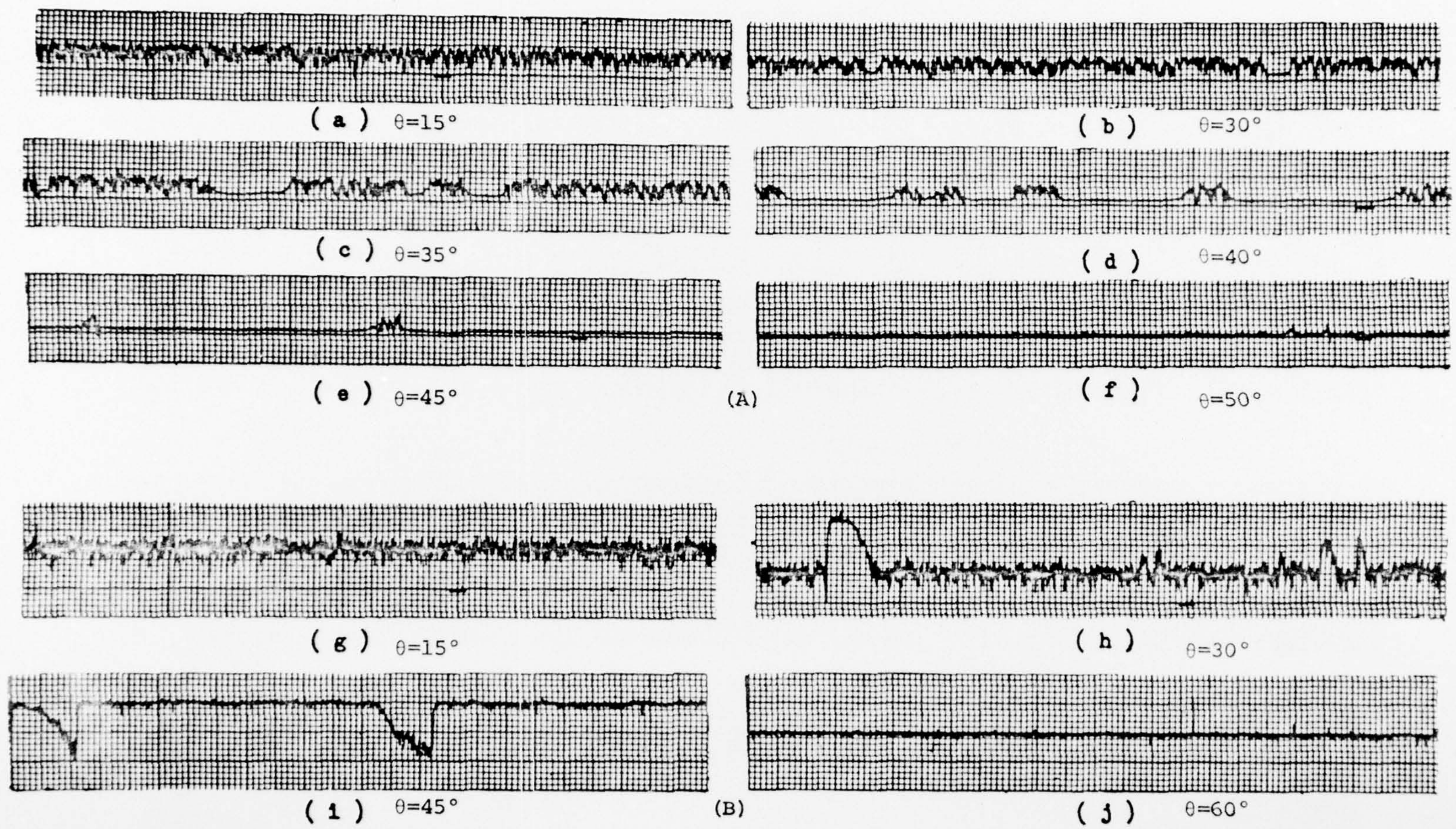

Figure 21. Typical strip chart records of the LDA output signal in steady flow from experimental series 2
(A) r=18.4 mm (B) r=0

(a) f = 0.23 Hz, r=0

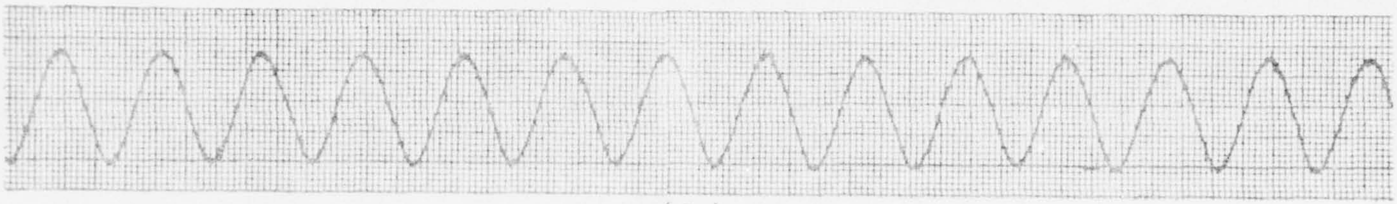

(b) f = 0.057 Hz, r=0

(c) f = 0.23 Hz, r=18.4 mm

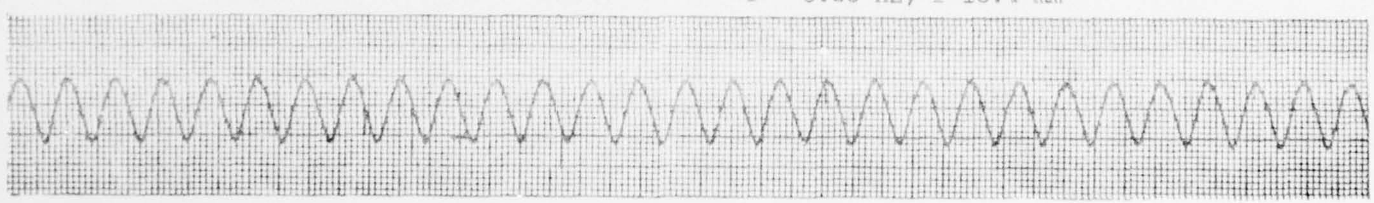

(d) f = 0.057 Hz, r=18.4 mm

Figure 22. Typical strip chart records of the LDA output signal in oscillatory flow from experiment series 2.
Intervals marked T denotes periods when the velocity trace is distorted from the normal laminar shape (shown by dotted lines) and are hence assumed to represent dutations of turbulent puffs

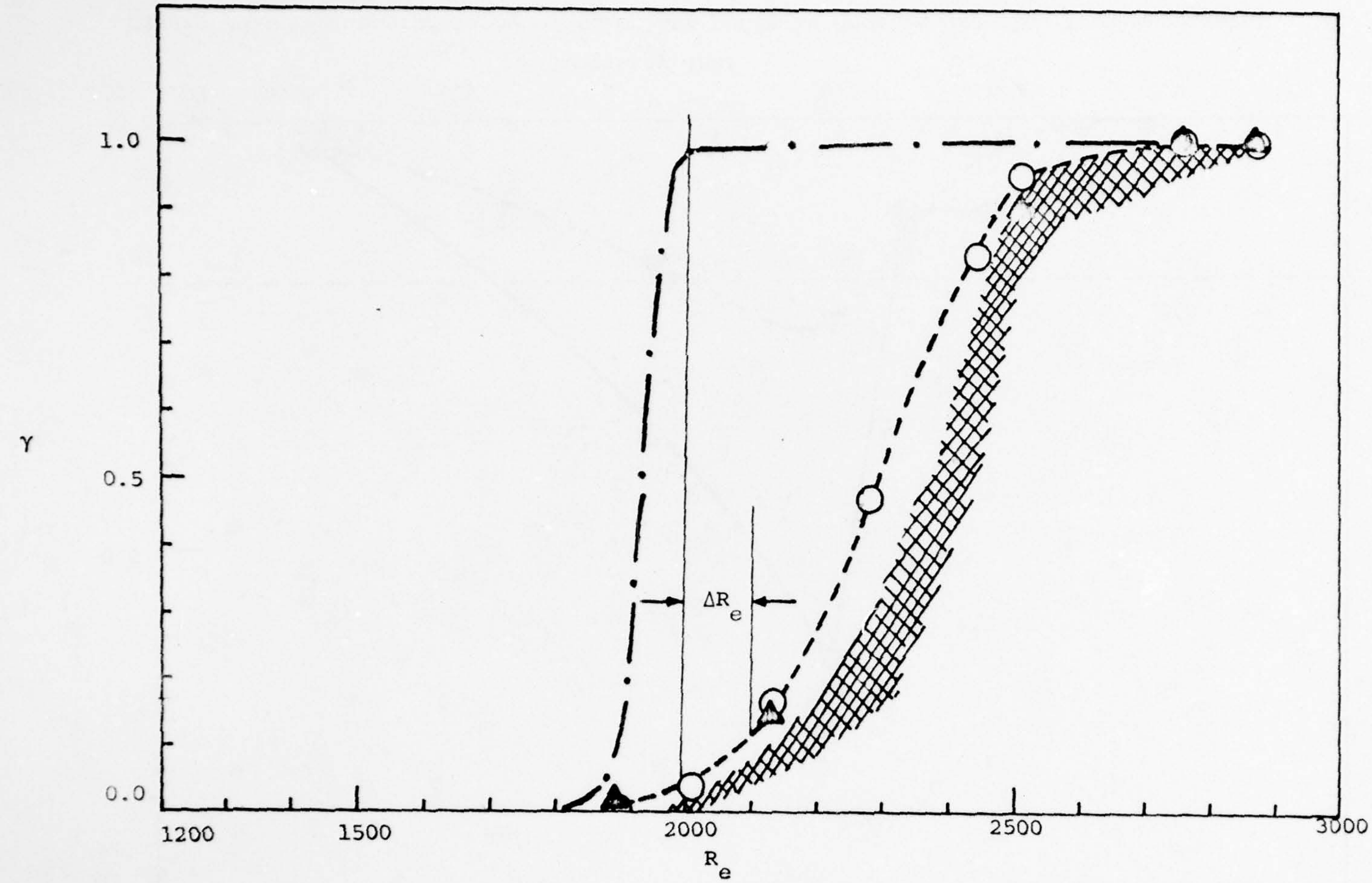

Figure 23. The intermittency of turbulent puffs in steady flow. Data from present series 2 experiments: --▲--, r =0; --0--, r =18.4 mm. —·—, (estimated) intermittency data for steady flow experiments of series 1; ▩, data of Wygnanski and Champagne (1973)

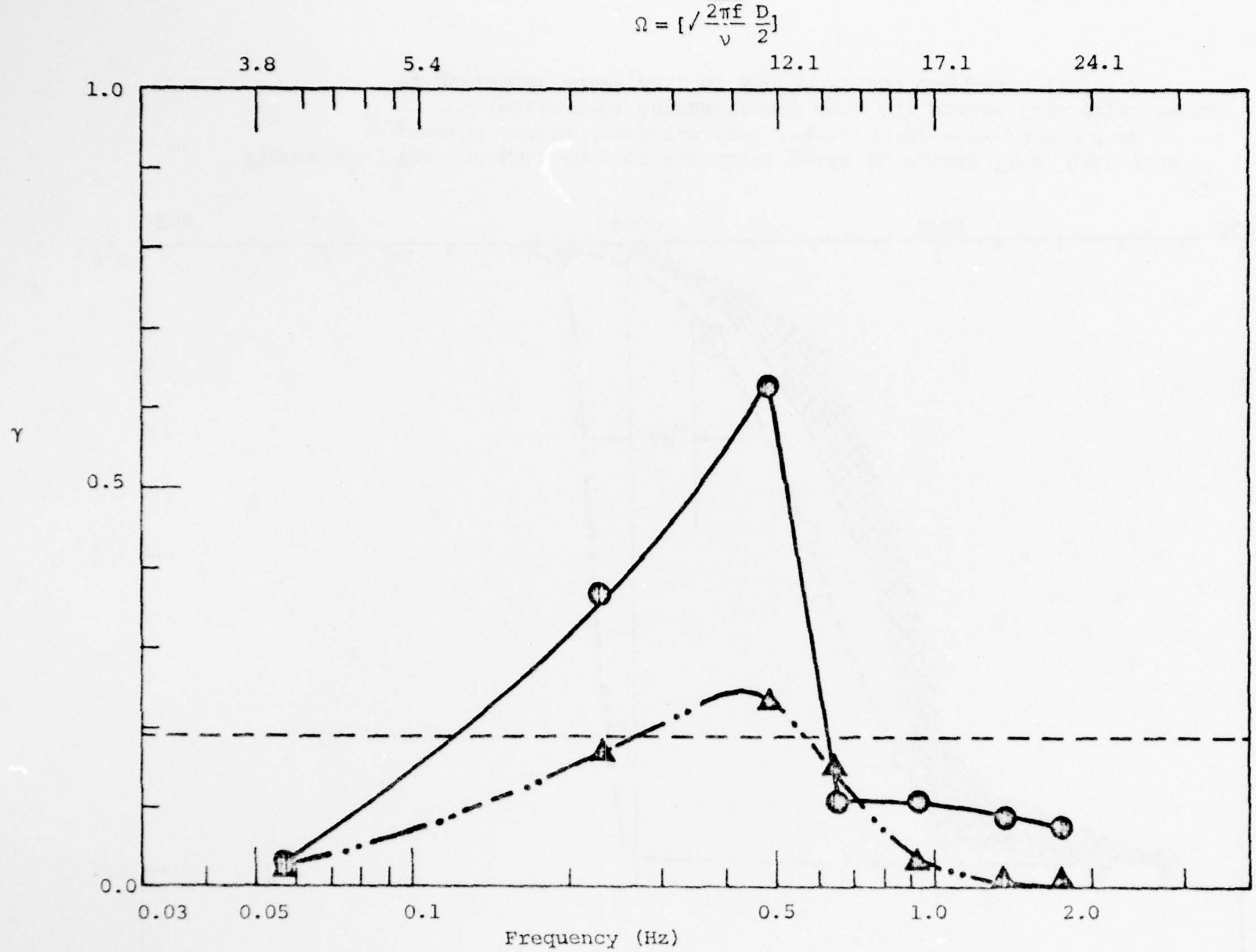

Figure 24. The intermittency of turbulent puffs in oscillatory flow from experiment series 2

—●—, r=0mm; —··—△—··—, r=18.4 mm; -----, mean quasi-steady flow at Re=2100 (θ=90°)

APPENDIX A

Description of the LDA System at IIHR and sample calculations of velocity from LDA signals

Description of the IIHR LDA System

A. The LDA System

The simple channel LDA system at IIHR is shown schematically in figure A.1. The system consists of a SPECTRAPHYSICS 5 mw He-Ne laser, ill'minating TSI (Thermo System Inc.) optics. The optics consists of a beam splitter which splits the laser beam into two beams each of half the original strength and spaced 50 mm apart. Each of the beams is then passed through an accousto-optic Bragg cell which shifts the frequency of the laser light by a preset amount. The Bragg-cells and the associated electronics were supplied by Opto-Elektronische-Instrumente. It's possible to shift the frequency of each beam independently by 7 selectable discrete frequencies ranging from 38.0 MHz to 44.0 MHz. By shifting the two beams by different frequencies one can obtain a relative frequency shift between the two outcoming beams. In the present case, a relative frequency shift of 0.3 MHz was used. The dual beams from the Bragg cells are focussed by the focussing lens of 104.1 mm focal length at the point (in reality, a finite sampling volume) in the fluid where the velocity is to be measured. The light scattered by a particle which passes through this volume is picked up by the receiving optics shown in the figure. The receiving optics consists of a pair of lenses and a prism that focusses the scattered light on to a photodiode. The photodiode converts the optical signal to an electrical signal which is then amplified.

In this particular arrangement, known as the dual beam system, the scattered light is essentially a mixture of the light scattered by the particle from the two incident beams. Let ν_o be the original laser beam frequency, ν_{B1} and ν_{B2} be the frequency shifts caused by the Bragg cell on the two incident beams, $\vec{n}_{i1}$ and $\vec{n}_{i2}$, the unit vectors in the directions of the incident beams, $\vec{r}$ the unit vector in the direction of collection (see figure A-1). Then, for an idealized case of scattering occurring due to a single particle travelling with a velocity $\vec{V}$ as shown, assuming uniform plane waves, one can write

$$\nu_1 = \nu_o + \nu_{B1} + \{\vec{V}\cdot\frac{\vec{r}-\vec{n}_{i1}}{\lambda_L}\} \qquad (A.1)$$

$$\nu_2 = \nu_o + \nu_{B2} + \{\vec{V}\cdot\frac{\vec{r}-\vec{n}_{i2}}{\lambda_L}\} \tag{A.2}$$

where ν_1 and ν_2 are the frequencies of scattered light from the two beams, and the bracketed terms represent the Doppler shift frequency in each case. The light picked up by the photodiode is a mixture of the above two. From the principle of hetrodyning, it can be shown that the resulting light will contain the mixture of the sum and difference of the above two frequencies. Of these, the difference equal to

$$(\nu_{B1} - \nu_{B2}) + \vec{V}\cdot[\frac{\vec{n}_{i2}-\vec{n}_{i1}}{\lambda_L}] \tag{A.3}$$

is the frequency of interest. This frequency is detected in the output signal by a frequency tracker. A TSI model 1090 tracker is used for this purpose. The tracker output, which is a linear function of the instantaneous velocity of the flow is low-pass filtered at 150 Hz to remove unwanted noise and then connected to the IIHR Data Acquisition System. The low-pass filtering frequency of 150 Hz was found to be high enough to include all significant turbulent frequencies in the flow. It is seen from Eq. A.3 that the output signal frequency is independent of the collection direction $\vec{r}$ (through the intensity of the collected light does depend on $\vec{r}$). It is also seen that at zero velocity, the output frequency will be $\nu_{B1} - \nu_{B2}$ i.e., equal to the imposed relative frequency shift.

It is appropriate to mention here briefly some of the problems encountered in LDA measurements. One of them, viz., directional ambiguity has been overcome in the present studies by using frequency shifting technique. Secondly, particle size and distribution introduce complexities, not encountered in the simple single particle analysis. The particle size influences scattered light distribution and intensity, the ability of a particle to follow the flow and the signal to noise ratio. Also, the higher the particle concentration, the more will be the background noise due to phase differences between particles arriving at the sampling volume. Low particle concentrations, on the other hand, limit the velocity versus time information as well as generally increase the complexity of data processing

due to discontinuity in the data, or "signal drop out". Signal drop out can also be caused by large variations in velocity with time as can occur in highly turbulent flows, very low velocities and in oscillatory flows. In these cases, the accompanying frequency changes are too large to be tracked by the tracker. The use of frequency shifting, in fact, has the added advantage of bringing the range of frequency variations into the most efficient region of tracker operation. Ideally, the particles should have a high refractive index, be uniform in size, and be as large as possible (up to 5μ) while still following the flow. The concentration should be low enough to minimize Doppler ambiguity while high enough to obtain adequate time information on flow characteristics. To approach this ideal seeding is generally required. However, naturally occurring particulates in the fluid may often be adequate to give satisfactory results, as in the present study. Thirdly, the spatial resolution of LDA is limited by the requirement of a finite sampling volume. With reference to figure A-1 the dimensions L_m and D_m of the sampling volume depend on the intersection angle ϕ of the beams in the fluid and the diameter of the beam. In the present experiments the dimensions L_m and D_m are 1.1 mm and 0.7 mm respectively. The dimension L_m is very much larger than the diameter of a hot-wire (2.5 μm) but comparable to the diameter of a total head tube. It is, however, to be noted that since oil was used in the present studies, the dimension L_m is still less than the thickness ($\cong$1.5 mm) of the viscous sublayer. The calculations required for obtaining the value of velocity from the LDA output are described in Appendix B.

B. <u>The Traverse Mechanism for LDA</u>

A simple one dimensional traverse mechanism was built for traversing the LDA optics along a horizontal diameter of the test section. The construction of this traverse can be seen from figure A-2. The upper alluminium channel slides over the bottom alluminium channel. The latter rests on a mild steel framework and can be adjusted to be level by using the four levelling screws. The upper channel is moved longitudinally by a spindle and has a travel of 50 mm. A dial indicator of 0.01 mm least count is mounted in such a way as to measure the displacement of

the upper channel. The laser, the entire optics and the photodiode are all mounted on wooden bases fixed to the upper alluminium channel and thus move together as one unit.

Because of the refraction effect, through the tube wall and the liquid, the actual displacement of the focal point (sampling volume) is not equal to the physical displacement of the traverse (apparent displacement). Knowing the thickness of the pipe wall and the refractive indices of the pipe wall and the oil, one can calculate the actual displacement of the focal point for a given apparent displacement. It was, however, felt that a practical calibration would be more desirable, as well as concenient, in the present case. A temporary arrangement consisting of an L-shaped point gage traversed by a precision micrometer (0.025 mm least count) was used for this purpose. The point gage was traversed through a hole in the tube wall, located at such a position that the tip of the gage travelled along the LDA axis. The location of the focal point could be easily determined from observing the light scattered by the tip of the gage as it moved along the axis of the LDA. The focal point was given a series of prescribed apparent displacements as measured by the dial indicator and the corresponding actual displacements as measured by the micrometer were obtained. The resulting calibration curve is shown in A.3 and is seen to be linear (as expected). This result was used in all subsequent experiments to obtain the actual displacement of the focal point. Theoretically, the uncertainty involved in the calibration was equal to the dimension "L_m" of the sampling volume. In practice, however, it was much less than this since it was possible to locate the two "extremes" of this region and set the point gage at the middle of these two positions. The finite length of the sampling volume did present some difficulty in fixing the "zero" distance from the wall during the velocity traverses. This difficulty was overcome by matching the velocity profile in steady laminar flow with the theoretical parabolic distribution. The "zero" so determined was used for the turbulent flow traverse also. In the unsteady flow, the location of the "zero" position was taken to be the point at which the oscillation amplitude (as observed on the oscilloscope) would suddenly go to zero. This was a very well defined point and could be located with

excellent repeatability.

C. Sample Calculation of Velocity from the LDA Signal

If f_D is the Doppler frequency shift, from Eq. (A.3)

$$f_D = \frac{n\vec{V}}{\lambda_L} \cdot (\vec{n}_{i1} - \vec{n}_{i2})$$

From Fig. A.1 $|\vec{n}_{i2} - \vec{n}_{i1}| = 2 \sin \phi/2$

hence, $f_D = \frac{n\vec{V}}{\lambda_L} \cdot \vec{n}_{i2} - \vec{n}_{i1} = 2 \frac{nU}{\lambda_L} \sin \phi/2$

where U is the velocity component normal to the bisector of $\vec{n}_{i1}$ and $\vec{n}_{i2}$. The value of n is taken as unity in air and the angle as $\tan^{-1}$ (d/2L,) where d is the original beam spacing introduced by the beam splitter and L is the focal length of the focussing lens. It can be easily shown that even when the beams pass through media of different refractive indices (in the present experiment, for example, they pass through the plexiglass tube wall and then through the oil), the produce ($n \cdot \sin \phi/2$) can still be calculated using the above values for n and ϕ. Hence Eq. (A.3) can be written as

$$f_D = \frac{2U \sin [\mathrm{Tan}^{-1} (d/2L)]}{\lambda_L}$$

or

$$U = f_D [\frac{\lambda_L}{2 \sin [\tan^{-1} (d/2L)}] = K f_D$$

For the present LDA system, $\lambda_L = 632.8$ nm, L = 104.1 mm and d = 50 mm. Hence,

$$K = 1.313 \text{ m/s/MHz}$$

If the relative frequency shift introduced by the Bragg cells is f_s and the measured frequency is f_m

$$U = (f_m - f_s) K$$

As already mentioned, the value of f_s in the present experiments was 0.3 Hz. The tracker output voltage E is proportional to f_m or $E = cf_m$. Hence,

$$U = (\frac{E}{C} - f_s)K \; (E - Cf_s) \frac{K}{C} = \frac{(E-E_o)K}{C}$$

where E_o is the tracker output voltage at zero velocity. In he present experiments c was 1 volt/MHz ± 0.4%. Thus,

$$U = (E - 0.3) \times 1.313 \text{ m/s}$$

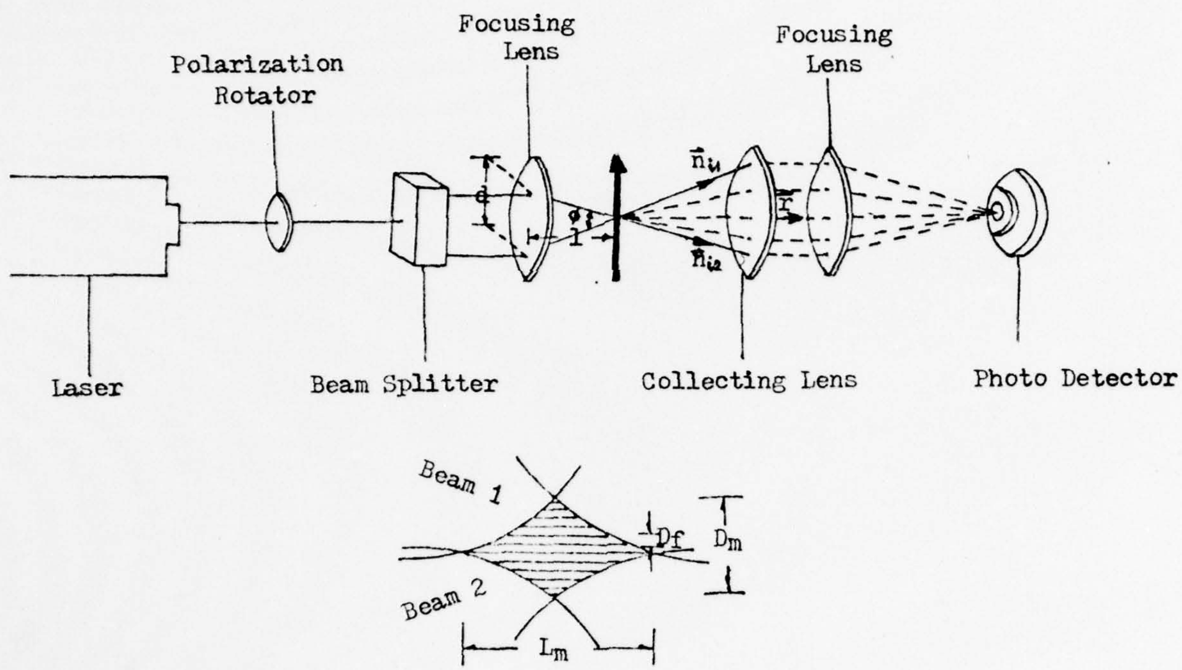

FIG. A1. A DESCRIPTION OF THE IIHR LDA IN DUAL BEAM, FORWARD SCATTER MODE

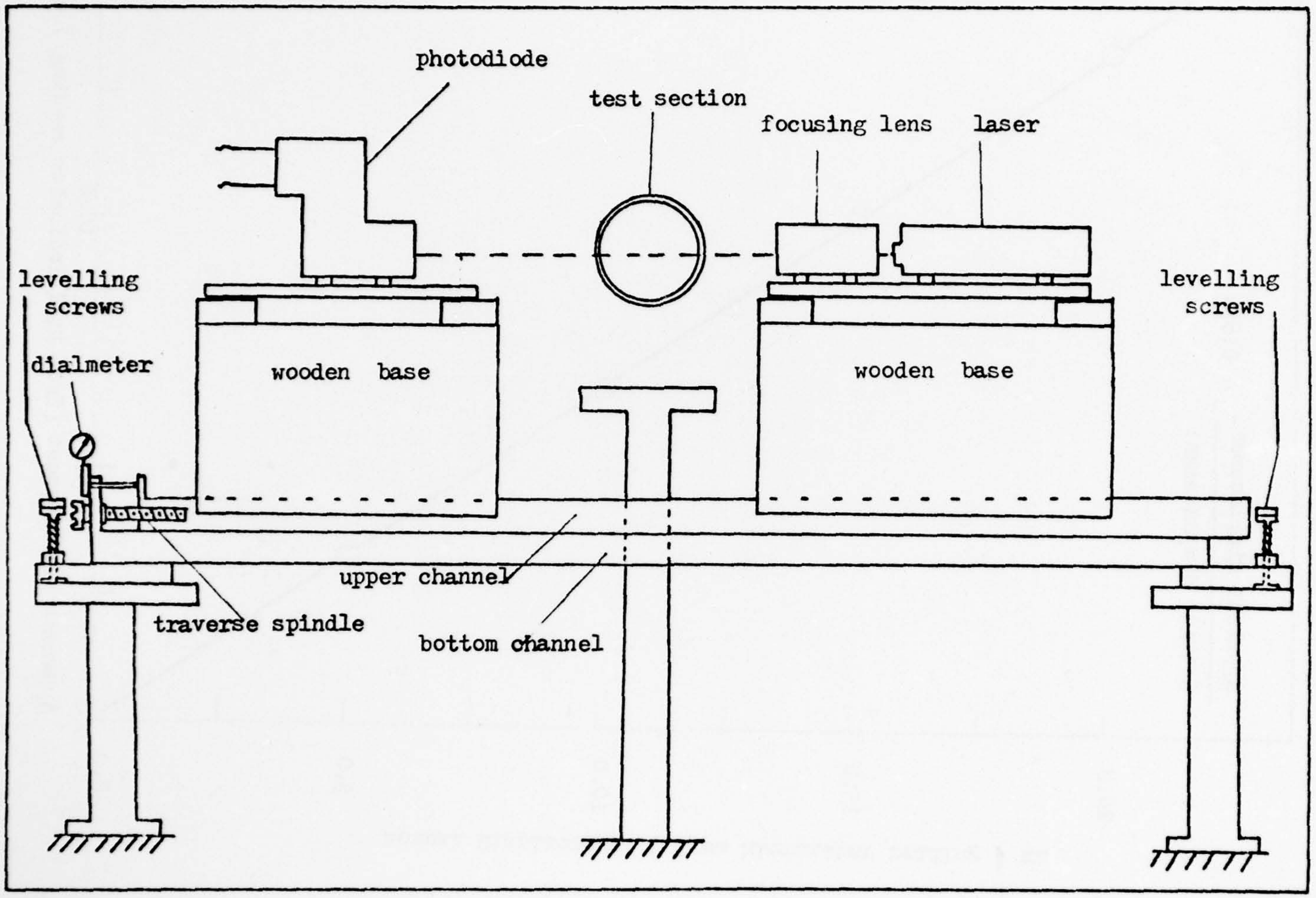

FIG. A2. DETAILS OF THE LDA TRAVERSE

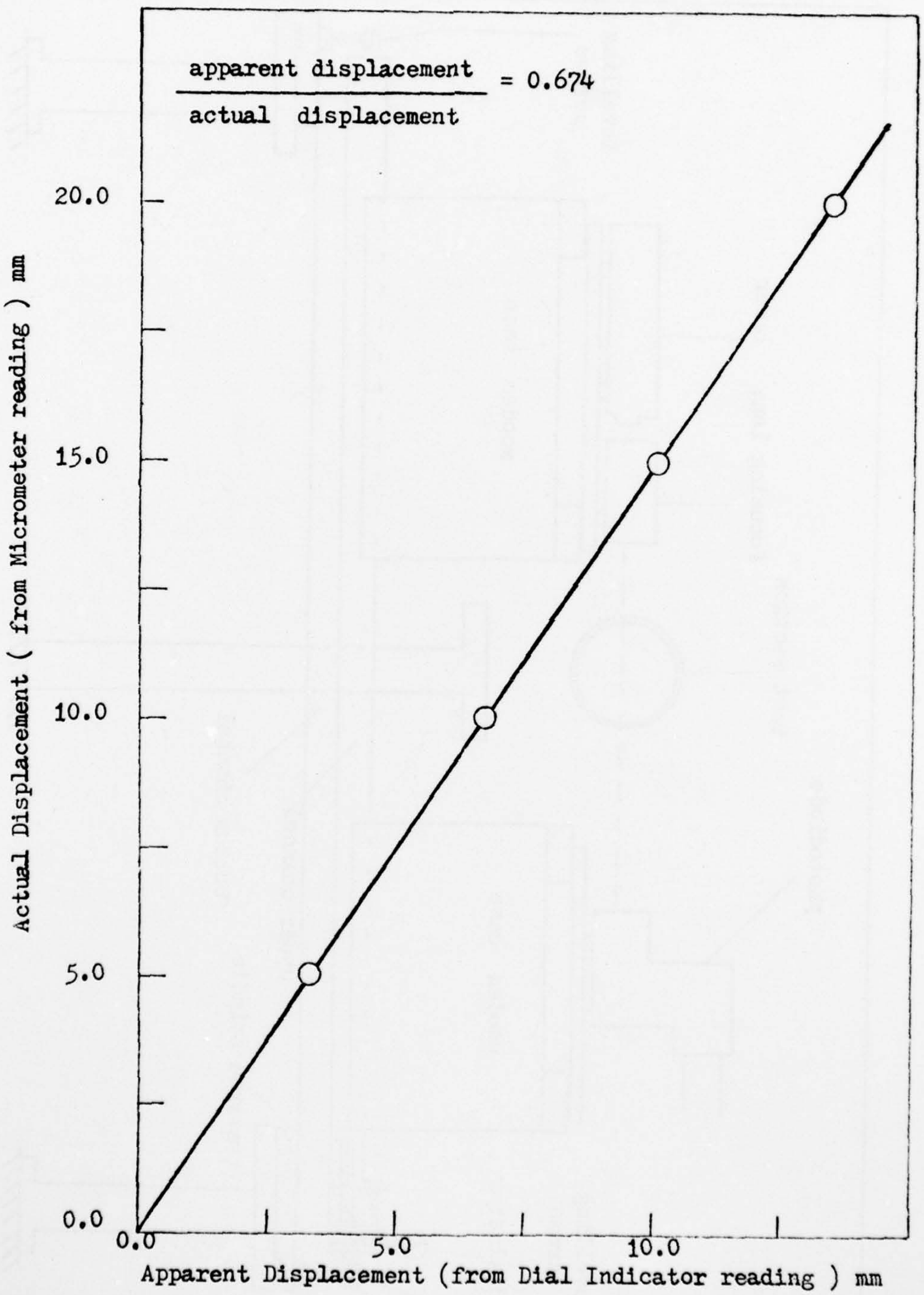

FIG. A3. CALIBRATION OF THE LDA TRAVERSE

APPENDIX B

Experimental Data

AD-A081 180   IOWA INST OF HYDRAULIC RESEARCH IOWA CITY   F/G 20/4
EXPERIMENTS ON TRANSITIONAL OSCILLATORY PIPE FLOW,(U)
AUG 79 B R RAMAPRIAN, S W TU   DAAG-29-79-G-0017

UNCLASSIFIED   IIHR-221   NL

2 OF 2
AD
A081180

END
DATE
FILMED
3-80
DDC

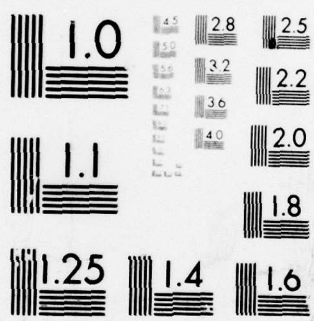

MICROCOPY RESOLUTION TEST CHART
NATIONAL BUREAU OF STANDARDS-1963-A

TABLE 1.

STEADY PRESSURE DROP

$\nu = 1.384 \times 10^{-5}$ m^2/s

x/D \ Δp^* \ Re	2872	2760	2513	2132	1818	1402	1278
6	0.0	0.0	0.0	0.0	0.0	0.0	0.0
12	0.561	0.458	0.475	0.589	0.687	1.506	0.941
24	-	1.479	1.989	1.267	1.153	1.442	-
36	1.415	1.532	1.617	1.624	1.914	2.266	2.578
42	1.553	-	-	-	-	-	2.874
48	-	2.022	2.144	2.302	2.552	2.844	3.171
54	2.033	-	-	-	-	-	3.567
60	-	2.628	2.618	2.819	3.018	3.339	3.915
66	2.575	-	-	-	-	-	4.262
72	-	3.246	3.093	3.336	3.558	3.874	4.608
78	3.184	-	-	-	-	-	4.956
84	-	3.788	3.825	3.854	4.098	4.781	5.253
90	3.715	-	-	-	-	-	5.649
96	-	4.299	4.428	4.370	4.540	5.399	5.945
102	4.304	-	-	-	-	-	6.244
108	-	4.863	4.993	4.959	4.982	5.977	6.541
114	4.854	-	-	-	-	-	-
120	-	5.416	5.532	5.405	5.448	6.553	7.186
126	5.395	-	-	-	-	-	-
132	-	6.076	6.186	5.958	5.840	7.172	7.831
138	5.965	-	-	-	-	-	-
144	-	6.726	6.777	6.547	6.282	7.789	8.424
150	6.486	-	7.123	-	-	-	-
156	-	7.236	7.393	7.153	6.649	8.326	8.969
162	7.075	-	7.726	-	6.943	-	9.265
168	7.390	7.864	7.996	7.795	7.189	8.821	9.564

$\bar{U}$ave :(m/s) , dp/dx : (newton/m^2/m)

$\bar{U}$ ave	0.780	0.750	0.683	0.580	0.494	0.381	0.348
-dp/dx	233.73	224.78	191.95	140.59	74.93	57.65	49.95
$\lambda \cdot 10^{+2}$	4.620	4.850	5.000	5.090	3.730	4.820	5.020

TABLE 2.

MEASUREMENTS IN STEADY FLOW

η	Re= 2872 ($\theta = 0°$)						Re = 1278 ($\theta = 90°$)	
	RUN 12				RUN 22		RUN 11	RUN 21
	$<\bar{U}>/<\bar{U}>_{max}$	$<\bar{U}>/\bar{U}_*$	$y\bar{U}_*/\nu$	$u'/\bar{U}_*$	$<\bar{U}>/<\bar{U}>_{max}$	$u'/\bar{U}_*$	$<\bar{U}>/<\bar{U}>_{max}$	$<\bar{U}>/<\bar{U}>_{max}$
0.0	0.0	0.0	0.0	0.0	0.0	0.0	0.0	0.0
0.039	0.218	4.15	4.14	1.55	0.327	1.70	0.095	0.099
0.118	0.619	11.48	12.42	2.35	0.631	2.39	0.221	0.236
0.197	0.745	13.98	20.71	2.21	0.759	2.23	0.362	0.372
0.276	0.828	15.36	28.99	1.90	0.832	1.91	0.470	0.484
0.354	0.851	16.11	37.28	1.60	0.866	1.65	0.582	0.583
0.433	0.894	16.59	45.56	1.46	-	-	0.675	-
0.512	0.926	17.17	53.84	1.28	0.957	1.12	0.769	0.749
0.591	0.943	17.49	62.13	1.19	-	-	0.826	-
0.670	0.969	17.97	70.41	1.05	-	-	0.880	0.877
0.748	0.983	18.23	78.69	0.92	-	-	0.927	-
0.827	0.986	18.34	86.98	0.85	0.991	0.9	0.964	0.962
0.945	1.0	18.55	99.40	0.80	1.0	0.85	1.0	1.0
$<\bar{U}>_{max}$ (m/s)	1.06				1.07		0.709	0.711
$\bar{U}_{ave}$ (m/s)	0.783				*		0.351	*
$\bar{U}_*$ (m/s)	0.057**						-	-

* In RUN 21 and RUN 22, measurements were made at only a few points to check RUN 11 and RUN 12, hence enough points were not available to calculate $\bar{U}$ave. However, $\bar{U}$ave in these experiments can be assumed to be the same as in RUN 11 and RUN 12 respectively.

** Based on pressure drop measurements.

TABLE 3.

MEASUREMENTS IN UNSTEADY FLOW (RUN 23)

$\bar{U}_{max}$=1.086m/s, $(U_{qm})_{pmax}$= 0.43 m/s , $\bar{u}_*$ =0.0344 m/s

η	$\bar{u}/\bar{u}_{max}$	$u_{pmax}/(U_{qm})_{pmax}$	$\bar{u}/\bar{u}_*$	$y\bar{u}_*/\nu$	ϕ_*(degrees)
0.0	0.0	0.0	0.0	0.0	-
0.04	0.078	0.365	2.516	2.486	-60.8
0.08	0.163	0.602	5.164	4.972	-72.0
0.158	0.297	0.696	9.380	9.944	-79.2
0.197	0.361	0.672	11.400	12.430	-82.8
0.236	0.414	0.652	13.056	14.916	-86.4
0.276	0.470	0.647	14.827	17.402	-90.0
0.315	0.522	0.640	16.475	19.888	-79.2
0.354	0.572	0.647	18.043	22.374	-86.4
0.394	0.619	0.640	19.531	24.860	-82.8
0.472	0.700	0.640	22.10	29.831	-82.8
0.551	0.775	0.643	24.464	34.803	-82.8
0.630	0.836	0.659	26.404	39.775	-86.4
0.709	0.884	0.656	27.919	44.747	-82.8
0.787	0.929	0.656	29.327	49.719	-82.8
0.866	0.962	0.656	30.381	54.691	-86.4
0.984	1.0	0.656	31.568	62.149	-86.4

TABLE 4.

MEASUREMENTS IN UNSTEADY FLOW (RUN 24)

$\bar{U}_{max}$ = 1.11 m/s , $(U_{qm})_{pmax}$ = 0.43 m/s , $\bar{u}_*$ =0.036 m/s

η	$\bar{u}/\bar{u}_{max}$	$u_{pmax}/(U_{qm})_{pmax}$	$\bar{u}/\bar{u}_*$	$y\bar{u}_*/\nu$	ϕ_*(degree)
0.0	0.0	0.0	0.0	0.0	-
0.04	0.082	0.214	2.541	2.583	- 7.2
0.08	0.170	0.395	5.286	5.166	+ 14.4
0.158	0.328	0.769	10.256	10.331	+ 14.4
0.236	0.461	1.029	14.365	15.497	+ 14.4
0.315	0.584	1.205	18.210	20.662	+ 14.4
0.394	0.691	1.367	21.535	25.828	0
0.472	0.780	1.463	24.322	30.994	0
0.551	0.856	1.607	26.667	36.160	- 14.4
0.630	0.910	1.743	28.372	41.325	- 7.2
0.709	0.954	1.771	29.719	46.491	- 7.2
0.787	0.998	1.983	31.117	51.657	- 21.6
0.866	1.007	1.914	31.364	56.822	- 14.4
0.984	1.000	1.897	31.151	64.571	- 21.6

TABLE 5.

MEASUREMENTS IN UNSTEADY FLOW (RUN 13)

$\bar{U}_{max}$=0.818 m/s , $(U_{qm})_{pmax}$=0.43 m/s , $\bar{u}_*$ = 0.0535 m/s

η	$\bar{u}/\bar{u}_{max}$	$u_{pmax}/(U_{qm})_{pmax}$	$\bar{u}/\bar{u}_*$	$y\bar{u}_*/\nu$	ϕ_*(degrees)	$u'/\bar{u}_*$	$u'/\bar{u}_{max}$
0.0	0.0	0.0	0.0	0.0	-	0.0	0.0
0.04	0.266	0.546	4.068	3.864	- 51.4	1.35	0.0883
0.08	0.370	0.652	5.664	7.729	- 64.3	1.66	0.1083
0.158	0.625	0.713	9.556	15.457	- 70.7	1.97	0.1284
0.236	0.741	0.651	11.339	23.186	- 77.1	1.86	0.1213
0.315	0.806	0.634	12.330	30.915	- 77.1	1.70	0.1115
0.394	0.867	0.675	13.265	38.643	- 70.7	1.44	0.0944
0.472	0.894	0.660	13.675	46.372	- 70.7	1.30	0.0850
0.551	0.921	0.643	14.091	54.101	- 64.2	1.19	0.0778
0.630	0.955	0.679	14.604	61.829	- 77.1	1.11	0.0721
0.709	0.975	0.660	14.923	69.558	- 83.6	1.01	0.0662
0.787	0.980	0.634	15.003	77.287	- 70.7	1.03	0.0670
0.866	0.993	0.638	15.197	85.016	- 83.6	0.974	0.0636
0.984	1.000	0.624	15.293	96.609	- 77.1	1.02	0.0667

APPENDIX C

Assembler Language Program for Sampling and Processing Periodic Turbulent Flows on the IIHR IBM/1800 System

```
// JOB   0000011111
// ASM AGSV3
*LIST
                         **************************************************
                         *          PROCESS PROGRAM AGSV3                 *
                         *  THIS PROGRAM TAKES DATA FROM MPXR PTS         *
                         *  /1016,/1017,/1018. A SYNCHRONIZING SIGNAL     *
                         *  MUST BE PRESENT FOR EXTERNAL SYNC ON THE ADC. *
                         *  EXITS AFTER 25 SECOND DELAY IF NO SYNC.       *
                         *  THE NO. OF WAVES, THE NO. OF POINTS PER WAVE, *
                         *  AND THE DELAY TIME BETWEEN DATA POINTS ARE    *
                         *  OBTAINED FROM FIL20. THE DATA OF THE 3.CHANNEL *
                         *  ARE TESTED FOR LOCKON OF THE LDA-TRACKER.     *
                         *  THE RAW DATA FROM ALL THREE CHANNEL ARE       *
                         *  STORED ON DISK IN FIL03,FIL04,FIL05.          *
                         *  PROGRAMMED BY MUELLER BASED ON AGSV2          *
                         *  MARCH, 1977                                   *
                         **************************************************
*0000 0  0877          START XIO       LITON
 0001 30 17493093            CALL      PKLPL
 0003 20 2EE63A15            LIBF      WRTYN
 0004 0  2002                DC        /2002
 0005 1  1000                DC        MTS5-1
 0006 0  0800          ON    DC        /0800
 0007 20 2EE63A15            LIBF      WRTYN
 0008 0  0002                DC        /0002
 0009 0  70FD                MDX       *-3
 000A 01 0C0001DE            XIO   L   IOCCA
 000C 0  E050                AND       M0200
 000D 0  4808                BSC       +
 000E 0  700C                MDX       NOCNG
 000F 30 22505093            CALL      SPECL
 0011 30 03201547            CALL      CHANG
 0013 30 24558000            CALL      UNC
 0015 30 011E2073            CALL      AGSV3
 0017 0  0001                DC        1
 0018 0  085D                XIO       LITOF
 0019 30 25241E00            CALL      VIAO
 001B 01 C40001CB      NOCNG LD    L   WDCNT      SET UP WORD COUNT TO STORE
 001D 01 D4000E69            STO   L   STDT1      DATA IN DISK.
 001F 01 D4000BEB            STO   L   STDT2
 0021 01 D400136D            STO   L   STDT3
 0023 0  10A0                SLT       32         SET ZERO IN A & Q REG.
 0024 01 DC000199            STD   L   AREAC+308
 0026 01 DC00019B            STD   L   AREAC+310
 0028 01 DC00019D            STD   L   AREAC+312
 002A 01 0C0001D0            XIO   L   IOCCD      SHUT OFF TIMERS.
 002C 00 C400000D            LD    L   /000D
 002E 01 D40002DE            STO   L   SAVE
 0030 00 C400000C            LD    L   /000C
 0032 01 D400019F            STO   L   AREAC+314
 0034 00 2C40000C            STS   L   /000C,/40
 0036 0  C02E                LD        ADDRT
 0037 00 D400000D            STO   L   /000D
 0039 0  C008                LD        DLY
 003A 00 D400000C            STO   L   /000C
 003C 01 0C0001CC            XIO   L   IOCCF
 003E 20 012578D5            LIBF      AIPTN
 003F 0  1010                DC        /1010
 0040 1  02F2                DC        DATAW+2
 0041 1  02F1                DC        DATAW+1
 0042 0  F3CB          DLY   DC        -3125      LOOP COUNT FOR DELAY FOR SYNC
 0043 20 012578D5            LIBF      AIPTN
 0044 0  0000                DC        /0000
```

```
0045 0  70FD              MDX      *-3
0046 01 0C0001C0          XIO   L  IOCCB
0048 01 C400002DF         LD    L  SAVE
004A 00 D400000D          STO   L  /000D
004C 0  7016              MDX      FORWD
004D 20 20C63A15    EXIT1 LIBF     WRTYN     TERMINATES IF NO SYNC.SIG.
004E 0  2002              DC       /2002
004F 1  1E5C              DC       DMES7-1
0050 0  0000              DC       0
0051 20 20C63A15          LIBF     WRTYN
0052 0  0002              DC       /0002
0053 0  70FD              MDX      *-3
0054 01 C40001DF    EXIT2 LD    L  AREAC+314
0056 00 D400000C          STO   L  /0006
0058 01 C400002DF         LD    L  SAVE
005A 00 D400000D          STO   L  /000D
005C 00 2041000D          STS   L  /000D,/41
005E 01 0C0001C6          XIO   L  IOCCE     START TIMERS
0060 0  0815              XIO      LITCF
0061 30 25241C00          CALL     VIAQ
0063 01 4C0001CA    FORWD BSC   L  PAUZ1
0065 0  0200        H0200 DC       /0200
0066 1  0067        ADDRT DC       TIMEW
0067 0  0000        TIMEW DC       *-*
0068 01 0C0001C0          XIO   L  IOCCB     SHUT OFF TIMERS
006A 01 0C0001C4          XIO   L  IOCCD     SENSE DSW.
006C 0  4878              BOSC     +Z-
006D 0  1000              NOP
006E 00 67000067          LDX   I3 103
0070 20 012578D5          LIBF     AIPTN
0071 0  3000              DC       /3000
0072 01 4C00004D          BSC   L  EXIT1
0074 0  0000        OFF   DC       0
0076    0000              BSS   E  0         INSURE THAT AREAA IS EVEN ADDRESS
0076 1  0074        LITCF DC       OFF
0077 0  617D              DC       /617D
0078 1  0006        LITON DC       ON
0079 0  617D              DC       /617D
007A 0  0004        AREAA DC       4
007B 31 06253C80    INFOM DSA      FIL20     INFORMATION STORED ON DISK.
007E 0  0000        DELAY DC       *-*       DELAY TIME.
007F 0  0000        PONTS DC       *-*       NO. OF POINTS ON A WAVE.
0080 0  0000        WAVES DC       *-*       NO. OF WAVES TAKEN.
0081 0  0000        CLICK DC       *-*       LOCATION OF RUN NO.
0082 0  0000        U00   DC       *-*
0083 0  0000        U11   DC       *-*
0084 0  0000        LIMT  DC       *-*
0085    0139        AREAC BSS      313
01BE    0000              BSS   E  0
01BE 0  0000        IOCCA DC       /0000     READ D.E.S INTO A  REG.
01BF 0  0740              DC       /0740
01C0 0  0000        IOCCB DC       /0000     SHUT OFF TIMERS
01C1 0  0420              DC       /0420
01C2 0  8000        IOCCC DC       /8000     TURN ON TIMER A
01C3 0  0420              DC       /0420
01C4 0  0000        IOCCD DC       /0000     SENSE DSW
01C5 0  0721              DC       /0721
01C6 0  2000        IOCCE DC       /2000     START TIMER C
01C7 0  0420              DC       /0420
01C8 0  0780        WDCNT DC       1920
01C9 0  3200        D128H DC       12800     LENGTH OF FILES 03 04 05
01CA 0  C005        PAUZ1 LD       WDCT2     SET UP WORD COUNT.
01CB 01 D400007B          STO   L  INFOM
01CD 20 04262495          LIBF     DISKN     READ INFORMATION FROM THE DISK.
01CE 0  1000              DC       /1000
01CF 1  007B              DC       INFOM
```

```
01D0 0  0140       WPCT2 DC        320
01D1 20 04262495         LIBF      DISKN
01D2 0  0100             DC        /0100
01D3 1  007B             DC        INFOM
01D4 0  70FC             MDX       *-4
01D5 20 26663A15         LIBF      WRTYN
01D6 0  2002             DC        /2002
01D7 1  1B48             DC        DMES6-1
01D8 0  0000             DC        0
01D9 20 26663A15         LIBF      WRTYN
01DA 0  0002             DC        /0002
01DB 0  70FD             MDX       *-3
01DC 20 23A17172         LIBF      TYPE2
01DD 1  007F             DC        DELAY
01DE 0  0003             DC        3
01DF 20 26663A15         LIBF      WRTYN
01E0 0  2002             DC        /2002
01E1 1  1B74             DC        DMES9-1
01E2 0  0000             DC        0
01E3 20 26663A15         LIBF      WRTYN
01E4 0  0002             DC        /0002
01E5 0  70FD             MDX       *-3
01E6 20 23A17172         LIBF      TYPE2
01E7 1  0082             DC        U00
01E8 0  0003             DC        3
01E9 01 C4000082         LD    L   U00        TRANSFER U0,U1,LIMIT
01EB 01 D40002C9         STO   L   U0
01ED 01 C4000083         LD    L   U11
01EF 01 D40002CA         STO   L   U1
01F1 01 C4000084         LD    L   LIMIT
01F3 01 D40002CC         STO   L   LIMIT
01F5 01 C4000080         LD    L   WAVES
01F7 01 A400007F         M     L   PONTS
01F9 0  1090             SLT       16
01FA 0  B0CF             CMP       D128N      FILE LENGTH IS 40 SECTORS
01FB 0  7002             MDX       NGOOD
01FC 0  700A             MDX       GOOD
01FD 0  7009             MDX       GOOD
01FE 20 26663A15   NGOOD LIBF      WRTYN
01FF 0  2002             DC        /2002
0200 1  1BC4             DC        DMES8-1
0201 0  0000             DC        0
0202 20 26663A15         LIBF      WRTYN
0203 0  0002             DC        /0002
0204 0  70FD             MDX       *-3
0205 01 4C00004D         BSC   L   EXIT1      OUT IF FILES TOO SMALL
0207 01 C4000080   GOOD  LD    L   WAVES
0209 01 D40002DC         STO   L   NUMBR      STORE NO. OF WAVES
020B 01 C400007F         LD    L   PONTS
020D 0  1001             SLA       1          MULTIPLY BY TWO
020E 01 D40002DD         STO   L   TWPTS      TWICE THE NUMBER OF POINTS
0210 0  1080             SLT       32         ZERO A AND Q REG.
0211 01 940002DD         S     L   TWPTS
0213 01 D40002DD         STO   L   TWPTS      MINUS TWICE THE NUMBER
0215 0  1010             SLA       16         ZERO A REG.
0216 01 9400007F         S     L   PONTS      OBTAIN  TWICE THE NUMBER
0218 01 D40002DE         STO   L   NNPTS      OF POINTS NEGATIVE.
021A 01 0C0001C0         XIO   L   IOCCB      SHUT OFF TIMER C
021C 00 C400000B         LD    L   /000B      SAVE THE ADDRESS OF IBM'S
021E 01 D40002DF         STO   L   SAVE       LEVEL ZERO INTER. ROUTINE.
0220 00 2C40000B         STS   L   /000B,64   UNWRITE STOR. PROT. BIT.
0222 01 C40002EB         LD    L   ADDRA      SUBSTITUTE OUR INTERRUPT
0224 00 D400000B         STO   L   /000B      ROUTINE ADDRESS.
0226 30 14062480         CALL      MASK
0228 1  1AE0             DC        MSK1
0229 1  1AE1             DC        MSK2
```

```
022A 01 C400007F      SYNCK LD    L  DELAY       SET UP DELAY INT TIMER  A
022C 00 D4000004            STO   L  /0004
022E 01 C5000288            LDX   I1 TNPTS       LOOP FOR DATA
0230 20 01257805            LIBF     AIPTN       TAKE FIRST PT. ONLY AFTER THE
0231 0  1010                DC       /1010       SYNC. SIGNAL IS RECEIVED.
0232 1  02F2                DC       DATAU+2
0233 1  02F1                DC       DATAU+1
0234 0  0000                DC       /0000
0235 20 01257805            LIBF     AIPTN
0236 0  0000                DC       /0000
0237 0  70FD                MDX      *-3
0238 0  0889                XIO      IOCCC       START TIMER A
0239 0  3000                WAIT                 WAIT FOR TIMER INTERRUPT
023A 0  70FE                MDX      *-2
023B 0  0000          TIMER DC       *-*         TIMER INTERRUPT ROUTINE
023C 0  0887                XIO      IOCCD       SENSE DESW
023D 0  4878                BOSC     +Z-         RESET INDICATORS
023E 0  1000                NOP
023F 01 C400007F            LD    L  DELAY
0241 00 D4000004            STO   L  /0004       RESET TIMER A
0243 20 01262615            LIBF     AISQN       OBTAIN DATA SEQUENTIALLY.
0244 0  2000                DC       /2000
0245 1  02E0                DC       DATAU
0246 1  02F8                DC       ERROR
0247 20 01262615            LIBF     AISQN       TEST FOR COMPLETION.
0248 0  0000                DC       /0000
0249 0  70FD                MDX      *-3
024A 01 C40002E2            LD    L  DATAU+2
024C 01 D400046B      DKST1 STO   L  STDT1+2     FOR CHANNEL1.
024E 01 7401024D            MDX   L  DKST1+1,1
0250 01 C40002F3            LD    L  DATAU+3
0252 01 D40008ED      DKST2 STO   L  STDT2+2     STORE CHAN.2 DATA IN DISK AREA.
0254 01 74010253            MDX   L  DKST2+1,1   SET UP FOR NEXT CSL STORE.
                      *                          TEST FOR TRACKER
0256 01 C40002F4            LD    L  DATAU+4     TEST IF U1>U0
0258 0  8010                A        U0
0259 0  4810                BSC      -
025A 0  7015                MDX      OK
025B 01 C40002F4            LD    L  DATAU+4     TEST /UI-UI-1/>U1
025D 0  9009                S        LAST
025E 0  4810                BSC      -
025F 0  7003                MDX      LIMTE
0260 0  D007                STO      MEMO
0261 0  1010                SLA      16
0262 0  9005                S        MEMO
0263 0  B006          LIMTE CMP      U1
0264 0  700B                MDX      OK
0265 0  7008                MDX      NOK
0266 0  7007                MDX      NOK
0267 0  0000          LAST  DC       *-*
0268 0  0000          MEMO  DC       *-*
0269 0  0640          U0    DC       1600        U0=100MVOLT
026A 0  0020          U1    DC       32          U1=2MVOLT
026B 0  0000          COUNT DC       *-*
026C 0  000A          LIMIT DC       10
026D 0  0000          ZERO  DC       0
026E 01 7401026B      NOK   MDX   L  COUNT,1
0270 01 C40002F4      OK    LD    L  DATAU+4
0272 0  D0F4                STO      LAST
0273 01 D400136F      DKST3 STO   L  STDT3+2     STORE CHAN .3 DATA ON DISK.
0275 01 74010274            MDX   L  DKST3+1,1   SET UP FOR NEXT CSL STORE.
0277 0  7102                MDX    1 +2          DECREMENT INDEX REGISTER.
0278 0  7001                MDX      TIMEX       RETURN FOR NEXT SAMPLE ON THIS WAVE
0279 0  7002                MDX      NWAVE       END SAMPLING . NEXT WAVE.
027A 01 4C80023B      TIMEX BSC   I  TIMER       END OF TIMER INTER. ROUTINE.
027C 01 0C0001C0      NWAVE XIO   L  IOCCP       SHUT OFF TIMERS.
```

```
027D 0  C0FC              LD        COUNT      TEST NO OF BAD POINTS
027E 0  90FC              S         LIMIT
0280 0  4808              BSC       +
0281 0  7012              MDX       GOON
0282 20 23A17172          LIBF      TYPE2
0283 1  026B              DC        COUNT
0284 0  0001              DC        1
0285 0  C0C7              LD        DKST1+1    RESTORES ADDRESS CH.1
0286 01 9400007F          S     L   PONTS
0288 0  D0C4              STO       DKST1+1
0289 0  C0C9              LD        DKST2+1    RESTORES ADDRSS CH.2
028A 01 9400007F          S     L   PONTS
028C 0  D0C6              STO       DKST2+1
028D 0  C0E6              LD        DKST3+1    RESTORES ADDRESS CH.3
028F 01 9400007F          S     L   PONTS
0290 0  D0E3              STO       DKST3+1
0291 0  C0DB              LD        ZERO       RESET COUNT
0292 0  D0D8              STO       COUNT
0293 0  709E              MDX       SYNCK
0294 0  C0D8       GOON   LD        ZERO
0295 0  D0D5              STO       COUNT
0296 0  C0B6              LD        DKST1+1
0297 01 94000468          S     L   ADD07
0299 01 B4000168          CMP   L   WRCNT      CHECK TO SEE IF THE DISK
029B 0  7001              MDX       OUT        AREA IS FULL.
029C 0  7002              MDX       DCRNT
029D 01 44000429   OUT    BSI   L   ODISK      GO TO DISK OUTPUT SUBROUTINE.
029F 01 74FF02DC   DCRNT  MDX   L   NUMBR,-1   DECREMENT NUMBER OF WAVES.
02A1 0  7008              MDX       SYNCK      GO BACK TO SYNCK LOOP.
02A2 01 44000429          BSI   L   ODISK
02A4 0  C03A       EXITS  LD        SAVE       RESTORE 1800'S LEVEL ZERO
02A5 00 D400000D          STO   L   /000D      INTER. ROUTINE ADDRESS.
02A7 00 2C41000D          STS   L   /000D,C5   WRITE STORAGE PROT. BIT.
02A9 30 24554480          CALL      UNMK
02AB 1  1AF0              DC        MSK1
02AC 1  1AF1              DC        MSK2
02AD 01 0C0001CE          XIO   L   IOCCE      TURN ON TIMER C.
02AF 30 034D6002          CALL      CLOCK      OBTAIN RUN NUMBER.
02B1 1  0081              DC        CLICK
02B2 0  C03A              LD        DE320
02B3 01 D400007B          STO   L   INFOM
02B5 20 04262495          LIBF      DISKN      WRITE OUT THE DATA ON DISK.
02B6 0  3000              DC        /3000      DATA MAY BE USED FOR PLOTTING.
02B7 1  007B              DC        INFOM
02B8 0  0000              DC        /0000
02B9 20 04262495          LIBF      DISKN
02BA 0  0100              DC        /0100
02BB 1  007B              DC        INFOM
02BC 0  70FC              MDX       *-4
02BD 01 C4000081          LD    L   CLICK
02BF 20 02255103          LIBF      BINDC      CONVERT RUN NUMBER FOR
02C0 1  1B07              DC        INPUT      PRINTOUT.
02C1 20 085935D9          LIBF      HOLEB
02C2 0  0000              DC        /0000
02C3 1  1B07              DC        INPUT
02C4 1  1AFA              DC        OTPUT
02C5 0  0006              DC        6
02C6 20 23A17155          LIBF      TYPEN      PRINT RUN NUMBER.
02C7 0  2002              DC        /2002
02C8 1  1AF2              DC        DMES3-1
02C9 0  0000              DC        0
02CA 20 23A17155          LIBF      TYPEN      TEST OP. COMPLETE.
02CB 0  0000              DC        0
02CC 0  70FD              MDX       *-3
02CD 30 24558000          CALL      UNC
02CF 30 011F2973          CALL      AGSV3
```

```
02D1 1  0435                DC       UNK
02D2 30 18985985            CALL     QUEUE
02D4 30 03543CF3            CALL     CCMPT
02D6 0  0001                DC       1
02D7 0  0000                DC       0
02D8 01 0C00007C            XIO   L  LITOF
02DA 30 75241C00            CALL     VIAQ
02DC 0  0000         NUMBR  DC       *-*      NUMBER OF WAVES TO BE SAMPLED
02DD 0  0000         TNPTS  DC       *-*      TWICE NO. OF POINTS.
02DE 0  0000         MNPTS  DC       *-*      MINUS TWICE NO. OF PTS.
02DF 0  0000         SAVE   DC       *-*      SAVED ADDRESS IN /000D
02E0 0  0004         DATAW  DC       4
02E1 0  101C                DC       /101C
02E2 1  02E2                DC       DATAW+2
02E3 1  02E3                DC       DATAW+3
02E4 1  02E4                DC       DATAW+4
02E5    0003                BSS      3
02E8 0  0000         ERROR  DC       *-*
02E9 01 4C0002E8            BSC   I  ERROR
02EB 1  023B         ADDRA  DC       TIMER    ADDRESS OF TIMER ROUTINE
02EC 0  2717         SCALE  DC       10007    SCALING COEF.
02ED 0  0140         DE320  DC       320      CONSTANT USED FOR DISKN
02EE    0000                BSS   E  0
02EE    013B         AREAR  BSS      315      DISKN AREA
0429 0  0000         ODISK  DC       *-*      DISK OUTPUT SUBROUTINE.
042A 20 04262495            LIBF     DISKN    RUN RAW DATA INTO DISK
042B 0  3000                DC       /3000    FOR CHAN1.
042C 1  0469         ADC01  DC       STDT1
042D 0  0000                DC       0
042E 20 04262495            LIBF     DISKN
042F 0  0100                DC       /0100
0430 1  0469                DC       STDT1
0431 0  70FC                MDX      *-4
0432 20 04262495            LIBF     DISKN    RUN RAW DATA INTO DISK
0433 0  3000                DC       /3000    FOR CHAN.2.
0434 1  0BEB         ADC02  DC       STDT2
0435 0  0001         UNK    DC       1
0436 20 04262495            LIBF     DISKN
0437 0  0100                DC       /0100
0438 1  0BEB                DC       STDT2
0439 0  70FC                MDX      *-4
043A 20 04262495            LIBF     DISKN    RUN RAW DATA INTO DISK
043B 0  3000                DC       /3000    FOR CHAN.3.
043C 1  136D         ADC03  DC       STDT3
043D 0  0000                DC       0
043E 20 04262495            LIBF     DISKN
043F 0  0100                DC       /0100
0440 1  136D                DC       STDT3
0441 0  70FC                MDX      *-4
0442 01 C4000BEC            LD    L  STDT2+1
0444 0  8022                A        DEC6     CHANGE OF SECTOR ADDRESS.
0445 01 D4000BEC            STO   L  STDT2+1
0447 01 C400136E            LD    L  STDT3+1
0449 0  801D                A        DEC6     CHANGE OF SECTOR ADDRESS.
044A 01 D400136E            STO   L  STDT3+1
044C 0  C01D                LD       STDT1+1
044D 0  8019                A        DEC6     CHANGE OF SECTOR ADDRESS.
044E 0  D01B                STO      STDT1+1
044F 01 74010466            MDX   L  STCNT,1
0451 0  C010                LD       ADC04
0452 01 D400024D            STO   L  DKST1+1  RESTORE STORE ADDRESS.
0454 0  C00F                LD       ADC05
0455 01 D4000253            STO   L  DKST2+1
0457 0  C00C                LD       ADC06
0458 01 D4000274            STO   L  DKST3+1
045A 0  C00B                LD       STCNT
```

```
045B 0  B009             CMP    DEC12
045C 0  7003             MDX    ENDIT
045D 0  7000             MDX    OUT2
045E 01 4C800429   OUT2  BSC  I OPISK
0460 01 4C000244   ENDIT BSC  L EXITS
0462 1  046B       ADC04 DC     STDT1+2
0463 1  0BED       ADC05 DC     STDT2+2
0464 1  136F       ADC06 DC     STDT3+2
0465 0  000C       DEC12 DC     12
0466 0  0000       STCNT DC     *-*
0467 0  0006       DEC6  DC     6
0468 1  046A       ADC07 DC     STDT1+1
0469 31 06253C33   STDT1 DSA    FIL03      SEDIMENT CONCENTRATION.
046C    077F             BSS    1919
0BEB 31 06253C34   STDT2 DSA    FIL04      HORIZONTAL VELOCITY COMPONENT.
0BEE    077F             BSS    1919
136D 31 06253C35   STDT3 DSA    FIL05      VERTICAL VELOCITY COMPONENT.
1370    077F             BSS    1919
1AEF 0  FE3F       PIPPS DC     /FE3F
1AF0 0  0FFC       MSK1  DC     /0FFC      MASKING CONSTANT
1AF1 0  FFFF       MSK2  DC     /FFFF      MASKING CONSTANT
1AF2 0  000A             DC     DMESX-DMES3
1AF3    000F       DMES3 DMES   '2DRUN NUMBER  'E
1AFA    0003       OTPUT BSS    3
1AFD    0000       DMESX BES    0
1AFD 0  000C             DC     DMESB-DMES4+3
1AFF    0012       DMES4 DMES   'DAVERAGE VALUE = 'E
1B07    0000       DMESB BSS    0
1B07    0006       INPUT BSS    6
1B0D 0  003A             DC     DMESC-DMES5
1B0E    001F       DMES5 DMES   '2DDATA COLLECTION FOR SEDIMENT '
1B1D    001F             DMES   CONCENTRATION AND TWO VELOCITY '
1B2D    001F             DMES   COMPONENTS.'DTO CHANGE PROGRAM '
1B3C    0018             DMES   CONSTANTS, SET D.E.S. B.'E
1B48    0000       DMESC BES    0
1B48 0  000D             DC     DMESQ-DMES6
1B49    001A       DMES6 DMES   '2D   DELAY  POINTS   WAVES'E
1B56    0000       DMESQ BES    0
1B56 0  000D             DC     DMESP-DMES7
1B57    001A       DMES7 DMES   'R'AEXIT1, NO SYNC SIGNAL.'R'E
1B64    0000       DMESP BES    0
1B64 0  000F             DC     DMESO-DMES8
1B65    001F       DMES8 DMES   'RFILES 03 04 05 ARE TOO SMALL'E
1B74    0000       DMESO BES    0
1B74 0  0
104 14.818 02        1442 NOT READY 00D            DC      DMESM-DMES9
1B75    001A       DMES9 DMES   'R     U0        U1        LIMIT'E
1B82    0000       DMESM BES    0
1B82    0000             END    START
    NO ERRORS IN ABOVE ASSEMBLY.
ACSV3
DUP FUNCTION COMPLETED
```

```
// JOB   0000011111
// ASM COMPT
*LIST
                         ************************************************
                         *              PROGRAM : COMPT                 *
                         * THIS PROGRAM COMPUTES THE PERIODIC MEAN      *
                         * AND THE RMS OF THE RANDOM COMPONENT          *
                         * OF THE SIGNALS FOR 3 CHANNELS FROM THE DATA  *
                         * STORED ON DISK BY THE PROCESS PROGRAM AGSV3. *
                         * PROGRAMMED BY A.MUELLER, APRIL 1977          *
                         ************************************************
0000 01 0C000152    START XIO  L  LITON
0002 01 C40006F9          LD   L  STDT1+1    SAVE SECTOR ADDRESS.
0004 01 D400007A          STO  L  SECSV
0006 01 C4000370          LD   L  DE320      SET UP WORD COUNT TO OBTAIN
0008 01 D4000163          STO  L  INFOM      EXPERIMENTAL PARAMETERS.
000A 20 04262495          LIBF    DISKN      READ FIL20 FROM DISK
000B 0  1000              DC      /1000      WHICH CONTAINS THE
000C 1  0163              DC      INFOM      NUMBER OF POINTS PER WAVE,
000D 0  0000              DC      /0000      THE NUMBER OF WAVES SAMPL-
000E 20 04262495          LIBF    DISKN      ED AND THE RUN NUMBER.
000F 0  0100              DC      /0100
0010 1  0163              DC      INFOM
0011 0  70FC              MDX     *-4
0012 01 C4000168    LOOP1 LD   L  WAVES      SET UP COUNTER FOR NUMBER
0014 01 D400015A          STO  L  NUMDR      OF AVERAGES COMPUTED.
0016 01 C4000167          LD   L  PONTS      COMPUTE TWICE THE NUMBER
0018 0  1001              SLA     1          OF POINTS.
0019 01 D4000158          STO  L  TNPTS
001B 0  10A0              SLT     32         CLEAR STORAGE FOR
001C 01 65800158          LDX  I1 TNPTS      ACCUMULATION OF SUMS.
001E 01 DD0002A6    CLEAR STD  L1 AREAC-2    AREAC : USED FOR ACCUMULA-
0020 0  71FE .            MDX   1 -2          TION OF SUMS.
0021 0  70FC              MDX     CLEAR
0022 00 6500FDC0          LDX  L1 -576       CLEAR AREAD.
0024 01 D50005B5    CLER2 STO  L1 AREAD+576
0026 0  7101              MDX   1 1
0027 0  70FC              MDX     CLER2
0028 01 94000158          S    L  TNPTS      OBTAIN MINUS TWICE THE
002A 01 D4000158          STO  L  TNPTS      NUMBER OF POINTS. TNPTS
002C 01 C400007C          LD   L  XR4        CONTAINS -2*PONTS.
002E 01 B400007B          CMP  L  TWO        CHECK FOR LOOP. SET UP OF
0030 0  7002              MDX     NSKIP      ADDRESSES.
0031 0  701B              MDX     SKIP
0032 0  701A              MDX     SKIP
0033 0  C02F        NSKIP LD      ADDD1+1
0034 01 94000158          S    L  TNPTS      MODIFY ADDRESSES FOR
0036 0  D02C              STO     ADDD1+1    ACCUMULATION AND
0037 0  D02D              STO     ADDD1+3    MANIPULATION OF DATA.
0038 01 D4000099          STO  L  LDDD1+1
003A 01 C400011C          LD   L  ADDD2+1    SET UP ADDRESSES.
003C 01 94000158          S    L  TNPTS      DO FOR FIRST LOOP ONLY.
003E 01 D400011C          STO  L  ADDD2+1
0040 01 D400011E          STO  L  ADDD2+3
0042 0  1010              SLA     16         ZERO A REG.
0043 01 94000167          S    L  PONTS      COMPUTE MINUS THE
0045 01 D4000159          STO  L  MNPTS      NUMBER OF POINTS.
0047 01 C4000167          LD   L  PONTS
0049 01 84000114          A    L  SUBCP+1
004B 01 D4000114          STO  L  SUBCP+1
004D 01 C4000157    SKIP  LD   L  WDCNT      SET UP WORD COUNT FOR
004F 01 D40006F8          STO  L  STDT1      DISK READ.
0051 20 04262495    READD LIBF    DISKN      READ IN THE FIRST SET OF
0052 0  1000              DC      /1000      DATA STORED ON DISK IN
```

```
0053 1  06F8                  DC        STDT1
0054 0  0000                  DC        /0000
0055 20 04262495              LIBF      DISKN
0056 0  0100                  DC        /0100
0057 1  06F8                  DC        STDT1
0058 0  70FC                  MDX       *-4
0059 01 65800158       AGAIN  LDX    I1 TNPTS       LOAD INDEX REGISTERS TO
005B 01 66800159              LDX    I2 MNPTS       BEGIN SIGNAL AVERAGING.
005D 01 C40006FA       LOAD1  LD     L  STDT1+2
005F 0  D019                  STO       SAVE1
0060 0  C018                  LD        SAVE1
0061 0  1890                  SRT       16          COMPUTE SIGNAL AVERAGED
0062 01 8D0002A8       ADDD1  AD     L1 AREAC       RESULTS.
0064 01 DD0002A8              STD    L1 AREAC
0066 01 7401005E              MDX    L  LOAD1+1,1 MODIFY ADDRESS.
0068 0  C0F5                  LD        LOAD1+1     CHECK FOR END OF DATA BLOCK.
0069 01 9400015B              S      L  ADC01
006B 01 B4000157              CMP    L  WDCNT
006D 0  400F                  BSI       MORDT       MORE DATA REQUIRED.
006E 0  7001                  MDX       MCOMP       COMPUTATIONS CONTINUE.
006F 0  400D                  BSI       MORDT       MORE DATA REQUIRED.
0070 0  7201           MCOMP  MDX     2 1           DECREMENT XR2.
0071 0  1000                  NOP
0072 0  7102                  MDX     1 +2          DECREMENT XR1.
0073 0  70E9                  MDX       LOAD1       GO BACK FOR MORE DATA.
0074 01 74FF015A              MDX    L  NUMBR,-1    DECREMENT NUMBER OF WAVES.
0076 0  70E2                  MDX       AGAIN       GET ANOTHER WAVE SET.
0077 0  701C                  MDX       COMPT       GO TO COMPUTATION SCHEME.
0078 0  0000           TEMP   DC        *-A*         TEMPORARY STORAGE.
0079 0  0000           SAVE1  DC        *-*         TEMPORARY STORAGE.
007A 0  0000           SECSV  DC        *-*         SAVE SECTOR ADDRESS FOR
007B 0  0002           TWO    DC        2           RAW DATA.
007C 0  0003           XR4    DC        3           INDEX REGISTER FOR LOOP.
                       ****************************************************
                       * DISK DATA SUBROUTINE TO OBTAIN MORE DATA.        *
                       ****************************************************
007D 0  0000           MORDT  DC        *-*         SUBROUTINE TO GET
007E 01 C400015B              LD     L  ADC01       MORE DATA FROM DISK.
0080 01 D400005E              STO    L  LOAD1+1     RESET ADDRESSES OF LOADING
0082 01 D4000112              STO    L  LOAD2+1     OPERATION.
0084 01 C40006F9              LD     L  STDT1+1     UPDATE SECTOR ADDRESS.
0086 01 84000162              A      L  DEC6
0088 01 D40006F9              STO    L  STDT1+1
008A 20 04262495              LIBF      DISKN       CALL TO DISK FOR
008B 0  1000                  DC        /1000       MORE DATA.
008C 1  06F8                  DC        STDT1
008D 0  0000                  DC        /0000
008E 20 04262495              LIBF      DISKN
008F 0  0100                  DC        /0100
0090 1  06F8                  DC        STDT1
0091 0  70FC                  MDX       *-4
0092 01 4C80007D              BSC    I  MORDT       END SUBROUTINE.
                       ****************************************************
0094 01 65800158       COMPT  LDX    I1 TNPTS       LOAD INDEX REGISTERS
0096 01 66800159              LDX    I2 MNPTS       TO SCALE THE DATA.
0098 01 CD0002A8       LDDD1  LDD    L1 AREAC
009A 01 AC000168              D      L  WAVES
009C 01 D40005B8       STOR2  STO    L  CBQCD+2     UNSCALED SIGNAL AVERAGED
009E 01 7401009D              MDX    L  STOR2+1,1 RESULT STORED IN FIL27
00A0 0  7102                  MDX     1 +2          RESULT STORED BACK INTO
00A1 0  1000                  NOP                   AREAC.
00A2 0  7201                  MDX     2 +1
00A3 0  70F4                  MDX       LDDD1
00A4 01 74FF007C              MDX    L  XR4,-1      DECREMENT OF INDEX REG.
00A6 0  7001                  MDX       LUCKY       FOR LOOP COUNTER.
00A7 0  701B                  MDX       LOOP4
```

```
00A8 01 C400007C    LUCKY LD    L  XR4
00AA 01 B400007B          CMP   L  TWO
00AC 0  7016              MDX      LOOP4
00AD 0  700B              MDX      LOOP3
00AE 0  7000              MDX      LOOP2
00AF 01 C4000E7B    LOOP2 LD    L  STDT2+1     SET UP SECTOR ADDRESS FOR
00B1 01 D40006F9          STO   L  STDT1+1     CHANNEL 2.
00B3 01 C400015B          LD    L  ADCO1       CHANNEL2 & RESET LOAD
00B5 01 D400005E          STO   L  LOAD1+1     INSTRUCTION.
00B7 01 4C000012          BSC   L  LOOP1       GO BACK TO OPERATE ON
00B9 01 C4000E7E    LOOP3 LD    L  STDT3+1     CHANNEL 2 & GET SUM. OF CHAN.3.
00BB 01 D40006F9          STO   L  STDT1+1
00BD 01 C400015B          LD    L  ADCO1
00BF 01 D400005E          STO   L  LOAD1+1
00C1 01 4C000012          BSC   L  LOOP1       GO BACK TO OPERATE ON
00C3 01 C400007A    LOOP4 LD    L  SECSV       CHANNEL 3.
00C5 01 D40006F9          STO   L  STDT1+1     SAVE SECTOR ADDRESS FOR
00C7 01 7403007C          MDX   L  XR4,3       CHANNEL1.
00C9 0  C005              LD       CONST       SAVE SECTOR ADDRESS FOR
00CA 01 D40005B6          STO   L  CB@CD       CB@CD.
00CC 20 04262495          LIBF     DISKN       STORE UNSCALED SIGNAL
00CD 0  3000              DC       /3000       AVERAGED DATA (AREAE)
00CE 1  05B6              DC       CB@CD       INTO DISK.
00CF 0  0140        CONST DC       320
00D0 20 04262495          LIBF     DISKN
00D1 0  0100              DC       /0100
00D2 1  05B6              DC       CB@CD
00D3 0  70FC              MDX      *-4
00D4 01 C4000168    INDEX LD    L  WAVES
00D6 01 D400015A          STO   L  NUMBR
00D8 01 C400007C          LD    L  XR4         LOAD INDEX REGISTER TO
00DA 01 B400007B          CMP   L  TWO         CHECK THE LOOP STEP.
00DC 0  7028              MDX      READF
00DD 0  7014              MDX      LOOPB
00DE 01 C4000E7B    LOOPA LD    L  STDT2+1     LOAD & STORE THE DATA OF
00E0 01 D40006F9          STO   L  STDT1+1     CHANNEL 2 &.CHANGE ADDRESS
00E2 01 C4000114          LD    L  SUBCP+1
00E4 01 84000167          A     L  PONTS
00E6 01 D4000114          STO   L  SUBCP+1
00E8 01 C400015B          LD    L  ADCO1
00EA 01 D4000112          STO   L  LOAD2+1
00EC 0  C02F              LD       ADDD2+1     MODIFY ADDRESS FOR
00ED 01 94000158          S     L  TNPTS       ACCUMULATION & MANIPULATION
00EF 0  D02C              STO      ADDD2+1     OF DATA.
00F0 0  D02D              STO      ADDD2+3
00F1 0  7013              MDX      READF
00F2 01 C4000E7E    LOOPB LD    L  STDT3+1     LOAD & STORE THE DATA OF
00F4 01 D40006F9          STO   L  STDT1+1     CHANNEL 3 & CHANGE ADDRESS.
00F6 01 C4000114          LD    L  SUBCP+1
00F8 01 84000167          A     L  PONTS
00FA 01 D4000114          STO   L  SUBCP+1
00FC 01 C400015B          LD    L  ADCO1
00FE 01 D4000112          STO   L  LOAD2+1
0100 0  C01B              LD       ADDD2+1     MODIFY ADDRESS FOR
0101 01 94000158          S     L  TNPTS       ACCUMULATION & MANIPULATION
0103 0  D018              STO      ADDD2+1     OF DATA.
0104 0  D019              STO      ADDD2+3
0105 20 04262495    READF LIBF     DISKN       READ OUT THE SET OF DATA
0106 0  1000              DC       /1000       STORED ON DISK.
0107 1  06F8              DC       STDT1
0108 0  0000              DC       /0000
0109 20 04262495          LIBF     DISKN
010A 0  0100              DC       /0100
010B 1  06F8              DC       STDT1
010C 0  70FC              MDX      *-4
010D 01 65800158    AGAN1 LDX   I1 TNPTS       LOAD INDEX REGISTER TO
```

```
010F 01 66800159          LDX   I2 MNPTS      BEGIN SIGNAL AVERAGING.
0111 01 C40006FA   LOAD2  LD    L  STDT1+2    LOAD FROM DISK AREA.
0113 01 960005B8   SUBCP  S     L2 AREAE-1    SUBTRACT UNSCALED MEAN
0115 01 A400015C          M     L  SCALE      RAW DATA & MEAN VALUE.
0117 01 D4000078          STO   L  TEMP
0119 01 A4000078          M     L  TEMP
011B 01 80000374   ADDD2  AD    L1 AREAD-1
011D 01 DD000374          STD   L1 AREAD-1
011F 01 74010112          MDX   L  LOAD2+1,1 MODIFY ADDRESS.
0121 0  C0F0              LD       LOAD2+1    CHECK FOR END OF DATA BLOCK
0122 01 9400015B          S     L  ADC01
0124 01 B4000157          CMP   L  WDCNT
0126 0  7001              MDX      DATA1      MORE DATA REQUIRED.
0127 0  7002              MDX      MCMP1      MORE COMPUTATIONS.
0128 01 4400007D   DATA1  BSI   L  MORDT
012A 0  7201       MCMP1  MDX    2 1          DECREMENT XR2.
012B 0  1000              NOP
012C 0  7102              MDX    1 +2         DECREMENT XR1.
012D 0  70E3              MDX      LOAD2      GO BACK FOR MORE DATA.
012E 01 74FF015A          MDX   L  NUMBR,-1   DECREMENT NO. OF WAVES.
0130 0  70DC              MDX      AGAN1      GET ANOTHER WAVE SET.
0131 01 74FF007C          MDX   L  XR4,-1
0133 0  7001              MDX      LOOPZ
0134 0  7002              MDX      LAST
0135 01 4C0000D4   LOOPZ  BSC   L  INDEX
0137 01 C400013E   LAST   LD    L  WORDC
0139 01 D4000372          STO   L  CPVST      RANDOM COMPONENT OF THE
013B 20 04262495          LIBF     DISKN      CONC. FLUCTL TO DISK.
013C 0  3000              DC       /3000
013D 1  0372              DC       CPVST
013E 0  0240       WORDC  DC       576
013F 20 04262495          LIBF     DISKN
0140 0  0100              DC       /0100
0141 1  0372              DC       CPVST
0142 0  70FC              MDX      *-4
0143 20 04262495          LIBF     DISKN      READ IN ALL INFORMATIONS
0144 0  3000              DC       /3000      OF CONSTANTS ONTO INFOM.
0145 1  0163              DC       INFOM
0146 0  0000              DC       /0000
0147 20 04262495          LIBF     DISKN
0148 0  0100              DC       /0100
0149 1  0163              DC       INFOM
014A 0  70FC              MDX      *-4
014B 01 0C000150          XIO   L  LITOF
014D 30 25241600          CALL     VIAQ
0150    0000              BSS   E  0
0150 1  0155       LITOF  DC       OFF
0151 0  617D              DC       /617D
0152 1  0154       LITON  DC       ON
0153 0  617D              DC       /617D
0154 0  0200       ON     DC       /0200
0155 0  0000       OFF    DC       /0000
0156 0  0008       EIGHT  DC       8
0157 0  0780       WDCNT  DC       1920       WORD COUNT - READ IN DATA.
0158 0  0000       TNPTS  DC       *-*        MINUS TWICE NO. OF PTS.
0159 0  0000       MNPTS  DC       *-A*        MINUS NO. OF PTS.
015A 0  0000       NUMBR  DC       *-*        NBR. OF WAVES.
015B 1  06FA       ADC01  DC       STDT1+2    ADDR. CHECK ON ENOUGH DATA.
015C 0  2717       SCALE  DC       10007      SCALING COEF.
015D    0003       DVSER  BSS      3
0160 0  0000       AVRGE  DC       *-*
0162    0000              BSS   E  0
0162 0  0006       DEC6   DC       6
0163 31 06253CB0   INFOM  DSA      FIL20      INFORMATION STORED ON DISK.
0166 0  FFB0       DELAY  DC       -80        DELAY TIME.
0167 0  0060       PONTS  DC       96         NUMBER OF POINTS ON A WAVE.
```

```
0168 0  0064        WAVES DC       100      NUMBER OF WAVES.
0169 0  0000        CLICK DC       *-*      LOCATION OF RUN NUMBER.
016A    0060        AREAB BSS      96       DISKN AREA.
01CA    0003        AREAF BSS      3
01CD    0003        AREAG BSS      3
01D0    00D8        AREAH BSS      216
02A8    00C8        AREAC BSS   E  200      SCALED.
0370 0  0140        DE320 DC       320      CONSTANT.
0372    0000              BSS   E  0
0372 31 06253CB2    CPVST DSA      FIL22    USES FIL22 AND FIL23
0375    0240        AREAD BSS      576
05B6    0000              BSS   E  0
05B6 31 06253CB7    CBJCD DSA      FIL27    STORAGE OF UNSCALED SIGNAL
05B9    013F        AREAE BSS      319      AVERAGED RESULT.
06F8 31 06253C33    STDT1 DSA      FIL03    SEDIMENT CONCENTRATION.
06FB    077F              BSS      1919
0E7A 31 06253C34    STDT2 DSA      FIL04    HORIZONTAL VELOCITY COMPONENT.
0E7D 31 06253C35    STDT3 DSA      FIL05    VERTICAL VELOCITY COMPONENT.
0E80 0  0009        DEC9  DC       9
0E81 0  0019        DEC25 DC       25
0E82    0006        INPUT BSS      6
0E88    0000              END      START
     NO ERRORS IN ABOVE ASSEMBLY.
COMPT
DUP FUNCTION COMPLETED
 // JOB    0000011111
 // END OF ALL JOBS
```

```
// JOB   0000011111
// ASM CHANG
*LIST
                            *****************************************************
                            *                        CHANG                      *
                            *  THIS PROCESS PROGRAM IS CALLED BY A CALL SPECL  *
                            *  FROM THE SIGNAL AVERAGING PROGRAM AGSV3          *
                            *  AND ALLOWS THE USER TO CHANGE PROGRAM            *
                            *  CONSTANTS. THESE CONSTANTS ARE THE NUMBER OF     *
                            *  WAVES TO BE SAMPLED, THE NUMBER OF POINTS        *
                            *  PER WAVE, THE DELAY TIME IN MS BETWEEN DATA      *
                            *  POINTS, THE MIN.VALUE U0 IN MV, THE MAX.         *
                            *  DIFFERENCE U1 IN MV AND THE NUMBER LIMIT OF      *
                            *  ALLOWED BAD POINTS TO TEST THE LDA-TRACKER. ALL*
                            *  ENTRYS ARE MADE THROUGH THE DATA ENTRY           *
                            *  SWITCHES AND AN ECHO CHECK IS PRINTED.           *
                            *****************************************************
0000 20 23A17155      START LIBF     TYPEN      INTRODUCTORY MESSAGE.
0001 0  2002                DC       /2002
0002 1  02FC                DC       DMES0-1
0003 0  0000                DC       0
0004 20 23A17155            LIBF     TYPEN
0005 0  0002                DC       /0002
0006 0  70FD                MDX      *-3
0007 20 23A17155            LIBF     TYPEN
0008 0  2002                DC       /2002      AT PAUSE ENTER THE NUMBER
0009 1  01FF                DC       DMES1-1    OF WAVES TO BE SAMPLED.
000A 0  0000                DC       0
000B 20 23A17155            LIBF     TYPEN
000C 0  0002                DC       /0002
000D 0  70FD                MDX      *-3
000E 01 C400008B            LD    L  AREAA
0010 01 D400008C            STO   L  INFOR
0012 20 04262495            LIBF     DISKN      READ IN THE AREA FROM DISK
0013 0  1000                DC       /1000
0014 1  008C                DC       INFOR
0015 0  0000                DC       0
0016 20 04262495            LIBF     DISKN      ONLY THE FIRST 3 WORDS
0017 0  0100                DC       /0100      IN THE AREA WILL BE CHANGED.
0018 1  008C                DC       INFOR
0019 0  70FB                MDX      *-4
001A 20 17064885            LIBF     PAUSE      PROGRAMMED WAIT
001B 1  02F2                DC       ONE
001C 01 0C0000AA            XIO   L  IOCCA      READ CONTENTS OF DES. TO WA VES
001E 20 23A17155            LIBF     TYPEN      ECHO CHECK ON THE NUMBER
001F 0  2002                DC       /2002      OF WAVES ENTERED.
0020 1  022A                DC       DMES2-1
0021 0  0000                DC       0
0022 20 23A17155            LIBF     TYPEN
0023 0  0002                DC       /0002
0024 0  70FD                MDX      *-3
0025 01 C40000C1            LD    L  WAVES
0027 01 440002C0            BSI   L  PRINT
0029 20 23A17155            LIBF     TYPEN      MESSAGE TO ENTER THE
002A 0  2002                DC       /2002      NUMBER OF DATA POINTS
002B 1  0237                DC       DMES3-1
002C 0  0000                DC       0
002D 20 23A17155            LIBF     TYPEN
002E 0  0002                DC       /0002
002F 0  70FD                MDX      *-3
0030 20 17064885            LIBF     PAUSE      WAIT TO ENTER VIA DES.
0031 1  02F3                DC       TWO
0032 0  0879                XIO      IOCCB      READ DES TO POINTS
0033 20 23A17155            LIBF     TYPEN      ECHO CHECK ON THE NUMBER
```

```
0034 0  2002              DC        /2002     OF POINTS ENTERED.
0035 1  0248              DC        DMES4-1
0036 0  0000              DC        0
0037 20 23A17155          LIBF      TYPEN
0038 0  0002              DC        /0002
0039 0  70FD              MDX       *-3
003A 01 C4000000          LD    L   POINTS
003C 01 4400020B          BSI   L   PRINT
003E 20 23A17155          LIBF      TYPEN     MESSAGE TO ENTER  THE DELAY
003F 0  2002              DC        /2002     TIME VIA DES.
0040 1  0258              DC        DMES5-1
0041 0  0000              DC        0
0042 20 23A17155          LIBF      TYPEN
0043 0  0002              DC        /0002
0044 0  70FD              MDX       *-3
0045 20 17064885          LIBF      PAUSE     WAIT TO ENTER INFORMATION.
0046 1  02E4              DC        THREE
0047 0  0866              XIO       IOCCC     READ DES. TO DELAY
0048 20 23A17155          LIBF      TYPEN     ECHO CHECK ON THE NUMBER
0049 0  2002              DC        /2002     OF MILLISECONDS DELAY TIME.
004A 1  0269              DC        DMES6-1
004B 0  0000              DC        0
004C 20 23A17155          LIBF      TYPEN
004D 0  0002              DC        /0002
004E 0  70FD              MDX       *-3
004F 0  C0CF              LD        DELAY
0050 01 4400020B          BSI   L   PRINT
0052 0  1010              SLA       16        ZERO A REG
0053 0  90CC              S         DELAY     A REG. CONTAINS MINUS DELAY
0054 0  1003              SLA       3         MULTIPLY BY  8
0055 0  D0C9              STO       DELAY     STORE IN DELAY
0056 20 23A17155          LIBF      TYPEN     READ IN U0
0057 0  2002              DC        /2002
0058 1  0275              DC        DME10-1
0059 0  0000              DC        0
005A 20 23A17155          LIBF      TYPEN
005B 0  0002              DC        /0002
005C 0  70FD              MDX       *-3
005D 20 17064885          LIBF      PAUSE
005E 1  02F5              DC        FOUR
005F 0  0850              XIO       IOCCD
0060 20 23A17155          LIBF      TYPEN
0061 0  2002              DC        /2002
0062 1  02A5              DC        DME13-1
0063 0  0000              DC        0
0064 20 23A17155          LIBF      TYPEN
0065 0  0002              DC        /0002
0066 0  70FD              MDX       *-3
0067 01 C4000003          LD    L   U0
0069 01 4400020B          BSI   L   PRINT
006B 01 C4000003          LD    L   U0
006D 0  1004              SLA       4         MULTIPLY BY 16
006E 01 D4000003          STO   L   U0
0070 20 23A17155          LIBF      TYPEN     READ IN U1
0071 0  2002              DC        /2002
0072 1  0285              DC        DME11-1
0073 0  0000              DC        0
0074 20 23A17155          LIBF      TYPEN
0075 0  0002              DC        /0002
0076 0  70FD              MDX       *-3
0077 20 17064885          LIBF      PAUSE
0078 1  02F6              DC        FIVE
0079 0  0838              XIO       IOCCE
007A 20 23A17155          LIBF      TYPEN
007B 0  2002              DC        /2002
007C 1  02B1              DC        DME14-1
```

```
007D 0  0000                    DC       0
007E 20 23A17155                LIBF     TYPEN
007F 0  0002                    DC       /0002
0080 0  70FD                    MDX      *-3
0081 01 C4000004                LD    L  U1
0083 01 440002CB                BSI   L  PRINT
0085 01 C4000004                LD    L  U1
0087 0  1004                    SLA      4         MULTIPLY BY 16
0088 01 D4000004                STO   L  U1
008A 20 23A17155                LIBF     TYPEN     READ IN LIMIT
008B 0  2002                    DC       /2002
008C 1  020F                    DC       DMF12-1
008D 0  0000                    DC       0
008E 20 23A17155                LIBF     TYPEN
008F 0  0002                    DC       /0002
0090 0  70FD                    MDX      *-3
0091 20 17064885                LIBF     PAUSE
0092 1  02F7                    DC       SIX
0093 0  0820                    XIO      IOCCF
0094 20 23A17155                LIBF     TYPEN
0095 0  2002                    DC       /2002
0096 1  02DD                    DC       DMF15-1
0097 0  0000                    DC       0
0098 20 23A17155                LIBF     TYPEN
0099 0  0002                    DC       /0002
009A 0  70FD                    MDX      *-3
009B 01 C4000005                LD    L  LIMIT
009D 01 440002CB                BSI   L  PRINT
009F 20 04262495                LIBF     DISKN     READ OUT ONTO DISK
00A0 0  3000                    DC       /3000
00A1 1  00BC                    DC       INFOR
00A2 0  0000                    DC       /0000
00A3 20 04262495                LIBF     DISKN
00A4 0  0100                    DC       /0100
00A5 1  00BC                    DC       INFOR
00A6 0  70FC                    MDX      *-4
00A7 30 02063480                CALL     BACK
00AA    0000                    BSS   E  0
00AA 1  00C1          IOCCA DC       WAVES     READ DES TO LOC. WAVES
00AB 0  0240                DC       /0240
00AC 1  00C0          IOCCB DC       PONTS     READ DES. TO NO. OF PTS.
00AD 0  0240                DC       /0240
00AE 1  00BF          IOCCC DC       DELAY     READ DES. DELAY TIME.
00AF 0  0240                DC       /0240
00B0 1  00C3          IOCCD DC       U0        READ DES TO LOC. U0
00B1 0  0240                DC       /0240
00B2 1  00C4          IOCCE DC       U1        READ DES TO LOC. U1
00B3 0  0240                DC       /0240
00B4 1  00C5          IOCCF DC       LIMIT     READ DES TO LOC. LIMIT
00B5 0  0240                DC       /0240
00B6 0  0000          DATSW DC       /0000
00B7 0  0740                DC       /0740
00B8 0  0140          AREAA DC       320
00B9 31 06253C86      FILE  DSA      FIL26
00BC 31 06253CB0      INFOR DSA      FIL20
00BF 0  0000          DELAY DC       *-*
00C0 0  0000          PONTS DC       *-*       NUMBER OF POINTS
00C1 0  0000          WAVES DC       *-*       NO. OF WAVES
00C2 0  0000          CLICK DC       *-*
00C3 0  0000          U0    DC       *-*
00C4 0  0000          U1    DC       *-*
00C5 0  0000          LIMIT DC       *-*
00C6    0139                BSS      313
01FF 0  002A                DC       DMESZ-DMES1
0200    0020          DMES1 DMES     '2PENTRY OF CONSTANTS FOR SIGNAL '
0210    0012                DMES     AVERAGING PROGRAM.'E
```

```
0219      0022              DMES    'RENTER NUMBER OF WAVES AT PAUSE 1.'E
022A      0000        DMESZ BES     0
022A 0    000C              DC      DMESY-DMES2
022B      0018        DMES2 DMES    '2RTHE NO. OF WAVES IS     'E
0237      0000        DMESY BES     0
0237 0    0010              DC      DMESX-DMES3
0238      0020        DMES3 DMES    '2RNOW ENTER NO. OF DATA POINTS.'E
0248      0000        DMESX BES     0
0248 0    000F              DC      DMESW-DMES4
0249      001F        DMES4 DMES    '2RTHE NO. OF DATA POINTS IS    'E
0258      0000        DMESW BES     0
0258 0    0010              DC      DMESU-DMES5
0259      0020        DMES5 DMES    '2RNOW ENTER DELAY TIME IN MSEC.'E
0269      0000        DMESU BES     0
0269 0    000B              DC      DMESV-DMES6
026A      0016        DMES6 DMES    '2RTHE DELAY TIME IS    'E
0275      0000        DMESV BES     0
0275 0    000F              DC      DMESP-DME10
0276      001E        DME10 DMES    '2RNOW ENTER MIN.VAL. U0 IN MV'E
0285      0000        DMESP BES     0
0285 0    0010              DC      DMESO-DME11
0286      0020        DME11 DMES    '2RNOW ENTER MAX.DIFF. U1 IN MV.'E
0296      0000        DMESO BES     0
0296 0    000F              DC      DMESM-DME12
0297      001C        DME12 DMES    '2RNOW ENTER LIMIT OF BAD PT.'E
02A5      0000        DMESM BES     0
02A5 0    000B              DC      DMESM-DME13
02A6      0016        DME13 DMES    '2RTHE MIN.VALUE U0 IS'E
02B1      0000        DMESM BES     0
02B1 0    000B              DC      DMESL-DME14
02B2      001E        DME14 DMES    '2RTHE MAX.DIFF. U1 IS'E
02BD      0000        DMESL BSS     0
02BD 0    000D              DC      DMESK-DME15
02BE      001A        DME15 DMES    '2RTHE LIMIT OF BAD PT. IS'E
02C8      0000        DMESK BES     0
02C8 0    0000        PRINT DC      *-*          PRINTING SUBROUTINE
02C9 20   02255103          LIBF    BINDC        BINARY TO DECIMAL
02CD 1    02DC              DC      BNOUT
02CE 20   08593599          LIBF    HOLPR        HOLLERITH TO PRINTER
02CF 0    0000              DC      /0000
02D0 1    02DC              DC      BNOUT
02D1 1    02E9              DC      PTOUT
02D2 0    0006              DC      6
02D3 20   23A17155          LIBF    TYPEN        PRINT OUT NUMBER
02D4 0    2002              DC      /2002
02D5 1    02E8              DC      PTOUT-1
02D6 0    0000              DC      /0000
02D7 20   23A17155          LIBF    TYPEN
02D8 0    0002              DC      /0002
02D9 0    70FD              MDX     *-3
02DA 01   4C8002C8          BSC   I PRINT        END OF SUBROUTINE PRINT
02DC      0006        BNOUT BSS     6
02E2 0    0001        ONE   DC      1
02E3 0    0002        TWO   DC      2
02E4 0    0003        THREE DC      3
02E5 0    0004        FOUR  DC      4
02E6 0    0005        FIVE  DC      5
02E7 0    0006        SIX   DC      6
02E8 0    0003              DC      3
02E9      0003        PTOUT BSS     3
02EC 0    0012              DC      DMESR-DMES9
02ED
104 14.093 02        1462 NOT READY 001C        DMES9 DMES    '2R'AACSV3'B CONST
ANTS WILL BE '
02FB      0008              DMES    MODIFIED'E
02FF      0000        DMESR BES     0
```

THIS DOCUMENT IS BEST QUALITY PRACTICABLE.
THE COPY FURNISHED TO DDC CONTAINED A
SIGNIFICANT NUMBER OF PAGES WHICH DO NOT
REPRODUCE LEGIBLY.

```
0300    0000              END     START
     NO ERRORS IN ABOVE ASSEMBLY.
CHANG
DUP FUNCTION COMPLETED
```

```
// JOB    0000011111
// ASM CNVRT
*LIST
                                *****************************************************
                                *       PROGRAM : CNVRT                             *
                                *  THIS PROGRAM CONVERTS THE DATA IN MV. TO         *
                                *  (PPM) FOR CHANNEL 1 (SEDIMENT CONCENTRATION)     *
                                *  AND 1000*(FT/S) FOR CHANNEL 3 (VERTICAL VELOCIT*
                                *  Y) THROUGH THE SCALING PROCEDURE.                *
                                *  PROGRAMED BY LOCHER AND NAKATO                   *
                                *****************************************************
0000 01 C400013C        START LD   L   DEC10      SET UP WORD COUNT TO
0002 01 D4000204              STO  L   INFOM      GET INFORMATION
0004 20 04262495              LIBF     DISKN      READ FIL20
0005 0  1000                  DC       /1000
0006 1  0204                  DC       INFOM
0007 0  0140            WDCNT DC       320
0008 20 04262495              LIBF     DISKN
0009 0  0100                  DC       /0100
000A 1  0204                  DC       INFOM
000B 0  70FC                  MDX      *-4
000C 0  C0FA                  LD       WDCNT      LOAD WORD COUNT ON FIL27
000D 01 D4000346              STO  L   CB@CD
000F 20 04262495              LIBF     DISKN      READ FIL27 TO GET UNSCALED
0010 0  1000                  DC       /1000      (MEAN + PERIODIC)
0011 1  0346                  DC       CB@CD
0012 0  0000                  DC       /0000
0013 20 04262495              LIBF     DISKN
0014 0  0100                  DC       /0100
0015 1  0346                  DC       CB@CD
0016 0  70FC                  MDX      *-4
0017 01 C4000208              LD   L   PONTS
0019 0  1001                  SLA      1
001A 01 D4000140              STO  L   TNPTS
001C 0  1010                  SLA      16         SET UP ZERO IN A-REG.
001D 01 94000208              S    L   PONTS      SUBTRACT NO. OF PTS.
001F 01 D400013F              STO  L   MNPTS      MINUS NO. OF PONTS
0021 01 6580013F              LDX  I1  MNPTS      DO LOOP FOR CHANNEL1
0023 01 C4000348        LOOP1 LD   L   AREAE-1    LOAD (MEAN + PERI)
0025 01 84000142              A    L   ZERO1      ADD UNSCALED ZERO VOLY
0027 01 A4000143              M    L   SCALE      SCALING
0029 01 D4000144        ARRAG STO  L   AREAG
002B 01 74010024              MDX  L   LOOP1+1,1
002D 01 7401002A              MDX  L   ARRAG+1,1
002F 0  7101                  MDX   1  1          INCREASE INDEX REG.1 BY 1
0030 0  70F2                  MDX      LOOP1      GO TO LOOP1
0031 0  C0F2                  LD       LOOP1+1
0032 01 94000208              S    L   PONTS
0034 0  D0EF                  STO      LOOP1+1
0035 0  C0F4                  LD       ARRAG+1
0036 01 94000208              S    L   PONTS
0038 0  D0F1                  STO      ARRAG+1
0039 01 C4000488              LD   L   ADRE       CALCUL. ADRESS 3.CH.
003B 01 84000140              A    L   TNPTS
003D 01 9400013A              S    L   DEC1
003F 0  D003                  STO      LOOP2+1
0040 01 6680013F              LDX  I2  MNPTS      DO LOOP FOR CHANNEL 3
0042 00 C4000000        LOOP2 LD   L   *-*        LOAD MEAN + PERIODIC
0044 01 A4000143              M    L   SCALE
0046 01 D40001A4        ARRAH STO  L   AREAH
0048 01 74010043              MDX  L   LOOP2+1,1
004A 01 74010047              MDX  L   ARRAH+1,1
004C 0  7201                  MDX   2  1          RAISE INDEX REG.2 BY 1
004D 0  70F4                  MDX      LOOP2
```

```
004E 0  C0F7                 LD       ARRAH
004F 01 94000208             S     L  PONTS
0051 0  D0F5                 STO      ARRAH+1
0052 20 23A17171             LIBF     TYPE1      PRINT RUNNO
0053 1  020A                 DC       CLICK
0054 0  0001                 DC       1
0055 01 0C0000E4             XIO   L  IOCCA      READ DATA ENTRY SWITCH
0057 01 E40000E7             AND   L  MASC2      TEST FOR SWITCH 2
0059 0  4820                 BSC      Z          SKIP IF DES 2 IS NOT SET
005A 0  700D                 MDX      SKIPP      SKIPP OUTPUT CHANNEL 1
005B 20 26663A15             LIBF     WRTYN      WRITE MESSAGE FOR SEDIMENT
005C 0  2001                 DC       /2001
005D 1  0489                 DC       DMES1-1
005E 0  0000                 DC       /0000
005F 20 26663A15             LIBF     WRTYN
0060 0  0001                 DC       /0001
0061 0  70FD                 MDX      *-3
0062 01 C4000208             LD    L  PONTS
0064 0  D002                 STO      NOP
0065 20 23A17171             LIBF     TYPE1      TYPE OUT SED. CONCENTRATION
0066 1  0144                 DC       AREAG      IN PPM UNIT
0067 0  0000           NOP   DC       *-*
0068 20 26663A15       SKIPP LIBF     WRTYN      WRITE MESSAGE FOR V-COMP
0069 0  2001                 DC       /2001
006A 1  049A                 DC       DMES2-1
006B 0  0000                 DC       /0000
006C 20 26663A15             LIBF     WRTYN
006D 0  0001                 DC       /0001
006E 0  70FD                 MDX      *-3
006F 01 C4000208             LD    L  PONTS
0071 0  D002                 STO      NNOP
0072 20 23A17171             LIBF     TYPE1      TYPE OUT V-COMP.
0073 1  01A4                 DC       AREAH      IN 1000*(FT/S) UNIT
0074 0  0000           NNOP  DC       *-A*
0075 01 0C0000E4             XIO   L  IOCCA      READ DATA ENTRY SWITCH
0077 01 E40000E6             AND   L  MASC
0079 0  4808                 BSC      +
007A 0  7067                 MDX      OUT
007B 20 03059115             LIBF     CARDN      FEEDS 1 CARD
007C 0  3000                 DC       /3000
007D 0  0000                 DC       0
007E 20 03059115             LIBF     CARDN
007F 0  0000                 DC       /0000
0080 0  70FD                 MDX      *-3
0081 01 C400020A             LD    L  CLICK      PUNCH RUNNO
0083 20 02255103             LIBF     BINDC
0084 1  00E9                 DC       OUTPT
0085 01 C4000209             LD    L  WAVES      PUNCH NO OF WAVES
0087 20 02255103             LIBF     BINDC
0088 1  00EF                 DC       OUTPT+6
0089 01 C400013D             LD    L  DEC12
008B 0  D05C                 STO      AREA
008C 20 03059115             LIBF     CARDN
008D 0  2000                 DC       /2000
008E 1  00E8                 DC       AREA
008F 0  0000                 DC       0
0090 20 03059115             LIBF     CARDN
0091 0  0000                 DC       /0000
0092 0  70FD                 MDX      *-3
0093 01 C400013E             LD    L  DEC72      PUNCH MEAN AND
0095 0  D052                 STO      AREA       PERIODIC ON CARDS
0096 01 65800208             LDX  11  PONTS
0098 0  620C           PUNCH LDX   2  12         12 VALUES PER CARD
0099 01 C40001A4       CONV  LD    L  AREAH
009B 20 02255103             LIBF     BINDC
009C 1  00E9           OTP   DC       OUTPT
```

```
009D 01 7406009C            MDX  L  OTP,6       FIELD FOR NEXT VALUE
009F 01 7401009A            MDX  L  CONV+1,1    NEXT VALUE.
00A1 0  72FF                MDX   2 -1
00A2 0  70F6                MDX     CONV
00A3 20 03059115            LIBF    CARDN
00A4 0  2000                DC      /2000
00A5 1  00E8                DC      AREA
00A6 0  0000                DC      0
00A7 20 03059115            LIBF    CARDN
00A8 0  0000                DC      /0000
00A9 0  70FD                MDX     *-3
00AA 01 74B8009C            MDX  L  OTP,-72     RESTORES 1. OUTPUT AD.
00AC 0  71F4                MDX   1 -12
00AD 0  70EA                MDX     PUNCH
00AE 01 C4000208            LD   L  PONTS       PRINTOUT OF REST
00B0 0  1890                SRT     16
00B1 01 AC00013D            D    L  DEC12
00B3 0  1090                SLT     16
00B4 01 B4000139            CMP  L  ZERO
00B6 0  7002                MDX     GOON
00B7 0  7024                MDX     RSTOR
00B8 0  7023                MDX     RSTOR
00B9 01 D4000141      GOON  STO  L  REST
00BB 01 A400013B            M    L  DEC6
00BD.0  1090                SLT     16
00BE 01 D40000E8            STO  L  AREA
00C0 0  C0D9                LD      CONV+1      SET ADRESS IN AREAH
00C1 0  D006                STO     CONVV+1
00C2 01 84000141            A    L  REST
00C4 0  D0D5                STO     CONV+1
00C5 01 66800141            LDX  I2 REST
00C7 00 C4000000      CONVV LD   L  *-*
00C9 20 02255103            LIBF    BINDC
00CA 1  00E9          OTTP  DC      OUTPT
00CB 01 740600CA            MDX  L  OTTP,6
00CD 01 740100C8            MDX  L  CONVV+1,1
00CF 0  72FF                MDX   2 -1
00D0 0  70F6                MDX     CONVV
00D1 20 03059115            LIBF    CARDN
00D2 0  2000                DC      /2000
00D3 1  00E8                DC      AREA
00D4 0  0000                DC      0
00D5 20 03059115            LIBF    CARDN
00D6 0  0000                DC      /0000
00D7 0  70FD                MDX     *-3
00D8 0  C0F1                LD      OTTP        RESTORES OTTP
00D9 01 940000E8            S    L  AREA
00DB 0  D0EE                STO     OTTP
00DC 01 C400009A      RSTOR LD   L  CONV+1      RESTORES ADR. IN CONV+1
00DE.01 94000208            S    L  PONTS
00E0 01 D400009A            STO  L  CONV+1
00E2 30 059C98C0      OUT   CALL    EXIT
00E4    0000                BSS  E  0
00E4 0  0000          IOCCA DC      /0000       READ DATA ENTRY SW.
00E5 0  0740                DC      /0740
00E6 0  0001          MASC  DC      /0001
00E7 0  0002          MASC2 DC      /0002       MASK FOR DES 2
00E8 0  0000          AREA  DC      *-A*         OUTPUT AREA FOR CARDS
00E9    0050          OUTPT BSS     80
0139 0  0000          ZERO  DC      0
013A 0  0001          DEC1  DC      1
013B 0  0006          DEC6  DC      6
013C 0  0068          DEC10 DC      104
013D 0  000C          DEC12 DC      12
013E 0  0048          DEC72 DC      72
013F 0  0000          MNPTS DC      *-*
```

```
0140 0   0000        TNPTS DC     *-*
0141 0   0000        REST  DC     *-*
0142 0   0000        ZERO1 DC     0          ZERO SHIFT CHAN.1
0143 0   2717        SCALE DC     10007
0144     0060        AREAG BSS    96         PPM FOR SED. CONC.
01A4     0060        AREAH BSS    96         1000*(FT/S)FOR V-COMP.
0204 31  06253CB0    INFOM DSA    FIL20
0207 0   0000        DELAY DC     *-*
0208 0   0000        POINTS DC    *-*
0209 0   0000        WAVES DC     *-*
020A 0   0000        CLICK DC     *-*
020B     0060        AREAB BSS    96
026B     00DB        AREAF BSS    219
0346 31  06253CB7    CBQCD DSA    FIL27
0349     013F        AREAE BSS    319
0488 1   0349        ADRE  DC     AREAE
0489 0   0010              DC     DMESA-DMES1
048A     000B        DMES1 DMES   '2RPRESSURE '
048F     0013              DMES   (MEAN AND PERIODIC)'E
0499 0   8105              DC     /8105
049A     0000        DMESA BES    0
049A 0   0015              DC     DMESB-DMES2
049B     0014        DMES2 DMES   '2RVELOCITY COMPONENT'
04A5     0014              DMES   (MEAN AND PERIODIC)'E
04AF 0   8105              DC     /8105
04B0     0000        DMESB BES    0
04B0     0000              END    START
    NO ERRORS IN ABOVE ASSEMBLY.
CNVRT
DUP FUNCTION COMPLETED
 // JOB    0000011111
 // END OF ALL JOBS
```

```
// JOB    0000011111
// ASM CONVT
*LIST
                    ****************************************************
                    *    PROGRAM : CONVT                               *
                    *  THIS PROGRAM CONVERTS VOLTAGE UNIT OF RANDOM    *
                    *  FLUCTUATIONS FOR PRINTOUT. AND PUNCHES CARDS.   *
                    *  DES1 UP : CARDS ARE PUNCHED                     * *
                    *  DES2 UP : PRINTOUT CHANNEL 1 IS SUPRESSED       *
                    *  PROGRAMMED BY A. MUELLER      MARCH 1977        *
                    ****************************************************
0000 01 C400022C    START LD   L  DEC9       LOAD WORD COUNT ON FIL20
0002 01 D4000234          STO  L  INFOM
0004 20 04262495          LIBF    DISKN      GET INFORMATION
0005 0  1000              DC      /1000
0006 1  0234              DC      INFOM
0007 0  0000              DC      /0000
0008 20 04262495          LIBF    DISKN
0009 0  0100              DC      /0100
000A 1  0234              DC      INFOM
000B 0  70FC              MDX     *-4
000C 01 C4000487          LD   L  WORDC      LOAD WORD COUNT ON FIL22
000E 01 D4000242          STO  L  CPVST
0010 20 04262495          LIBF    DISKN      GET SQUARE VALUE OF
0011 0  1000              DC      /1000      RANDOM FLUCTUATION
0012 1  0242              DC      CPVST
0013 0  0000              DC      /0000
0014 20 04262495          LIBF    DISKN
0015 0  0100              DC      /0100
0016 1  0242              DC      CPVST
0017 0  70FC              MDX     *-4
0018 0  1010              SLA     16         SET A REGISTER ZERO
0019 01 94000238          S    L  PONTS
001B 01 D400022D          STO  L  MNPTS      MINUS NO. OF PONTS
001D 0  1001              SLA     1          MULTIPLY BY TWO
001E 01 D400022E          STO  L  TNPTS      -2* NO. OF PONTS
0020 0  1001              SLA     1
0021 01 D400022F          STO  L  FNPTS      -4* NO. OF PONTS
0023 01 C4000239          LD   L  WAVES
0025 0  1890              SRT     16         SET UP DOUBLE PRECISION
0026 30 051064E3          CALL    EDFLT      FLOAT NO. OF WAVES
0028 20 058A3580          LIBF    ESTO       STORE FLOATED WAVES
0029 1  0230              DC      DVSER
002A 20 23A17171          LIBF    TYPE1      PRINT RUNNO
002B 1  023A              DC      CLICK
002C 0  0001              DC      1
002D 01 0C000112          XIO  L  IOCCA      READ DATA ENTRY SWITCH
002F 01 E4000115          AND  L  MASC2      TEST FOR SWITCH 2
0031 0  4820              BSC     Z          SKIP IF DES 2 IS NOT SET
0032 0  7037              MDX     SKIPP      SKIPP OUTPUT CHANNEL 1
0033 20 26663A15          LIBF    WRTYN      CARRAGE RETURN
0034 0  2001              DC      /2001
0035 1  0488              DC      CARIG.
0036 0  0000              DC      0
0037 20 26663A15          LIBF    WRTYN
0038 0  0001              DC      /0001
0039 0  70FD              MDX     *-3
003A 20 26663A15          LIBF    WRTYN
003B 0  2001              DC      /2001
003C 1  0494              DC      DMES1-1    HEADING FOR CHANNEL 1
003D 0  0000              DC      0
003E 20 26663A15          LIBF    WRTYN
003F 0  0001              DC      /0001
0040 1  003E              DC      *-3
```

```
0041 20 26663A15           LIBF     WRTYN      CARRAGE RETURN
0042 0  2001               DC       /2001
0043 1  0488               DC       CARIG
0044 0  0000               DC       0
0045 20 26663A15           LIBF     WRTYN
0046 0  0001               DC       /0001
0047 0  70FD               MDX      *-3
0048 01 6580022E           LDX   I1 TNPTS      SET UP INDEX REG. 1
004A 01 CC000244   LOOP1   LDD   L  AREAD-1    LOOP FOR CHANNEL 1
004C 30 051064E3           CALL     EDFLT      FLOAT THE VALUE
004E 20 05109940           LIBF     EDIV       DEVIDE BY NO. OF WAVES
004F 1  0230               DC       DVSER
0050 30 05898640           CALL     ESQR       TAKE SQUARE ROOT
0052 20 091899C0           LIBF     IFIX       CONVERT TO INTEGER
0053 01 D400016C   ADO     STO   L  AREAG
0055 01 74010054           MDX   L  ADO+1,1
0057 01 7402004B           MDX   L  LOOP1+1,2
0059 0  7102       LOOPC   MDX    1 2
005A 0  70EF               MDX      LOOP1
005B 01 C4000238           LD    L  PONTS
005D 0  D002               STO      NPON
005E 20 23A17171           LIBF     TYPE1      PRINTOUT 1.CHANNEL
005F 1  016C               DC       AREAG
0060 0  0000       NPON    DC       *-*
0061 0  C0F2               LD       ADO+1      RESTORES ADR. IN AREAG
0062 01 94000238           S     L  PONTS
0064 01 D4000054           STO   L  ADO+1
0066 0  C0E4               LD       LOOP1+1
0067 01 8400022E           A     L  TNPTS
0069 0  D0E1               STO      LOOP1+1
006A 20 26663A15   SKIPP   LIBF     WRTYN      CONVERSION CHANNEL 3
006B 0  2001               DC       /2001
006C 1  0488               DC       CARIG
006D 0  0000               DC       0
006E 20 26663A15           LIBF     WRTYN
006F 0  0001               DC       /0001
0070 0  70FD.              MDX      *-3
0071 20 26663A15           LIBF     WRTYN      HEADING FOR CHANNEL 3
0072 0  2001               DC       /2001
0073 1  04A2               DC       DMES2-1
0074 0  0000               DC       0
0075 20 26663A15           LIBF     WRTYN
0076 0  0001               DC       /0001
0077 0  70FD               MDX      *-3
0078 20 26663A15           LIBF     WRTYN      CARRAGE RETURN
0079 0  2001               DC       /2001
007A 1  0488               DC       CARIG
007B 0  0000               DC       0
007C 20 26663A15           LIBF     WRTYN
007D 0  0001               DC       /0001
007E 0  70FD               MDX      *-3
007F 01 6580022E.          LDX   I1 TNPTS
0081 01 C4000485           LD    L  ADRD       SETS ADR. FOR 3.CHANNEL
0083 01 9400022F           S     L  FNPTS
0085 01 94000486           S     L  DEC1
0087 0  D001               STO      LOOP2+1
0088 00 CC000000   LOOP2   LDD   L  *-*        LOOP FOR CHANNEL 3
008A 30 051064E3           CALL     EDFLT      FLOAT THE VALUE
008C 20 05109940           LIBF     EDIV       DIVISION ROUTINE
008D 1  0230               DC       DVSER.
008E 30 05898640           CALL     ESQR       SQUARE ROOT
0090 20 091899C0           LIBF     IFIX       CONVERTS TO INTEGER
0091 01 D40001CC   AD1     STO   L  AREAH      FIELD FO INT. VALUE
0093 01 74010092           MDX   L  AD1+1,1
0095 01 74020089           MDX   L  LOOP2+1,2
0097 0  7102       LOOPB   MDX    1 2
```

```
0098 0  70EF                MDX      LOOP2
0099 01 C4000238            LD    L  PONTS
009B 0  D002                STO      NPPON
009C 20 23A17171            LIBF     TYPE1         PRINTOUT 3.CHANNEL
009D 1  01CC                DC       AREAH
009E 0  0000         NPPON  DC       *-*
009F 0  C0F2                LD       AD1+1         RESTORES 1.ADR. IN AREAH
00A0 01 94000238            S     L  PONTS
00A2 0  D0EF                STO      AD1+1
00A3 01 0C000112            XIO   L  IOCCA         READ DATA ENTRY SWITCH
00A5 01 E4000114            AND   L  MASC
00A7 0  4808                BSC      +
00A8 0  7066                MDX      OUT
00A9 20 03059115            LIBF     CARDN         FEEDS 1 CARD
00AA 0  3000                DC       /3000
00AB 0  0000                DC       0
00AC 20 03059115            LIBF     CARDN
00AD 0  0000                DC       /0000
00AE 0  70FD                MDX      *-3
00AF 01 C400023A            LD    L  CLICK         PUNCH RUNNO
00B1 20 02255103            LIBF     BINDC
00B2 1  0117                DC       OTPUT
00B3 01 C4000239            LD    L  WAVES
00B5 20 02255103            LIBF     BINDC
00B6 1  011D                DC       OTPUT+6
00B7 01 C4000169            LD    L  DEC12
00B9 0  D05C                STO      AREA
00BA 20 03059115            LIBF     CARDN
00BB 0  2000                DC       /2000
00BC 1  0116                DC       AREA
00BD 0  0000                DC       0
00BE 20 03059115            LIBF     CARDN
00BF 0  0000                DC       /0000
00C0 0  70FD.               MDX      *-3
00C1 01 C400016A            LD    L  DEC72         PUNCH MEAN AND
00C3 0  D052                STO      AREA          PERIODIC ON CARDS
00C4 01 65800238            LDX   I1 PONTS
00C6 0  620C         PUNCH  LDX   2  12            12 VALUES PER CARD
00C7 01 C40001CC     CONV   LD    L  AREAH
00C9 20 02255103            LIBF     BINDC
00CA 1  0117         OTP    DC       OTPUT
00CB 01 740600CA            MDX   L  OTP,6         FIELD FOR NEXT VALUE
00CD 01 740100C8            MDX   L  CONV+1,1      NEXT VALUE
00CF 0  72FF                MDX   2  -1
00D0 0  70F6                MDX      CONV
00D1 20 03059115            LIBF     CARDN
00D2 0  2000                DC       /2000
00D3 1  0116                DC       AREA
00D4 0  0000                DC       0
00D5 20 03059115            LIBF     CARDN
00D6 0  0000                DC       /0000
00D7 0  70FD                MDX      *-3
00D8 01 74B800CA            MDX   L  OTP,-72       RESTORES 1. OUTPUT AD.
00DA 0  71F4                MDX   1  -12
00DB 0  70EA                MDX      PUNCH
.00DC 01 C4000238           LD    L  PONTS         PRINTOUT OF REST
00DE 0  1890                SRT      16
00DF 01 AC000169            D     L  DEC12
00E1 0  1090                SLT      16
00E2 01 B4000167            CMP   L  ZERO
00E4 0  7002                MDX      GOON
00E5 0  7023                MDX      RSTOR
00E6 0  7022                MDX      RSTOR
00E7 01 D400016B     GOON   STO   L  REST
00E9 01 A4000168            M     L  DEC6
00EB 0  1090                SLT      16
```

```
00EC 01 D4000116          STO   L  AREA
00EE 0  C0D9              LD       CONV+1      SET ADRESS IN AREAH
00EF 0  D0D6              STO      CONVV+1
00F0 01 8400016B          A     L  REST
00F2 0  D0D5              STO      CONV+1
00F3 01 6680016B          LDX  12  REST
00F5 00 C4000000   CONVV  LD    L  *-*
00F7 20 02255103          LIBF     BINDC
00F8 1  0117       OTTP   DC       OTPUT
00F9 01 740600F8          MDX   L  OTTP,6
00FB 01 740100F6          MDX   L  CONVV+1,1
00FD 0  72FF              MDX   2  -1
00FE 0  70F6              MDX      CONVV
00FF 20 03059115          LIBF     CARDN
0100 0  2000              DC       /2000
0101 1  0116              DC       AREA
0102 0  0000              DC       0
0103 20 03059115          LIBF     CARDN
0104 0  0000              DC       /0000
0105 0  70FD              MDX      *-3
0106 0  C0F1              LD       OTTP        RESTORES OTTP
0107 0  900E              S        AREA
0108 0  D0EF              STO      OTTP
0109 01 C40000C8   RSTOR  LD    L  CONV+1      RESTORES ADR. IN CONV+1
010B 01 94000238          S     L  PONTS
010D 01 D40000C8          STO   L  CONV+1
010F 30 059C98C0   OUT    CALL     EXIT
0112    0000              BSS   E  0
0112 0  0000       IOCCA  DC       /0000       READ DATA ENTRY SW.
0113 0  0740              DC       /0740
0114 0  0001       MASC   DC       /0001
0115 0  0002       MASC2  DC       /0002       MASK FOR DES 2
0116 0  0000       AREA   DC       *-*         OUTPUT AREA FOR CARDS
0117    0050       OTPUT  BSS      80
0167 0  0000       ZERO   DC       0
0168 0  0006       DEC6   DC       6
0169 0  000C       DEC12  DC       12
016A 0  0048       DEC72  DC       72
016B 0  0000       REST   DC       *-*
016C    0060       AREAG  BSS      96          STOR. 1. CHANNEL
01CC    0060       AREAH  BSS      96          STOR. 2. CHANNEL
022C 0  0009       DEC9   DC       9
022D 0  0000       MNPTS  DC       *-*
022E 0  0000       TNPTS  DC       *-*
022F 0  0000       FNPTS  DC       *-*
0230    0003       DVSER  BSS      3
0234    0000              BSS   E  0
0234 31 06253CB0,  INFOM  DSA      FIL20       INFORMATIONE FOR EXP.CONST
0237 0  0000       DELAY  DC       *-*
0238 0  0000       PONTS  DC       *-*
0239 0  0000       WAVES  DC       *-*
023A 0  0000       CLICK  DC       *-*
023B    0006              BSS      6
0242    0000              BSS   E  0
0242 31 06253CB2   CPVST  DSA      FIL22       USES FIL22 AND FIL23
0245    0240       AREAD  BSS      576         SQUARE OF RANDOM FLUCTU.
0485 1  0245       ADRD   DC       AREAD
0486 0  0001       DEC1   DC       1
0487 0  0240       WORDC  DC       576
0488 0  0001       CARIG  DC       1
0489 0  8181              DC       /8181
048A 0  0008              DC       8
048B    0008       OUTPT  BSS      8
0493 0  2121              DC       /2121
0494 0  000D              DC       DMESA-DMES1
0495    0018       DMES1  DMES     '2RRMS VALUES OF PRESSURE'E
```

```
04A1 0  8105              DC      /8105
04A2    0000        DMESA BES     0
04A2 0  001B              DC      DMESB-DMES2
04A3    001B        DMES2 DMES    '2RRMS VALUES OF THE RANDOM '
04B0    0019              DMES    COMPONENT OF THE VELOCITY'E
04BD 0  8105              DC      /8105
04BE    0000        DMESB BES     0
04BE    0000              END     START
     NO ERRORS IN ABOVE ASSEMBLY.
CONVT
DUP FUNCTION COMPLETED
// JOB   0000011111
// END OF ALL JOBS
```